Study of Dynamic Cavitation in Variable Displacement Axial Piston Pumps

Liviu Theodorescu

A Thesis

in

The Department

of

Mechanical and Industrial Engineering

Presented in Partial Fulfillment of the Requirements

for the degree of Master of Applied Science (Mechanical Engineering) at

Concordia University

Montreal, Quebec, Canada

Your file Votre référence
ISBN: 0-494-10274-8
Our file Notre référence
ISBN: 0-494-10274-8

"Discovery consists of seeing what everybody has seen

and thinking what nobody has thought."

Albert Von Szent-Gyorgy

ABSTRACT

Study of Dynamic Cavitation in Variable Displacement Axial Piston Pumps

Liviu Theodorescu

The scope of this study is to identify and modify the design parameters of the variable displacement axial piston pump in order to reduce its sensitivity to cavitation when operated in a hydraulic system with pre-established characteristics.

An exhaustive analysis of existing theory explaining the cavitation phenomenon is performed and a new approach using the relationship between matter and energy is provided to complete and simplify the description of cavitation.

A detailed mathematical model of the axial piston pump is created in order to evaluate the contribution of the pump's geometrical characteristics to cavitation. This model is validated using results from tests performed on two test units.

Based on this, an evaluation method of the pump cavitation at the design stage is established and design recommendations are provided.

ACKNOWLEDGMENTS

Although the completion of this thesis proved to be a challenging event that took the author through the entire collection of human emotions, he may finally affirm that the elaboration of this document allowed him to acquire important academic and scientific knowledge. However, the author believes that the most valuable development did not occur on a professional level but on a personal level. The creation of such a paper shall allow the writer to enhance his capabilities of analyzing, synthesizing, and presenting information. Moreover, the involvement in this process shall teach the author to shape and defend his own opinions. Finally, the creation of such a document shall lead the author into pushing his own limits until the desired goal is attained. For all these reasons, the author hopes that, along with acquiring valuable knowledge, some positive and permanent changes occurred in his personality.

However, all these accomplishments could not be made possible without the significant support of several valuable and passionate people.

First, the author wishes to express his sincere gratitude to the supervising professor for this study, Dr. Jaroslav Svoboda, who unfortunately is not with us anymore to enjoy the results of his guidance and support. The assistance of Dr. Jaroslav Svoboda from the beginning of this process was greatly appreciated and the author feels fortunate to have known and worked with such an outstanding teacher.

Second, the author is grateful to Dr. Georgios Vatistas for accepting to supervise the completion of this thesis. The enthusiastic support provided by Dr. Georgios Vatistas during this highly important stage and his extraordinary efforts put into completing this process were greatly appreciated by the author.

Finally, the author wishes to express his sincere appreciation to his family. Although occasional support and comprehension were provided by the family members, the importance assigned by the author to these moments made them extremely valuable. The author is also grateful for the assistance provided by his father during the elaboration of this document; his technical expertise in the hydraulic field was highly useful in validating and developing important ideas presented in this study.

In conclusion, the author hopes that this thesis will provide valuable information on the subject considered and it will constitute a new basis for initiating other related projects and ideas.

TABLE OF CONTENTS

LIST OF FIGURES

FIGURE

LIST OF TABLES

TABLE

LIST OF SYMBOLS

A_1	Cross-sectional area at location (1)
A_2	Cross-sectional area at location (2)
A_p	Piston cross-sectional area
A_{dk}	Discharge area
A_{sk}	Suction area
α	Angle of swash plate
B	Bulk modulus of liquid medium
c	Maximum travel of piston
C_0	Ideal flow coefficient
C_{0d}	Ideal flow coefficient of discharge
C_{0s}	Ideal flow coefficient of suction
C_A	Actual flow coefficient
C_{Ad}	Actual flow coefficient of discharge
C_{As}	Actual flow coefficient of suction
c.v.	Control volume contained within one cylinder of the pump
D_C	Distance between centers of pistons
f	Frequency
F_{body}	Body forces acting on the system
$F_{surface}$	Surface forces acting on the system
F_{sys}	External force acting on a system
g	Gravitational acceleration
γ	Specific weight
h_L	Head loss
k	Piston number

K_L	Leakage empirical factor
m	Mass of system
n	Drive shaft speed of rotation
p	Pressure along a streamline
P	Linear momentum of a system
p_1	Pressure at location (1)
p_2	Pressure at location (2)
p_c	Pump casing pressure
p_d	Discharge pressure
p_k	Pressure inside cylinder chamber
p_s	Suction pressure
q	Total number of pistons
Q	Volume flowrate
Q_{dk}	Discharge volume flowrate
Q_{in}	Flowrate entering the control volume
Q_{lk}	Internal leakage volume flowrate
Q_{out}	Flowrate exiting the control volume
Q_{sk}	Suction volume flowrate
Q_{vk}	Volume flowrate due to piston action
R	Radius of circle on which the pump pistons revolve
ρ	Density of liquid medium
s_k	Linear displacement of piston
t	Time
θ_{av}	Angular position of piston produced by drive shaft rotation
θ_k	Angular displacement of piston
θ_{pn}	Angular position of piston related to the total number of pistons

u	x component of velocity vector
v	y component of velocity vector
v	Velocity vector
v_1	Velocity at location (1)
v_2	Velocity at location (2)
v_{pk}	Piston velocity
ω	Angular velocity of drive shaft
z	Elevation
z_1	Elevation of location (1)
z_2	Elevation of location (2)
$\frac{\partial v}{\partial t}$	Partial derivative of velocity vector with respect to time
$\frac{\partial v}{\partial x}$	Partial derivative of velocity vector with respect to x component
$\frac{\partial v}{\partial y}$	Partial derivative of velocity vector with respect to y component
$\forall_0$	"Dead" volume of cylinder

CHAPTER 1

FUNDAMENTALS OF CAVITATION PHENOMENON

CHAPTER 1

FUNDAMENTALS OF CAVITATION PHENOMENON

1.1 INTRODUCTION

Cavitation is an important physical phenomenon encountered in most technical fields where fluids are involved. The occurrence of cavitation was noted by many scientists mostly from its damaging effects, but until the late nineteen century no significant experimental work and scientific studies were performed to further analyze it. In 1873, the British engineer Osborne Reynolds proposed a viable theoretical description of the phenomenon [1, 2, 3] that gave a valuable impulse to the analysis of cavitation and resulted in a significant increase of cavitation-related studies and publications. However, it must be emphasized that even if a great deal of effort was done in understanding cavitation, some aspects of this process are still obscure due to the complexity of the process, to calculation limitations, and to reduced accessibility to experimental observations. The objective of this chapter is to present the available scientific studies and introduce other existing concepts and theories of physics in the attempt to complete the description of the cavitation phenomenon.

1.2 FUNDAMENTALS OF CAVITATION PHENOMENON

The term *cavitation* is an extension of the word *cavity*, which is defined as "an unfilled space within a mass" [4]. However, as it will later be seen, this space is far from being empty as its contents play the primary role in the cavitation process.

Most publications dedicated to cavitation deal with specific aspects, while the information describing the origins of the phenomenon does not present the level of detail necessary to achieve a complete understanding of this segment. In addition, some relevant elements of the cavitation process are often neglected or combined in more general descriptions that reduce the comprehension of the process. However, the available literature represents a valuable source of complementary information that shall be used in conjunction with other available theories of physics to describe cavitation.

Fundamentally, *cavitation* may be defined as the *process that deals with the effects of energy on a given amount of matter.* This general definition includes all manifestations of cavitation and it is discussed below in greater detail. In addition, more specific definitions of cavitation shall be presented as the process is further analysed.

1.2.1 Description of Cavitation Process

The occurrence of the cavitation process is based on the interaction between matter and energy. For this reason, the Kinetic Theory of Matter, one fundamental theory of physics that describes the relationship between matter and energy, is the principal means used to explain the cavitation phenomenon.

Basically, the Kinetic Theory of Matter states that matter is composed of discrete particles (molecules for most substances, atoms for noble gases) that behave in defined ways under the influence of energy.

Without presenting all the details of the process, it is observed that energy produces two types of forces on a particle: *attractive* and *repulsive*. These forces oppose each other and are created by the electric charge developed by the particle.

However, the development of these forces is not identical; the magnitude of *attractive* (or cohesive) *forces* is limited to a certain value fixed by the internal energy level of the particle, whereas the magnitude of *repulsive* (or tension) *forces* can reach any value depending on the amount of energy provided to the particle [5, 6, 7].

When the magnitude of cohesive forces is superior to the magnitude of tension forces, the particles group together under specific structures and form the *solid state* of matter. Alternatively, when the tension forces exceed the cohesive forces, the particles translate randomly and the distances between them increase as a result of the internal stress developed. These characteristics are specific to the *fluid state* of matter (liquid or gas).

The *liquid state* initiates when the magnitude of tension forces surpasses the magnitude of cohesive forces. Under theses circumstances, the particles translate randomly but their range of movement is limited by the cohesive forces. The *gaseous state* forms when the added energy increases the magnitude of the tension forces until the cohesive forces effect becomes negligible. In this case, the particles translate randomly beyond any range of movement.

Based on this, it may be concluded that energy determines the behaviour of matter and its variation leads to the formation of different states of matter.

Although energy is present in nature under various forms (thermal, mechanical, chemical, electrical, nuclear, etc.), it may fundamentally be classified in two categories: *potential energy* and *kinetic energy. Potential energy represents stored energy accumulated by matter as position or heat,* while *kinetic energy denotes energy of movement* [8]. This categorization shall later be used to distinguish between the two different classes of cavitation.

Going back to the discussion of cavitation, a more specific definition of this process may now be formulated based on the above considerations. Hence, *cavitation may be identified as the process under which liquid is transformed into gas as energy is added to matter, followed by an accelerated process under which the resulting gas is retransformed into the initial liquid when energy is removed from* matter. These transformation processes are explained next in greater detail.

As it was previously mentioned, the *fluid state* (liquid or gas) is created by the occurrence of internal stress in matter. The development of this stress takes place along three stages, which are illustrated in Fig. 1.1. The first stage is specific to the liquid state. Here, the initiation of internal stress causes an increase of the distances between particles and their random movement. Although the space between particles increases, they remain under the influence of cohesive forces that limit their range of movement to a particular value. This value is fixed and it is specific to each type of substance.

The second stage of internal stress development occurs when its magnitude reaches a critical value where the random movement of particles generates the *first* region where the distances between particles exceed the influence of cohesive forces. Consequently, a *crack* (or pocket) filled with the gaseous state of the matter forms at this location. Since the distances between particles within a crack are superior to the others, the instantaneous density of matter at that location is lower than the overall density. Thus, the *liquid cracking process* represents the beginning of the transition towards the gaseous state. Analytical and experimental analyses reveal that, after the first crack forms, only a minor internal stress increase is necessary to continue the cracking process at other locations in the liquid [9]. As new cracks appear, the existing ones increase their size through the involvement of neighbouring particles in the process.

The final stage of internal stress development occurs when gas-filled cracks replace the entire amount of liquid. Here, the liquid fails to sustain any increase of stress and *ruptures*; the gaseous state is fully installed [10, 11].

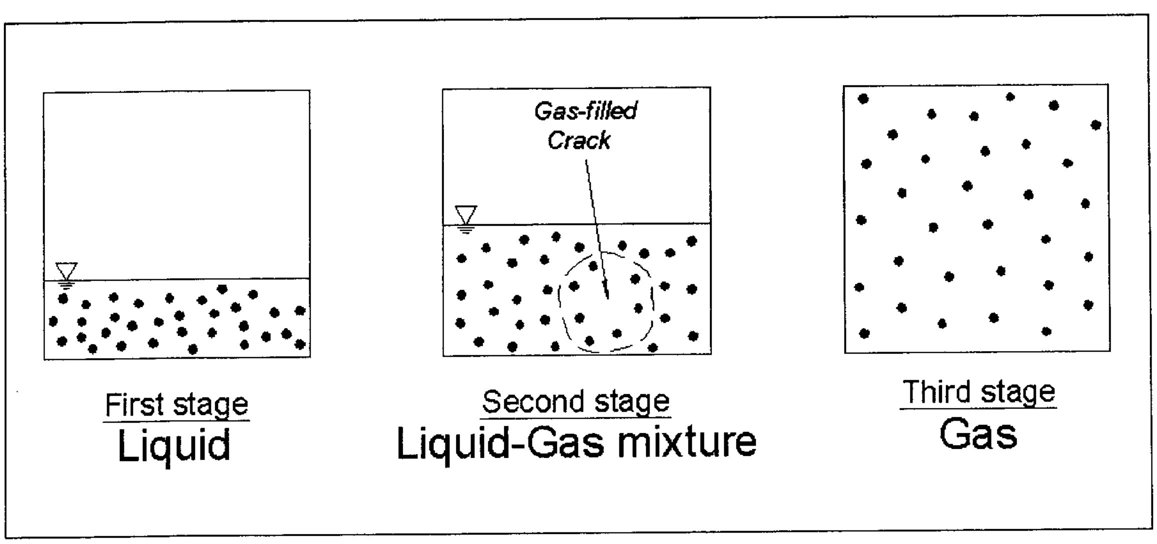

Fig. 1.1: Evolution of fluid state of matter

The transformation of gas into liquid is the inverse of the process presented above; the gas gradually turns into liquid as the magnitude of internal stresses decreases along with the distances between particles.

At this point, it is important to emphasize that, in order to remain consistent with the terminology employed by previous literature dedicated to this subject, the concept of gas-filled crack (or pocket) shall be replaced with the term *cavity*. Although this term, which fundamentally identifies a space deprived of matter, was believed by initial observers and scientists to describe the principal characteristic of the associated process, it is now proved that it does not correspond to the occurring situation. However, in order to provide continuity to the already existing studies and publications, the term *cavity* and the associated *cavitation process* are henceforth adopted.

The internal stress action is an event difficult to quantify. Since this stress affects the distances between particles and consequently the density, its action may indirectly be measured by pressure. Pressure determines the amount of movement for a group of particles by measuring the number of impacts with a given area [12]. Hence, when the distances between particles increase, the density and the number of impacts reduce. Therefore, an increase of internal stress translates into a decrease of fluid pressure, and vice-versa.

The cavitation process is exclusively associated with the evolution of gas-filled cavities and it is based on the series of transformations previously presented. Thus, as the energy of a liquid medium attains a certain level, cavities occur. A further addition of energy increases the number of cavities and the size of existing ones. However, in the case of cavitation, the addition of energy does not continue until the entire liquid medium transforms into gas. Instead, energy is removed from the liquid-gas medium and the occurring cavities are suppressed by retransforming into liquid. Another distinctive feature of cavitation process is that energy is removed from this medium at a much rapid rate as compared to the addition rate. Consequently, the gas-filled cavities compress and are constrained to explode in order to allow the release of the accumulated energy over the imposed shorter period of time.

Therefore, to conclude the general description of cavitation, it may be stated that this process includes three stages: *cavity inception*, *cavity development*, and *cavity suppression*. A more detailed description of these stages is presented in the next chapter.

1.2.1.1 Cavitation in other media

The scientific community agrees on assigning the occurrence of cavitation phenomenon only to the liquid state of matter. However, with the introduction of new states of matter – Bose-Einstein condensate and plasma – the concept of cavitation may be extended to other media. Thus, for example, the cavitation process may be expected to occur in a prevalent gaseous medium as plasma-filled cracks (or cavities) form. These cavities may subsequently follow the same process previously described as they are compressed and constrained to explode. Although the discussion of this process can make the object of a similar discussion, its analysis exceeds the objective of this study.

1.2.2 Classification of Cavitation

The cavitation phenomenon is classified using two criteria: *type of energy* and *nature of medium.*

1.2.2.1 Type of energy criterion

The cavitation stages are produced by varying the energy level of a prevalent liquid medium. As it was previously indicated, when energy is absorbed by matter, it is converted into *potential energy* and/or *kinetic energy.*

Potential energy represents stored energy that gives matter the capacity to perform work. Matter stores energy either through the enhancement of its relative *position (position gain)* or through the *accumulation of heat.* During this event, *matter remains stationary and stable* [13]. The *position gain* is mostly used when dealing with *macroscopic systems*, whereas the *accumulation of heat* has a greater importance in the analysis of *microscopic systems.* In the case of cavitation, the *position gain* may safely be neglected, while the *accumulation of heat* shall be the only aspect considered.

On the other hand, *kinetic energy represents the energy gained by matter as a result of its motion.* In contrast with potential energy, where energy is concealed as position or heat, kinetic energy may be acknowledged as an exposed type of energy expressed by movement [14].

Based on the energy criterion, two classes of cavitation may be defined: *static* and *dynamic.*

Static cavitation deals with the activity of gas-filled cavities in a *liquid at rest*, whereas *dynamic cavitation* is concerned with the activity of cavities resulting from *liquid motion*.

Static cavitation is produced by varying the amount of heat owned by the particles of a liquid. The only method to accomplish this is through the alteration of liquid's *temperature*; this action is achieved by exposing the particles of the liquid to various forms of potential energy: thermal, chemical, luminous, etc. Thus, when the temperature increases, the distances between particles augment and lower-density / lower-pressure regions occur. As temperature is further increased, gas-filled cavities form and develop. Boiling is a familiar term under which these two stages may be grouped. At this time, in order to remain consistent with the definition of cavitation process, the temperature of this medium shall be rapidly reduced. During this event, the gas-filled cavities are compressed and ultimately constrained to explode in order to release the accumulated energy over the imposed shorter period of time.

Alternatively, *dynamic cavitation* occurs in a moving liquid. This movement may be produced either by liquid flow, or by motion of a solid body (propeller, piston, etc.) through the mass of liquid. Thus, as the velocity of the liquid increases, the distances between particles augment, *pressure* decreases, and gas-filled cavities occur. A further increase of liquid velocity increases the size of these regions as the pressure is further reduced. Finally, when the liquid velocity is rapidly decreased, the cavities are suppressed by the resulting pressure increase. Dynamic cavitation is the most common type of cavitation to which liquid-handling machinery is exposed.

Combinations of static and dynamic cavitation may also occur. Thus, one or more stages of the cavitation process may be produced by potential energy (increase of temperature), while the subsequent stage(s) is(are) completed by kinetic energy (decrease of pressure). Furthermore, combinations of potential and kinetic energy may concurrently produce one or all stages of the cavitation process.

From the above considerations, it may be concluded that *the internal stress action is controlled either by temperature or by velocity variations.* Since the internal stress action may be identified as pressure action, it may be stated that *temperature or velocity variations in a fluid generate pressure variations, which lead to the occurrence of cavitation phenomenon. Temperature variations generate static cavitation, whereas velocity variations generate dynamic cavitation.*

1.2.2.2 Nature of medium criterion

As it was previously mentioned, cavitation is believed to occur in other media where the movement of particles, and therefore, the formation, development, and suppression of lower-density and lower-pressure regions are possible. However, the cavitation-related literature agrees on assigning this phenomenon only to a prevalent liquid medium. For the purpose of this study, the presentation of cavitation phenomenon is voluntarily limited to a prevalent liquid medium.

The medium where cavitation occurs may be a *pure liquid* or a *liquid-based mixture.*

Cavitation generated in a *pure liquid* is identified as v*aporous cavitation* [15]. During this process, *cavities filled with the gaseous state of the liquid medium* form, develop, and are suppressed as the magnitude of the internal stress varies in the liquid. As stated before, the cavities begin to form when the effect of cohesive forces becomes negligible at random locations; this point is characterized by a particular pressure identified as the *vapour pressure* of the liquid.

Theoretical analyses and experimental measurements reveal that pure liquids crack at very low absolute pressures. Most studies are concerned with this event since it determines the occurrence of the subsequent cavitation stages. If gage pressure terminology is employed, these pressures may also be regarded as negative (vacuum) pressures [16]. Although these conditions can be experimentally created to allow the occurrence of vaporous cavitation, they are virtually never encountered in any practical application. Moreover, combinations of these two conditions are not likely to occur in any liquid-handling machinery. Therefore, as it will later be seen, vaporous cavitation may be safely discarded from our future discussion.

Theoretical analyses and experimental measurements have been conducted on a reduced number of liquids. However, the existing data allows concluding that liquids characterized by higher viscosities crack at superior gage pressures. This is caused by the relationship that exists between viscosity and the magnitude of cohesive forces.

Cavitation may also occur in *liquid-based mixtures*. These mixtures are composed of *a prevalent pure liquid and at least another different substance.*

Depending on the temperature or velocity conditions that may affect the liquid, the state of this substance may be *solid, liquid, or gaseous.*

According to theoretical and experimental studies, the presence of a solid or liquid substance in a liquid medium leads to the formation of vaporous cavitation. In the first case, only a relatively large amount of the solid substance may have an impact on the temperature or velocity of the liquid; however, *vaporous cavitation* is the only process that may occur in a *liquid-solid mixture.*

For the second case, it is observed that a *liquid-liquid mixture* cavitates at conditions identical to the cavitation conditions of the "weaker" liquid; the "weaker" liquid is the one having inferior cohesive forces, and consequently, it is prone to modify its physical properties earlier. However, it can be concluded that this situation also leads to the occurrence of *vaporous cavitation* [17].

A different type of cavitation occurs in a *liquid-gas mixture.* This medium, composed of *a prevalent pure liquid* "contaminated" by at least one *non-condensable gas*, favours the formation of *gaseous cavitation* [18]. The qualificative "non-condensable" characterizes a substance that exists as gas at the temperature and/or velocity conditions of the surrounding liquid. Therefore, *the liquid contains a series of stable, non-miscible and non-soluble gas bubbles.*

The gaseous cavitation phenomenon may be regarded as a truncated process since cracks (or cavities filled with a non-condensable gas) already exists in the liquid. Thus, the initial stage of the process is not created by the internal stress action but it is allowed by the internal stress level of the liquid.

Under the internal stress action, the behaviour of this medium is dictated by the behaviour of the non-condensable gas cavities. As it was previously mentioned, when gas-filled cavities already exist in a medium, only a minor increase of the internal stress is required to trigger the development stage. The degree of this increase is situated below the vapour pressure limit of the prevalent pure liquid. Thus, in the case of gaseous cavitation, only the non-condensable gas cavities are involved in the process since the liquid cannot vaporise (or crack). Ultimately, the cavities are suppressed by a rapid increase of the internal stress.

The presence of non-condensable gas cavities in a liquid medium reduces considerably its resistance to internal stress. The pressure conditions may be achieved through relatively small increases of temperature or velocity [19, 20]. Consequently, *gaseous cavitation is the most common form of cavitation encountered in practical applications.*

The liquid-gas mixture is also favourable to the occurrence of a third form of cavitation: *pseudo cavitation* [21]. Pseudo cavitation occurs when the action of temperature and/or velocity in the mixture reaches the vapour pressure of the prevalent liquid. Under these circumstances, cavities filled with the gaseous state of the liquid add to the non-condensable gas cavities. However, as in the case of vaporous cavitation where the liquid cracking process requires extreme conditions of temperature and/or velocity, pseudo cavitation is virtually never encountered in any practical application. Therefore, as it will later be seen, this form of cavitation may also be safely discarded from future discussions.

CHAPTER 2

DETAILED DESCRIPTION OF GASEOUS CAVITATION

CHAPTER 2

DETAILED DESCRIPTION OF GASEOUS CAVITATION

2.1 INTRODUCTION

The previous chapter reveals that gaseous cavitation is the most common type of cavitation. This is primarily due to the fact that vaporous cavitation and pseudo cavitation require extreme conditions of either temperature or velocity that may only be created in laboratory using highly specialized equipment. In addition, liquid environments free of gaseous contaminants are virtually impossible to obtain. Thus, it may be stated that gaseous cavitation is at the origin of the majority of effects associated with the cavitation phenomenon. As it will later be seen, due to the operating conditions, *gaseous cavitation* is also the only type of cavitation encountered in axial piston hydraulic pumps. Therefore, this chapter proposes an extensive description of the gaseous cavitation process.

Although gaseous cavitation takes place in a prevalent liquid medium, only the gas-filled cavities are the protagonists of this process. The liquid medium is simply employed in transmitting the internal stress action, in allowing the evolution of the gas-filled cavities, and in concretizing the effects of gaseous cavitation.

The gaseous cavitation process includes three stages: *cavity inception*, *cavity development*, and *cavity suppression*.

2.2 CAVITY INCEPTION

The gaseous cavitation process begins with the occurrence of gas-filled cavities in a liquid medium. As it was previously mentioned, although these cavities are not the result of internal stress action, the internal stress level of the liquid medium allows the cavities to exist. Therefore, it is agreed to consider this stage as the equivalent of the liquid cracking process that characterizes the beginning of cavitation.

Also, as mentioned in the general description of gaseous cavitation, it is observed that the gas is able to maintain its state within the environment at which it is exposed. Numerous substances exist as gases at the operating conditions of most liquid-handling machinery. For example, air – the most common gas contaminant – at atmospheric pressure (101.325 KPa) requires a temperature of -195 °C to become liquid [22] and eventually mix with the prevalent liquid medium. Although this condition may occur, few prevalent media exist in liquid state under these circumstances. Moreover, combinations of these substances or operating conditions that may generate this environment are virtually never encountered in any practical application.

The occurrence of gas-filled cavities in a liquid medium made the object of numerous scientific studies. According to these studies, gas may be introduced in a liquid medium in two ways. First, for an open and dynamic system, gas exists above the liquid's free surface and may be introduced in this medium by the motion of the liquid. Also, for closed systems, static or dynamic, pockets of gas may occur in regions created by the system's boundaries. The gas trapped at these locations may be introduced in the liquid by *actions undertaken by the medium or the system* [23].

Second, gas may be introduced in a liquid medium *through the solid surfaces that contain it (boundaries), or by the solid particles that may contaminate it (impurities)*. This method was presented by Harvey et al. in 1947 as a theoretical model [24] and it was subsequently validated by experimental observations. The *Harvey Model* explains the occurrence of gas-filled cavities by assuming the *existence of crevices of microscopic dimensions in the solid surfaces that contain or contaminate the liquid medium*. Initially, these crevices are filled by the surrounding medium, which is generally a gas. When submerged by liquid, small amounts of gas shall get trapped in the crevices where they stabilize as gas-filled cavities when the pressure differential across the liquid-gas interface balances the surface tension at this interface [25]. Fig. 2.1 illustrates the process by which gas-filled cavities occur in a liquid medium according to Harvey Model. Table 2.1 gives the average depth of crevices that may be found on various solid surfaces, while Fig. 2.2 presents a magnification of a solid surface relief.

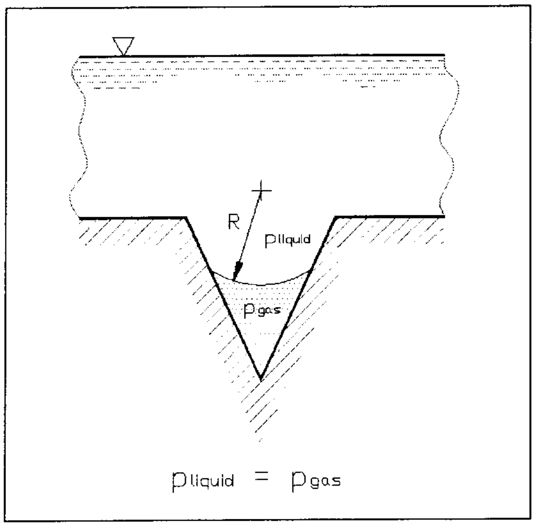

Fig. 2.1: Stabilization of gas-filled cavities in crevices of a solid surface [24, 26]

Table 2.1: Crevice depth for various solid materials [27]

Material	**Average crevice depth** [mm]
Drawn tubing	0.0015
Commercial steel or wrought iron	0.0450
Galvanized iron	0.1500
Cast iron	0.2600
Wood	0.1800 – 0.9000
Concrete	0.3000 – 3.0000
Riveted steel	0.9000 – 9.0000

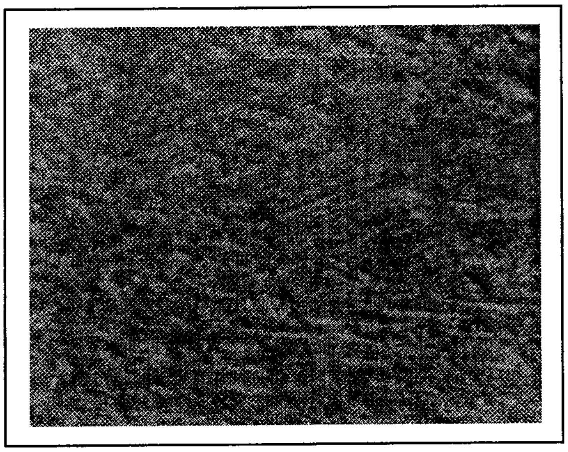

Fig. 2.2: Relief of a steel surface (magnified 200 times) [28]

Therefore, from the above discussion it may be concluded that *gaseous cavitation always initiates from a solid surface where gas-filled cavities are allowed to stabilize.*

2.3 CAVITY DEVELOPMENT

The second stage in gaseous cavitation evolution is *cavity development*. During this stage, Fig. 2.3, the occurring gas-filled cavities increase their dimensions as the pressure of the surrounding liquid decreases when either the temperature or the velocity increases.

The cavity size is controlled by the internal and external forces acting on it. In the beginning, cavity development is non-linear. Until the *first critical radius* is reached, the cavity is relatively stable and its size varies little as the pressure of the surrounding liquid decreases. However, when the pressure is sufficiently reduced and the cavity reaches its first critical size, the process becomes unstable and the cavity grows at a much faster rate [29].

The internal pressure of the cavity attempts to increase its size, while external liquid pressure and interfacial tension attempt to decrease cavity size.

A cavity grows on a solid surface until the contact line between the detached liquid and liquid still in contact with the solid interface reaches the locus of equilibrium between the tensile stress due to interfacial liquid tension and the pressure in the surrounding liquid [30]. When this equilibrium is broken in favour of the internal forces, the cavity detaches from the solid surface and begins to travel under the action of buoyancy force and eventual dynamic forces induced by flow.

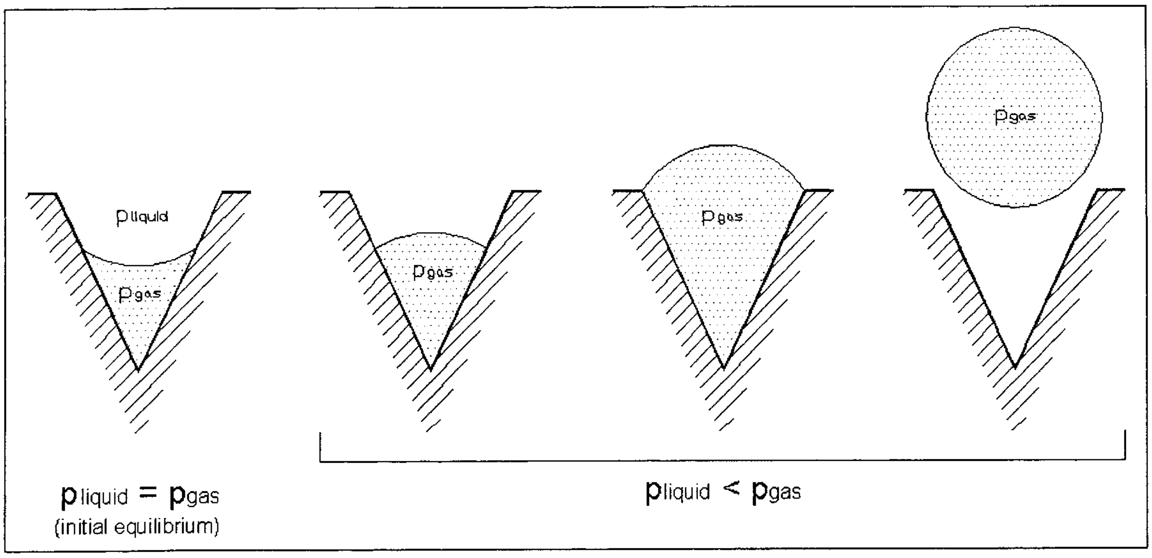

Fig. 2.3: Cavity development at solid interface [31, 32, 33]

A *travelling cavity* continues to grow if transported in a lower pressure region (higher temperature or higher velocity). The growth may be maintained until a *second critical radius* is reached, where the pressure inside the cavity is equal to the surface tension [34]. Although this event is not related to the cavitation process, it shall be mentioned that the cavity is not able to sustain any growth above this second critical radius and will eventually burst.

The shape of travelling cavities is not spherical since a non-uniform pressure field surrounds them as they experience motion. However, due to their relative small dimensions and to the fact that pressure variations around the cavities occur over relatively long time intervals which allows them to adapt, the scientific community agrees on assigning them a spherical shape under most circumstances. Also, beside the fact that a spherical shape shall simplify any desired computation at cavity level, it also maximizes the consequences of bubble explosion in terms of pressure, temperature, noise, or damage potential.

A non-spherical shape can diffuse the focus of the explosion and reduce the maximum velocities and temperatures that may result [35].

The phenomenon of complete cavity development can be easily observed in the common process of water heating. When water is heated in a container, it is noted that gas-filled bubbles first appear on the surface of the container although the temperature of this surface is the same as the liquid. The bubbles develop until the first critical size is reached. At this point, the bubbles detach from the solid surface and begin to travel under the action of buoyancy force. As the bubbles approach the liquid's free surface, the pressure in the medium decreases and the bubbles experience additional growth. Ultimately, the bubbles may burst in the liquid as they reach their critical dimensions under the effect of energy addition, or they may rupture at the liquid surface before attaining the critical dimensions. *Boiling* is a familiar term used to identify the process of cavity inception and cavity development until the bursting event occurs. Furthermore, it is observed that the boiling process may be produced either by static or dynamic means.

Another possibility for travelling cavities is to reach a higher pressure region (lower temperature or lower velocity) where they are suppressed before attaining the second critical radius. This corresponds to the last stage of cavitation and it also represents the most characteristic event of this process.

2.4 CAVITY SUPPRESSION

Cavity suppression is regarded as the most important stage of cavitation phenomenon since it encloses the majority of cavitation effects (erosion of material, vibrations, and noise). Although this stage made the object of extensive research, several aspects of this process are still not fully understood [36]. Therefore, the existing theory attempting to explain this stage is mostly based on experimental observations. However, the current study introduces known concepts and theories of physics in the attempt to complete the description of the cavity suppression stage.

Before proceeding with the description of this stage, it shall be mentioned that, in accordance with experimental observations, *only travelling cavities are involved in the suppression process* [37]. Also, it is important to recall that a spherical shape is assumed for the developed cavities entering the suppression stage.

The cavity suppression stage may be divided in three phases. During the first phase, the exposure of a travelling cavity to a sudden pressure increase produces the *implosion* (or *collapse*) of the cavity. Thus, the cavity experiences an *inward (or negative) acceleration* of volume decrease under the action of surrounding pressure. The shape of the cavity during this phase is assumed spherical despite the fact that a *non-uniform pressure field* compresses the cavity. However, since this phase occurs along a relatively long period of time when compared with the other cavitation stages, it is assumed that the cavity is able to adapt to these variations and adopt a spherical shape. Additionally, thermal effects associated with this first phase (heating of cavity and its surroundings) may safely be neglected [38].

The second phase of cavity suppression begins when the travelling cavity reaches the compressibility limit of its gaseous contents. At this moment, the non-uniform characteristic of the surrounding pressure becomes important as the cavity is no longer able to compensate for these variations. Consequently, the cavity deforms while maintaining its volume. The cavity deformation begins with the occurrence of a *dimple* at the surface of the cavity; the dimple is opposing the asymmetry that creates the local non-uniformity in the pressure field [38].

When the pressure acting on the cavity is further increased, the dimple develops and transforms into a *re-entrant stream* (or jet of liquid) that penetrates the cavity. The evolution of the re-entrant stream mechanism will be described later in greater detail as it represents an important event of the cavitation process. The second phase of cavity suppression ends when the re-entrant stream reaches the opposing cavity wall. Thermal effects during this phase shall also be considered minor and they may safely be neglected [39].

The last phase of the cavity suppression process is the *explosion* of the cavity. The cavity is constrained to adopt this action as it must release the amount of accumulated energy over the period of time imposed by the rapid pressure increase. This highly unstable phase of cavity suppression stage is characterized by an outward (or positive) acceleration of the cavity gaseous volume that increases in an explosive manner and is triggered when the re-entrant stream impacts the opposing cavity wall. The outcome is the cavity breakage into a series of smaller cavities that initially group together to form an agglomerate (or cloud) of cavitation bubbles. Subsequently, the resulting smaller cavities separate, while continuing to travel under the action of buoyancy force and eventual dynamic forces created by the flow of liquid. Next, the cavities may attain other lower pressure region where the development stage may resume.

The evolution of the cavity suppression stage can be observed in Fig. 2.4. Images 0 to 7 present the evolution of the implosion stage. Alternatively, images 8 to 13 show the development of the dimple and the re-entrant stream on the cavity. Finally, the last images present the explosion and breakage of the cavity.

As mentioned above, the cavity explosion is accompanied by a significant release of energy. During the development stage, the cavity accumulates potential energy by increasing the temperature and pressure levels of its contents. When the re-entrant stream impacts the opposing cavity wall, the explosion phase is initiated and the cavity releases its accumulated energy. Although the conditions of temperature and pressure inside the cavity that is about to break are not excessive, the sudden release of accumulated energy may generate relatively extreme temperatures and velocities [39].

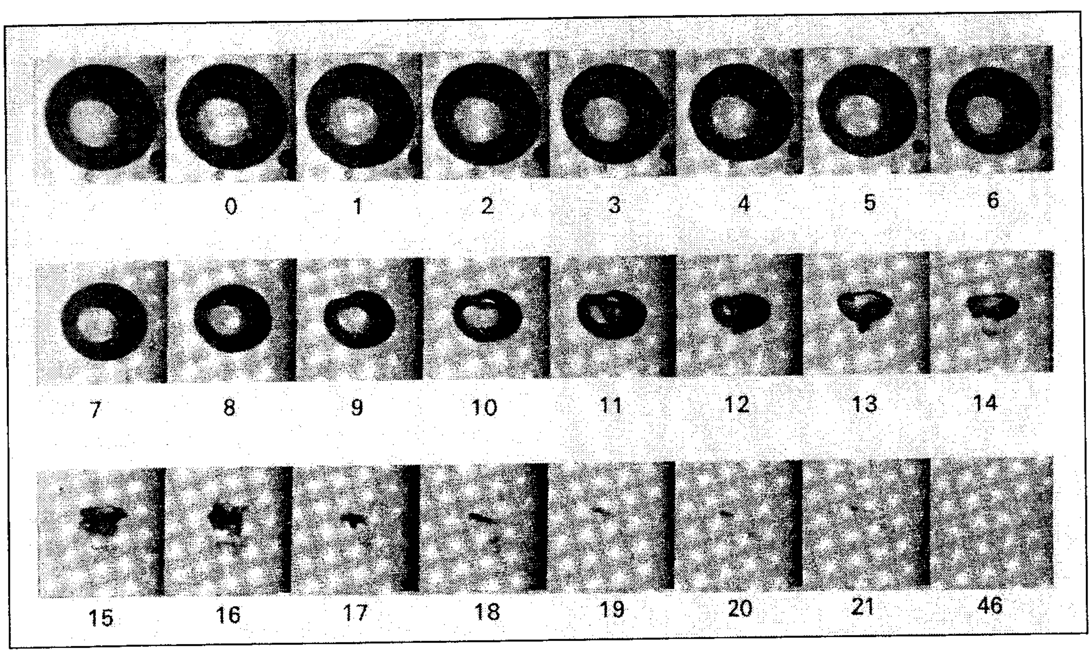

Fig. 2.4: Evolution of cavity suppression stage [40]

A cavity is suppressed when the difference between the pressure of the liquid medium outside the cavity and the pressure inside it reaches a critical value. This value is determined by both the elastic properties of cavity contents and surrounding medium, and by the capacity of the cavity contents to withstand compression before implosion takes place [41].

Thus, when pressure increases in a region where travelling cavities exist, the resulting internal forces elastically compress the liquid surrounding the cavities and their gaseous content. The liquid and gas media compress within specific limits given by their corresponding bulk moduli.

The liquid medium contained by a system (static or dynamic) is characterized by a *non-uniform pressure field*. The non-uniformity of the pressure field results from the interaction between the liquid medium and various system *asymmetries*, such as nearby *solid boundaries, proximity of other gas-filled cavities, and gravitational force* [42]. Consequently, higher pressure regions form and cavity implosion occurs at these locations.

Experimental observations determined that the duration of pressure variations around a cavity is extremely short (from 60 to 70 micro-seconds) [43]. Consequently, the cavity suppression time is also very short. The suppression time measured in most hydraulic components (pumps, valves, etc.) is about 100 pico-seconds [44].

As mentioned before, the cavity suppression stage produces the re-entrant stream mechanism and generates shock waves in the liquid. Since these events account for most of cavitation damage, they are presented below in greater detail.

2.4.1 Re-entrant Stream Mechanism

A re-entrant stream (Fig. 2.5 and Fig. 2.6) is produced when a cavity that has reached its compressibility limit is exposed to an additional pressure increase. The re-entrant stream penetrates the cavity and it is directed toward the asymmetry that created the local non-uniformity in the pressure field: nearby solid boundary, proximity of other cavities, or gravitational force.

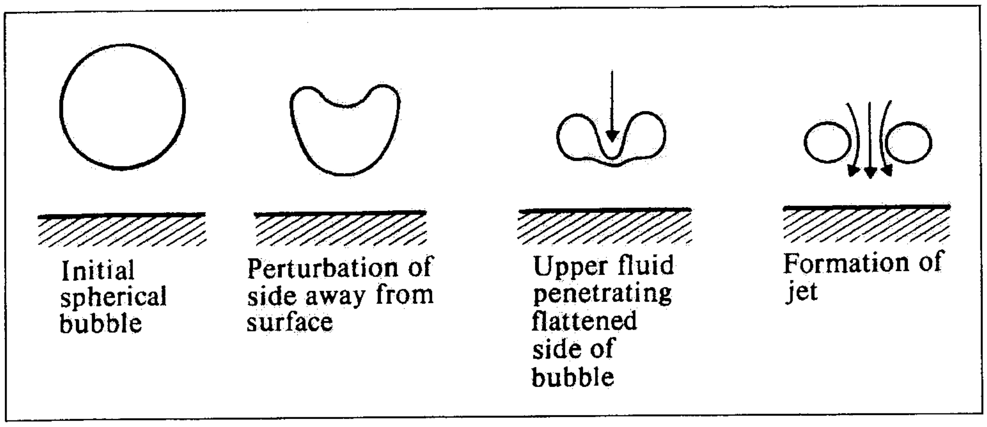

Fig. 2.5: Formation of re-entrant stream mechanism [45]

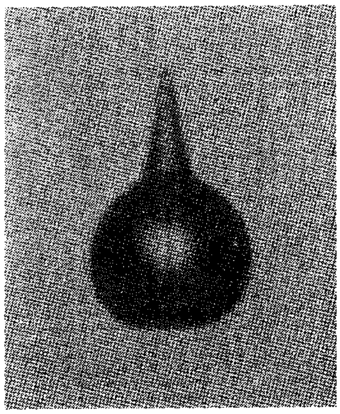

Fig. 2.6: Shape of a cavity at re-entrant stream phase [46]

The re-entrant stream action does not stop after it reached the opposing cavity wall and produced the cavity breakage, but it continues to propagate through the liquid, creating a shear layer between itself and the adjacent liquid [47]. Consequently, the re-entrant stream collides with neighbouring cavities and nearby solid surfaces.

When the re-entrant stream impacts other cavities, it penetrates and breaks them into a series of smaller cavities.

Of particular interest for cavitation damage is the impact of a re-entrant stream with a solid surface. Knowing that the re-entrant stream travels at speeds that can reach 1,000 to 1,200 m/sec [48], the damage produced by its energy of impact may be significant.

Although the re-entrant stream mechanism occurs over extremely short periods of time, its repetitive action may induce local surface fatigue and subsequent material erosion. A more detailed presentation of re-entrant stream effects is given in Chapter 4.

2.4.2 Shock Wave

The volume of a travelling cavity is reduced when the cavity is exposed to a surrounding pressure exceeding its internal pressure. During this compression process, the potential energy accumulated by the cavity "concentrates" through an increase of temperature and pressure of the cavity contents.

The cavity reaches its compressibility limit when the accumulated energy cannot be "concentrated" any further. If the surrounding pressure continues to increase beyond this point, the cavity breaks and releases its accumulated energy. This energy is released over a short time period as temperature and velocity increases. Consequently, the energy level of the liquid around the imploded cavity rises rapidly, creating a *compressive shock wave.* The shock wave propagates spherically in the liquid (see Fig. 2.7) and dissipates the temperature and pressure accumulated by the cavity [49, 50, 51].

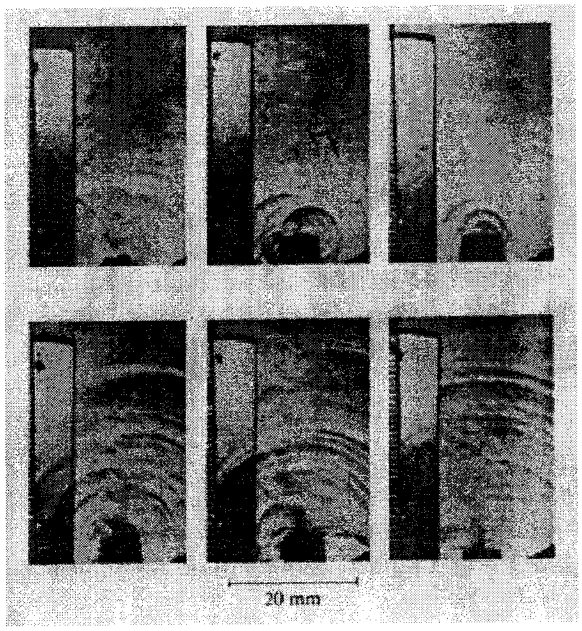

Fig. 2.7: Photograph of a spherical shock wave propagation in a liquid medium emanating from a single cavity explosion [52]

When a shock wave strikes a solid surface, it bounces back, producing a *reflected wave.* Furthermore, the reflected wave may combine with other shock waves and amplify the cavitation effects at that surface [49, 50, 51].

Theoretical analyses determined that, at the time of its formation, the shock wave travels at supersonic speeds (3-4 times the speed of sound in the given liquid medium). As it moves through the liquid, the shock wave decelerates and ultimately stabilizes at the speed of sound [49, 50, 51].

At this point it is important to recall that the re-entrant stream that is created during the second phase of cavity suppression stage travels at much lower speeds. Since the re-entrant stream continues to propagate through the liquid after the cavity breakage, the re-entrant stream has the possibility to be accelerated by the shock wave generated by the cavity explosion and the effects of the re-entrant stream are therefore amplified.

Cavity implosion generates extreme local conditions of temperature and pressure. Since these conditions are difficult to measure due to the short duration of the implosion process, theoretical calculations determined that the contents of a cavity during the first moments of implosion may reach temperatures as high 10,000 °C and pressures of 4,000 atm (~59 Kpsi) [53]. These conditions are transferred to the shock wave and ultimately to solid surfaces adjacent to the imploded cavity. Experimental measurements determined that, when a cavity implodes close to a surface, the surface may be locally exposed to a temperature rise of over 1,000 °C and a pressure shock of over 100 atm (~1,500 psi) [53, 54]. A detailed description of the shock wave effects is presented in Chapter 4.

Finally, the cavitation suppression stage produces a second shock wave. Since the first shock wave creates a vacuum at the cavity implosion site, liquid is absorbed toward this location. This event creates a much smaller *suction shock wave* that has negligible consequences.

CHAPTER 3

FACTORS INFLUENCING GASEOUS CAVITATION IN HYDRAULIC SYSTEMS

CHAPTER 3

FACTORS INFLUENCING GASEOUS CAVITATION IN HYDRAULIC SYSTEMS

3.1 INTRODUCTION

The gaseous cavitation process may be produced either by *static* or *dynamic* means and it may occur in either *open or closed systems*. In an *open system*, the liquid medium is characterized by a free surface which is usually exposed to atmospheric pressure, whereas in a *closed system* the liquid medium is isolated from the atmosphere and the system exposes it to superior pressures. A closed system involving liquid is also known as a *hydraulic system*.

As it was mentioned in Chapter 1, the static means that influence the gaseous cavitation process in either open or hydraulic systems are represented by *variations of temperature* in the liquid medium, whereas the dynamic means are represented by *variations of velocity*.

Although the occurrence of gaseous cavitation in an open system may make the subject of a similar presentation, the discussion in this study is voluntary limited to the occurrence of gaseous cavitation in a hydraulic system.

The factors influencing the occurrence of gaseous cavitation in a hydraulic system are associated with the solid, liquid, and gaseous media involved in the process. Therefore, these factors are organized in the following groups:

- *Factors associated with hydraulic system condition*;
- *Factors associated with gas condition*; and
- *Factors associated with liquid condition.*

3.2 FACTORS ASSOCIATED WITH HYDRAULIC SYSTEM CONDITION

A hydraulic system includes various hydraulic components: pumps, valves, lines, reservoirs, filters, etc. The first factor related to the condition of such a system is represented by its *operating conditions*. The operating conditions of a hydraulic system correspond to the intervals of temperature, flow velocities, and internal pressures at which its components function. Ideally, these conditions must foresee the avoidance of gaseous cavitation. However, in practical applications, due to reasons of output characteristics and space, the operating conditions are often exceeded and the gaseous cavitation phenomenon occurs more often than desired.

The second factor associated with the hydraulic system condition corresponds to the *quality of surfaces coming in contact with the liquid medium*. Thus, as it was previously stated, microscopic *crevices* present on the solid surface may harbour minute quantities of gas when submerged by liquid. These *attached gas-filled cavities*, which contaminate the liquid medium, initiate the gaseous cavitation process [24, 55].

The last factor related to the condition of a hydraulic system is represented by its *design*. This aspect may be divided in three distinctive parts. First, the design or, more specifically, the configuration of the system's boundaries, influences the temperature and/or velocity fields of the enclosed liquid medium. Consequently, the pressure field of the liquid medium is affected by the hydraulic system's design. As it was previously seen, the resulting pressure variations affect the development and suppression stages of cavitation process.

Second, the design of the system may allow the *entrapment of gas*. This gas, which differs from the gas trapped in the surface crevices, may either be a *requirement for the functioning of some hydraulic components* (reservoirs, valves, etc.) or it may result from *poor design of hydraulic components*. Under both circumstances, when the liquid-gas interface becomes sufficiently agitated, the gas may get entrained by the liquid medium, generating gaseous cavitation in the hydraulic system [56].

Finally, the system design may lead to the presence of *leakage (internal or external)*. Leakage in a hydraulic system results from inadequate tolerancing of hydraulic components or from excessive wear. Thus, leakage exposes the hydraulic system to at least one different pressure, and subsequently, it exposes the liquid medium to *gas ingestion*. As a result, leakage in a hydraulic system may also lead to the production of gaseous cavitation [57].

3.3 FACTORS ASSOCIATED WITH GAS CONDITION

The other group of factors that influences the occurrence of gaseous cavitation in a hydraulic system is assigned to the *gas condition* involved in the process. The only factor present in this group corresponds to the *nature of gas* implicated. The nature of any substance is associated with its level of intermolecular forces and establishes the physical characteristics of the substance at a given set of environmental conditions. Thus, the level of intermolecular forces for the gas-filled cavities present in the liquid environment affects their density, and consequently, their speed of development, their dimensions, and the explosion intensity.

In addition, the nature of the gas contained by the cavities may also produce *chemical reactions with the prevalent liquid medium and the system boundaries* [58]. This event may generate a series of reaction products (i.e., *lower-density* elements or compounds) that may contribute to the development stage of the cavities or increase the cavitation effects.

3.4 FACTORS ASSOCIATED WITH LIQUID CONDITION

The last group of factors influencing the occurrence and development of gaseous cavitation in a hydraulic system is *the condition of prevalent liquid medium*. As in the case of gaseous substance condition, the first factor included in this group corresponds to the *nature of liquid* involved in the process. The nature of liquid is determined by the intermolecular forces that affect its density, viscosity, bulk modulus, and surface tension. As a result, the nature of liquid influences the number of gas-filled cavities, their speed of development, their dimensions, the cavity suppression stage, and the effects produced.

Moreover, *chemical reactions between the liquid medium* and the solid surfaces may affect the evolution of gaseous cavitation process through the formation of lower-density elements or compounds and the corrosion of surfaces. The corrosion process may increase the number of crevices where additional gas quantities may be trapped [59].

The last factor assigned to the condition of prevalent liquid medium corresponds to the *presence of solid contaminants (or impurities) in the liquid*. Although this may be regarded as a minor factor, solid contaminants increase the overall temperature of the liquid medium by increasing its capacity to absorb and store heat. Thus, gaseous cavitation may occur more often and at other locations in a liquid medium that contains solid contaminants [60].

Furthermore, in a dynamic system, the abrasive action exerted by the impurities may increase the number of crevices in the bounding surfaces, and therefore, increase the number of locations from where gaseous cavitation may originate.

To resume this chapter, the factors that influence the occurrence and development of gaseous cavitation in a hydraulic system are presented in the table below:

Table 3.1: Factors influencing the occurrence and development of gaseous cavitation in a hydraulic system

Factors associated with Hydraulic System Condition	**Factors associated with Gas Condition**	**Factors associated with Liquid Condition**
- Operating conditions - Quality of surfaces coming in contact with the liquid medium - Design	- Nature of gas	- Nature of liquid - Solid contaminants

CHAPTER 4

EFFECTS OF GASEOUS CAVITATION IN HYDRAULIC SYSTEMS

CHAPTER 4

EFFECTS OF GASEOUS CAVITATION IN HYDRAULIC SYSTEMS

4.1 INTRODUCTION

Cavitation process is important as a consequence of its effects. These effects include the *alteration of pressure field exhibited by the liquid medium*, *lessening of forces applied to the liquid medium by any solid surface of the system and vice-versa*, *damage to the boundaries enclosing the liquid medium*, as well as some other *extraneous effects* (chemical reactions, vibration, noise, and luminescence) [61].

Since the effects of cavitation in hydraulic systems occur during all stages that form this process, they are organized in the following groups:

- *Effects associated with the inception stage*;
- *Effects associated with the development stage*; and
- *Effects associated with the suppression stage.*

4.2 EFFECTS ASSOCIATED WITH THE INCEPTION STAGE

During the inception stage, the presence of gas-filled cavities in either static or dynamic hydraulic systems may *disturb the continuity of the pressure field* exhibited by the liquid medium. Furthermore, the occurrence of cavities in a dynamic system may *alter the hydrodynamic characteristics of the liquid's flow*, which may produce or amplify the unsteadiness of this flow [62]. Consequently, *vibrations* may be introduced in the system. However, the level of these vibrations is relatively low and their effects may safely be neglected.

In addition, the occurrence of attached gas-filled cavities in either static or dynamic hydraulic systems reduces the *contact area* between the liquid medium and the system's boundaries, as well as the *bulk modulus* of the liquid medium. This effect is more significant in dynamic systems, where the reduced contact area and the reduced bulk modulus may affect the forces applied to the liquid medium by any solid surface of the system and vice-versa. Thus, a dynamic system may experience a *drop in efficiency and performance*, as well as an *increase of the head loss* [62, 63].

Finally, in either static or dynamic hydraulic systems, the presence of gas-filled cavities attached to the system's boundaries may *produce or accelerate chemical reactions* between the gas contained by the cavities, the liquid medium, and the solid surfaces. This may either induce or enhance the *oxidation or corrosion process* of these surfaces, or may cause other *chemical reactions that degrade the liquid medium* and/or produce *gaseous reactions products that increase the importance of gaseous cavitation* [64].

4.3 EFFECTS ASSOCIATED WITH THE DEVELOPMENT STAGE

As stated before, a cavity detaches from a solid surface when its internal pressure level exceeds the pressure level of the surrounding liquid. Subsequently, the gas-filled cavity starts to travel under the action of buoyancy force and eventual dynamic forces induced by any occurring flow.

The presence of travelling cavities in either static or dynamic hydraulic systems produces effects similar to those presented for the inception stage. Thus, the travelling cavities may *disturb the continuity of the pressure field* exhibited by the liquid medium. Furthermore, the occurrence of travelling cavities in a dynamic system may *alter the hydrodynamic characteristics of the liquid's flow*, which may produce or amplify the unsteadiness of this flow [62]. Consequently, *vibrations* may be introduced in the system. However, as before, the level of these vibrations is relatively low and their effects may safely be neglected.

In addition, the occurrence of developed travelling cavities in either static or dynamic hydraulic systems may reduce the *bulk modulus* of the liquid medium. This effect is more significant in dynamic systems, where this reduction may affect the magnitude of forces applied to the liquid medium by any solid surface of the system and vice-versa. Thus, a dynamic system may experience a *drop in efficiency and performance*, as well as an *increase of the head loss* [62, 63].

Finally, the presence of travelling cavities in either static or dynamic hydraulic systems may *produce or accelerate chemical reactions* between the gas contained by the cavities and the liquid medium. This may cause the *degradation of the liquid* medium, which may subsequently induce or enhance the *oxidation or corrosion process* of the system boundaries. Furthermore, the occurring reactions may produce *gaseous reactions products that increase the importance of gaseous cavitation* [64].

4.4 EFFECTS ASSOCIATED WITH THE SUPPRESSION STAGE

The effects associated with the suppression of gas-filled cavities in a liquid medium are the most significant of cavitation and represent the principal feature by which this process is most commonly recognized.

As presented before, the cavity suppression stage may be divided in three distinctive phases: *implosion* (or *collapse*) *of cavities*, *creation of the re-entrant stream mechanism*, and *explosion of cavities*. The effects associated with these phases include all the ones presented for the inception and development stages. However, an additional *direct damage effect* [65] induced by the explosion of gas-filled cavities and specific to this stage shall be introduced. Although most of these effects are common to all phases, some exceptions exist; these exceptions will be emphasized below as the effects associated with the suppression stage are presented.

During the phases of implosion and creation of the re-entrant stream mechanism, gas-filled cavities subsist in the liquid medium. In either static or dynamic hydraulic systems, this presence may *disturb the continuity of the pressure field* exhibited by the liquid medium. Furthermore, the presence of gas-filled cavities in a dynamic system may *alter the hydrodynamic characteristics of the liquid's flow*, which may *produce or amplify the unsteadiness of this flow* [62]. Consequently, *vibrations* may be introduced in the system. However, once again, the level of these vibrations is relatively low and their effects may be safely neglected.

On the other hand, in either static or dynamic hydraulic systems, the explosion of gas-filled cavities during the last phase of cavity suppression process generates *significant disturbances in the pressure field* exhibited by the liquid medium. The *shock waves* produced by these explosions propagate spherically into the liquid and may significantly affect the pressure field through the resulting increases in velocity and temperature. In the case of dynamic systems, the created disturbances *alter the hydrodynamic characteristics of the liquid's flow*, which may *produce or considerably amplify the unsteadiness of this flow* [62].

Furthermore, the occurrence of gas-filled cavities during the phases of implosion and creation of the re-entrant stream mechanism may reduce the *bulk modulus* of the liquid medium. This effect is more significant in dynamic systems, where this reduction may affect the magnitude of forces applied to the liquid medium by any solid surface of the system and vice-versa. Thus, a dynamic system may experience a *drop in efficiency and performance*, as well as an *increase of the head loss* [62, 63]. In contrast, in either static or dynamic systems, the explosion of gas-filled cavities during the last phase may *increase the magnitude of forces* applied by the liquid medium to any solid surface of the system and vice-versa. Also, during the explosion phase, the head loss associated with a cavitating system may experience a noticeable increase.

As stated before, the *mechanical damage directly induced by cavitation* to the system boundaries represents the most important effect associated with this process [65, 66]. *Direct damage* is produced during the cavity explosion phase. Thus, the explosion of a cavity produces one main shock wave that propagates spherically in the liquid medium and dissipates the energy accumulated by the cavity. When the shock wave strikes a solid surface, most of its energy is transferred to the surface as *pressure and heat*. Experimental measurements determined that such a shock wave may expose a surface to a localized pressure pulse of over 100 atm (~1,500 psi) and a temperature rise of over 1,000 °C [53, 54]. The eventual repetitive impact, as well as the cyclical *heating by the shock wave* and *cooling of the solid surface by the liquid medium* may *increase the surface hardness*. Consequently, *fatigue* may be induced into the solid surface, generating cracks and producing *material erosion* [67, 68].

Direct mechanical damage may also be produced by the *combined action of re-entrant stream mechanism and shock wave* [53]. As it was previously described, a re-entrant steam is created when a cavity which has reached its compressibility limit is exposed to an additional pressure increase. The re-entrant stream penetrates the cavity and it is directed toward the asymmetry that created the local non-uniformity in the pressure field. Most commonly, this asymmetry is represented by a *solid boundary*. The re-entrant stream action does not stop after it reached the opposing cavity wall and produced the cavity explosion, but it continues to propagate through the liquid, creating a *shear layer* between itself and the adjacent liquid. However, the spherical shock wave created by the cavity explosion travels faster than the re-entrant stream. Thus, the *re-entrant stream is accelerated* and *its action is amplified by the shock wave*. Moreover, since the shock wave travels faster than the re-entrant stream, the re-entrant stream reaches the solid boundary after the shock wave action. Consequently, the *re-entrant stream effect is intensified* as the solid boundary is already under the influence of pressure and heat increases produced by the shock wave [69]. The action of re-entrant stream mechanism on a solid surface produces characteristic *surface pits* that vary in depth and configuration as the process progresses. During the initial stages of attack, *shallow pits* form. As the attack continues, the pits may develop into deep *"worm-hole" pits* [70, 71]. Figure 4.1 illustrates the appearance of a solid surface affected by *cavitation pitting*, while Figure 4.2 depicts a solid surface severely affected by *cavitation erosion* [72].

Fig. 4.1: Pitting of a steel surface [70]

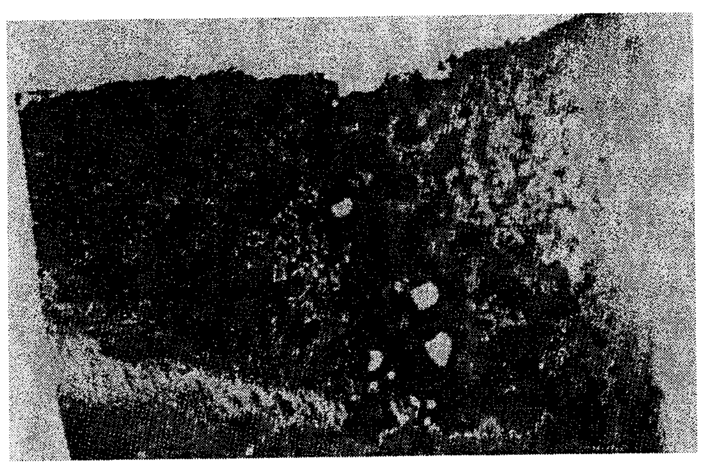

Fig. 4.2: Erosion of a stainless-steel impeller [72]

Therefore, as per the presentation presented above, the cavitation process may induce direct mechanical damage to the hydraulic system in which it occurs. This damage may affect the *integrity* and *strength* of a component or system, and produce *leakage*. The occurring leakage may introduce additional quantities of gas into the system (*gas ingestion*) [73], reducing the efficiency of the system [62, 63] and increasing the importance of gaseous cavitation [64].

Extraneous effects are the last effects associated with the suppression stage. As stated before, the presence of gas-filled cavities during the phases of implosion and creation of the re-entrant stream mechanism may *produce or accelerate chemical reactions* between the gas contained by the cavities and the liquid medium. This may cause the *degradation of the liquid medium*. Furthermore, the occurring reactions may produce *gaseous reactions products that increase the importance of gaseous cavitation* [64]. In addition, the *important temperatures and pressures generated during the explosion phase* may significantly increase the speed of any occurring chemical reaction. Consequently, the speeds at which the liquid medium may degrade, as well as any chemical reaction of oxidation, nitration, or carbonisation are increased.

Furthermore, the explosion of gas-filled cavities during the last phase of suppression may induce *significant vibrations* and *noise* into the hydraulic system. Hence, important *material damage* and *component fatigue* may be generated if one or more frequencies of vibration match the natural frequency of a component of the system [74].

In addition, the extreme conditions created by cavity explosion may also generate *cavity luminescence*. Cavity luminescence is a rather simple but fascinating phenomenon produced by the *high temperatures* that *heat up the matter at the explosion site* [75]. Hence, the temperature conditions excite the molecules in gaseous state, which relax through the release of photons [76]. Moreover, in inflammable liquid media, the high temperatures may cause *local ignition*; this phenomenon, also known as *dieseling* (terminology borrowed from the known phenomenon of ignition and explosion of liquid-gas mixtures in prevalent gaseous media), causes blackening of the liquid medium due to the creation of carbon deposits. However, cavity luminescence phenomenon is rarely encountered in practical applications as it involves extreme conditions of temperature and/or velocity. Figure 4.3 below illustrates the cavity luminescence phenomenon as created in a controlled experimental set-up. Here, light is generated by a small air-filled cavity within a prevalent water medium under the application of high frequency sound waves.

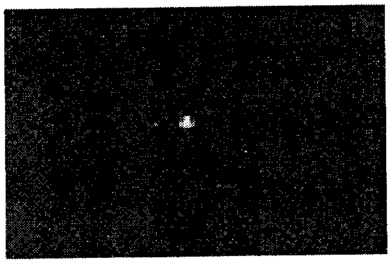

Fig. 4.3: Cavity luminescence phenomenon [77]

Finally, in order to summarize the effects associated with the cavitation phenomenon in hydraulic systems, the table below is presented:

Table 4.1: Effects of cavitation on hydraulic systems

	Inception	**Development**	**Suppression**
Disturbance of pressure field	- Minor vibrations; - Unsteady flow.	- Minor vibrations; - Unsteady flow.	- Implosion and creation of re-entrant stream mechanism phases: minor vibrations, unsteady flow; - Explosion phase: major vibrations, highly unsteady flow.
Lessening of forces applied to liquid medium by any solid surface of the system and vice-versa	- Drop in efficiency and performance; - Increase of Head Loss.	- Drop in efficiency and performance; - Increase of Head Loss.	- Implosion and creation of re-entrant stream mechanism phases: drop in efficiency and performance, increase of Head Loss; - Explosion phase: rise in efficiency and performance, decrease of Head Loss.
Damage	–	–	- Hardening of solid surface, fatigue, pitting, erosion, leakage.
Extraneous	- Chemical reactions.	- Chemical reactions.	- Chemical reactions, major vibrations, noise, luminescence

CHAPTER 5

CAVITATION IN PUMPS

CHAPTER 5

CAVITATION IN PUMPS

5.1 INTRODUCTION

A hydraulic system is composed of various hydraulic components: pumps, valves, lines, reservoirs, filters, etc. Although the cavitation process may be encountered in any of these hydraulic devices, this study is principally concerned with the occurrence of gaseous cavitation in pumps.

A pump is a device that converts mechanical power into hydraulic power. The source of mechanical power may be a combustion engine, an electric motor, or any other mechanical device that can impart force and motion to operate the pump [78, 79].

Pumps may be classified in two categories:

- *Dynamic* (or *Non-Positive Displacement*) *pumps*, and
- *Static* (or *Positive Displacement*) *pumps* [80, 81].

Dynamic pumps, Fig. 5.1, are used for low-pressure and high-volume flow applications. Most dynamic pumps operate by centrifugal force whereby liquids entering the center of the pump housing are projected to the outside by means of an impeller. The output pressure of a dynamic pump is increased when the speed of its impeller is increased. However, the design characteristics of this type of pump make its *discharge pressure dependent of the inlet pressure*. Due to the low discharge pressure, the dynamic pumps are not suited for actuation systems but are typically used for the transfer of fluids [82, 83].

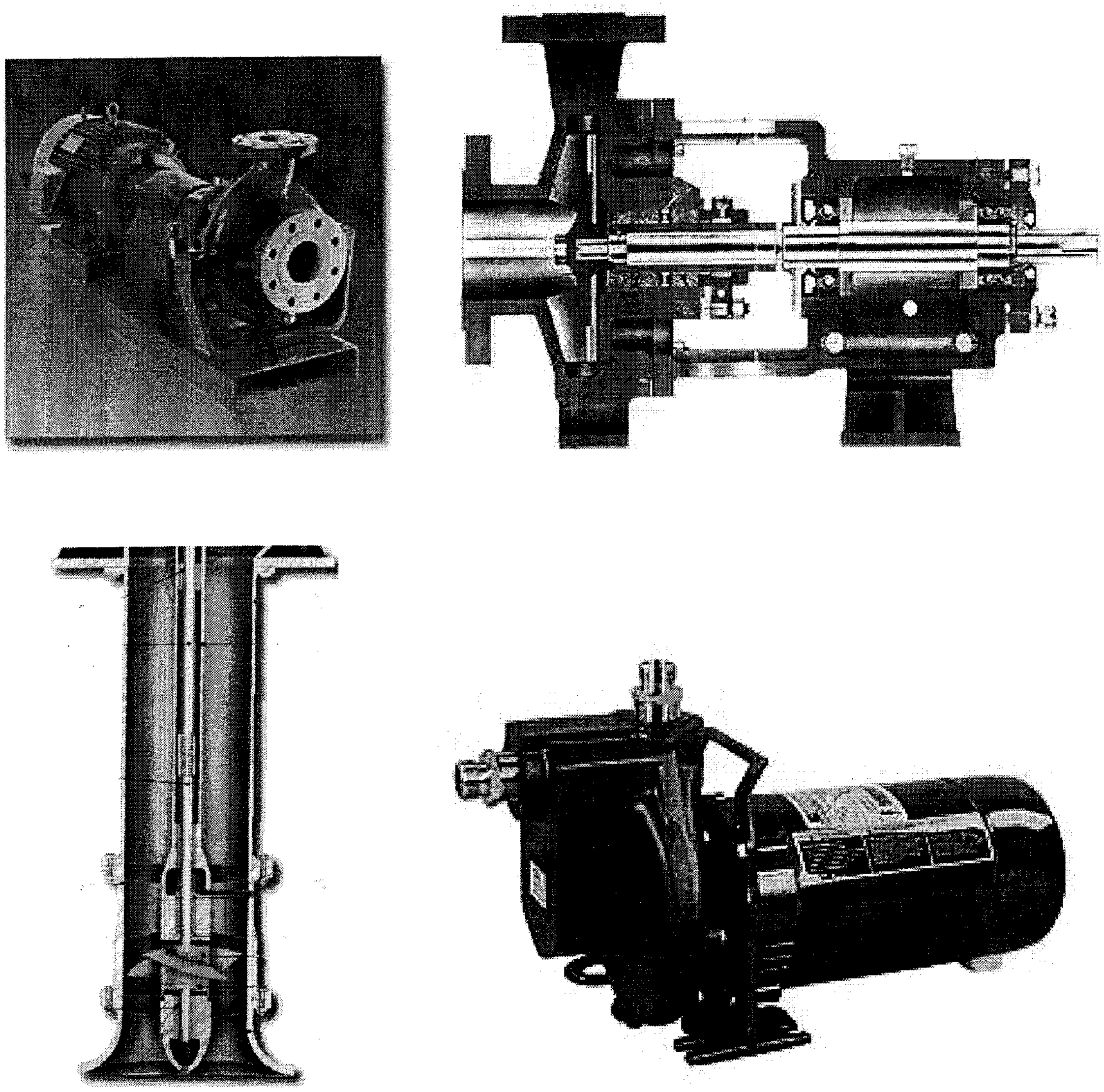

Fig. 5.1: Examples of industrial dynamic pumps [84]

Static pumps, Fig. 5.2, are designed to transmit hydraulic power since their *discharge pressure is independent of the inlet pressure*. As a result, static pumps are principally employed in actuation systems. Most static pumps are piston-type designs (radial, axial, or reciprocating plunger) and they operate by converting the rotary motion of the drive shaft into reciprocating piston motion. Hence, the pump provides a definite amount of fluid to the hydraulic system for each revolution of the drive shaft.

Static pumps may be further classified in two categories: *fixed displacement* and *variable displacement*. A fixed displacement static pump provides an unchanging volume displacement per revolution. A variable displacement pump is a device in which the displacement per cycle can be mechanically varied; pumps of this design provide variable volume from zero to the maximum volumetric capacity [82, 83].

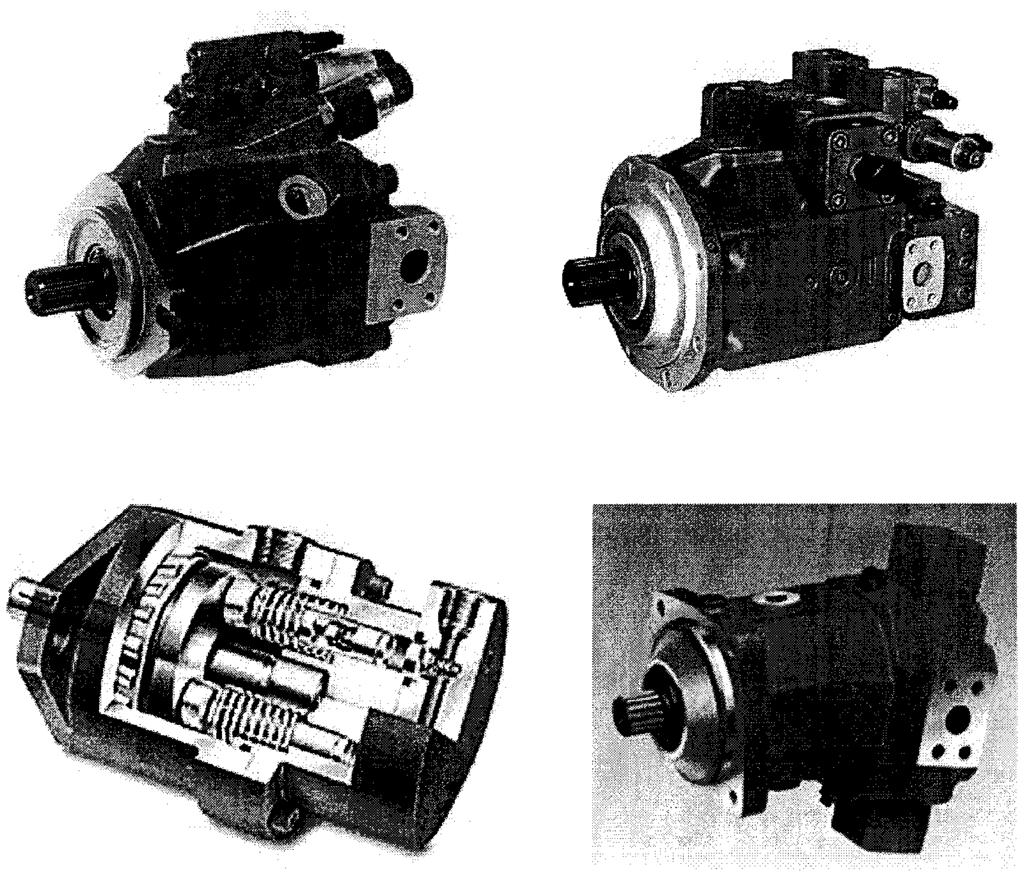

Fig. 5.2: Examples of industrial static pumps [84]

Both types of pumps, *static* and *dynamic*, are reversible units. This means that they may either be used as pumps to convert mechanical power into hydraulic power, or as turbines (static) / hydraulic motors (dynamic) to convert hydraulic power into mechanical power.

The axial piston pump with variable displacement is extensively employed in the aviation industry as source of hydraulic power dedicated to operate various heavy actuation systems of the aircraft: flight controls, nose and main landing gear actuation, nose wheel steering, and thrust reverser system.

Because the cavitation phenomenon is relatively frequent within the hydraulic power system of the aircraft, the scope of study is voluntarily limited to the analysis of cavitation occurrence in variable displacement axial piston pumps.

This analysis is determined by a real necessity: the reliability of the AC Motor Pump 3A from the hydraulic system #3 of the *XYZ* aircraft is continuously penalized by the effects of cavitation.

For better understanding of the pump functioning in the context of aircraft operation, a brief description of hydraulic power system of this aircraft is included below.

5.2 AIRCRAFT HYDRAULIC POWER SYSTEM

Typically, on an aircraft there are three independent hydraulic systems that ensure the actuation redundancy necessary to meet the safety requirements.

The hydraulic power system of an aircraft performs the following functions:

- Generates the hydraulic power under required flow and pressure characteristics;
- Supplies the hydraulic power to users;
- Conditions the hydraulic fluid for the established temperature range and cleanliness level;

- Controls the system parameters (flow rate, pressure limits, temperature range, etc.) during operation of users;
- Protects the system from high and low pressure, high and low temperature, and fluid contamination.

The block diagram showing the distribution of users on each hydraulic system of the *XYZ* aircraft is presented in Fig. 5.3 below.

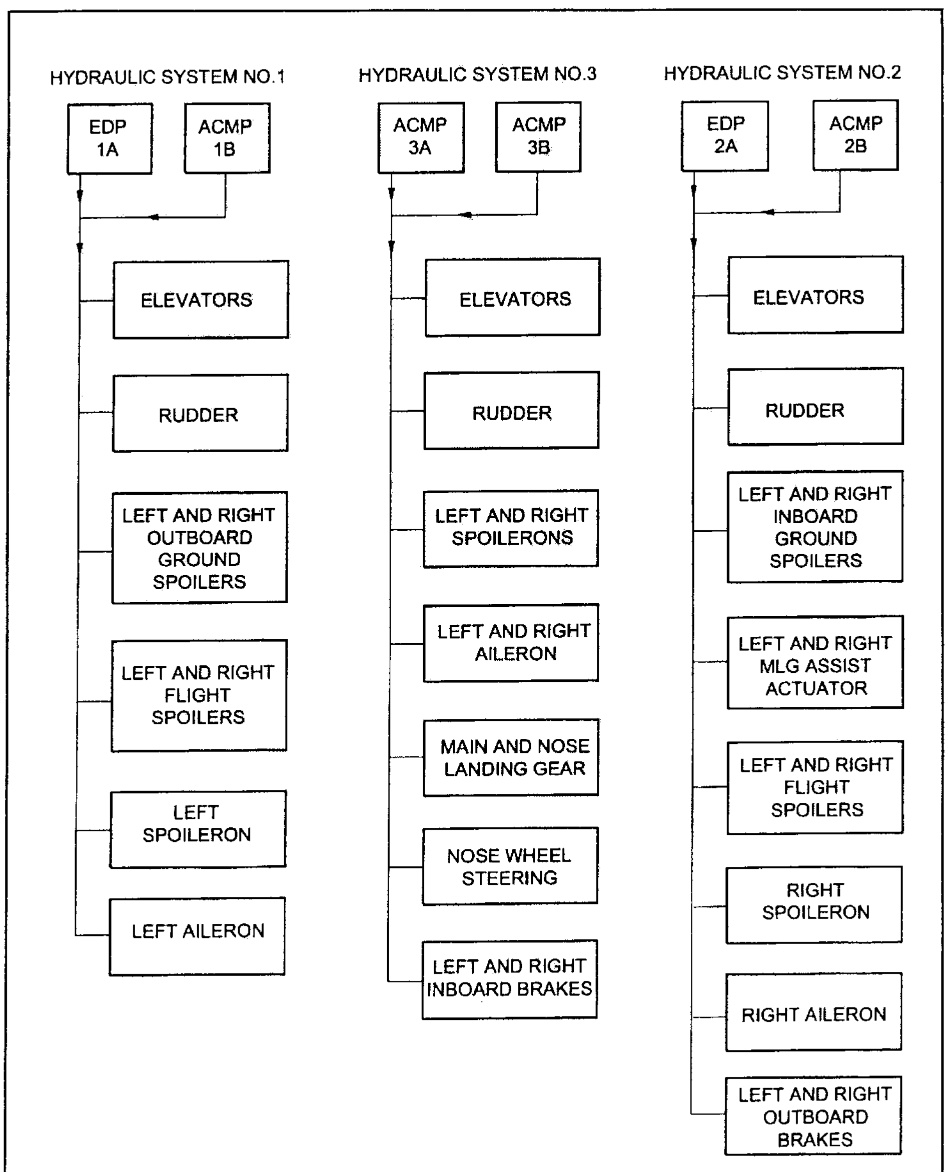

Fig. 5.3: Hydraulic power system distribution on the *XYZ* aircraft

The block diagram in Fig. 5.3 was conceived using the following criteria:

- *Redundancy* of the hydraulic power supply for the major actuation systems of the aircraft (flight control, landing gear, brakes, and thrust reversers);
- *Optimization* of flow capacity for each hydraulic system as a function of flow demand required by the users for all ground and flight phases.

There are several reasons for using hydraulic power actuation on the aircraft:

- Low ratio of weight vs. power for all hydraulic components;
- High efficiency (85-87%) for hydraulic power generation;
- High efficiency (90-95%) of components used to convert the hydraulic power into mechanical power for the actuation of power assisted systems;
- No impact / no interference on the adjacent systems sharing the same location / environment, other than eventual chemical effects of hydraulic fluid caused by external leakage;
- Heat rejection resulting from hydraulic system operation is dissipated within the hydraulic circuits, with no significant impact on the other aircraft systems.

At the actual development standard of the aviation industry, there is no other source of power for the actuation systems that can offer more advantages, in spite of the efforts deployed by some specialized companies to replace hydraulic power actuation by electrical actuation.

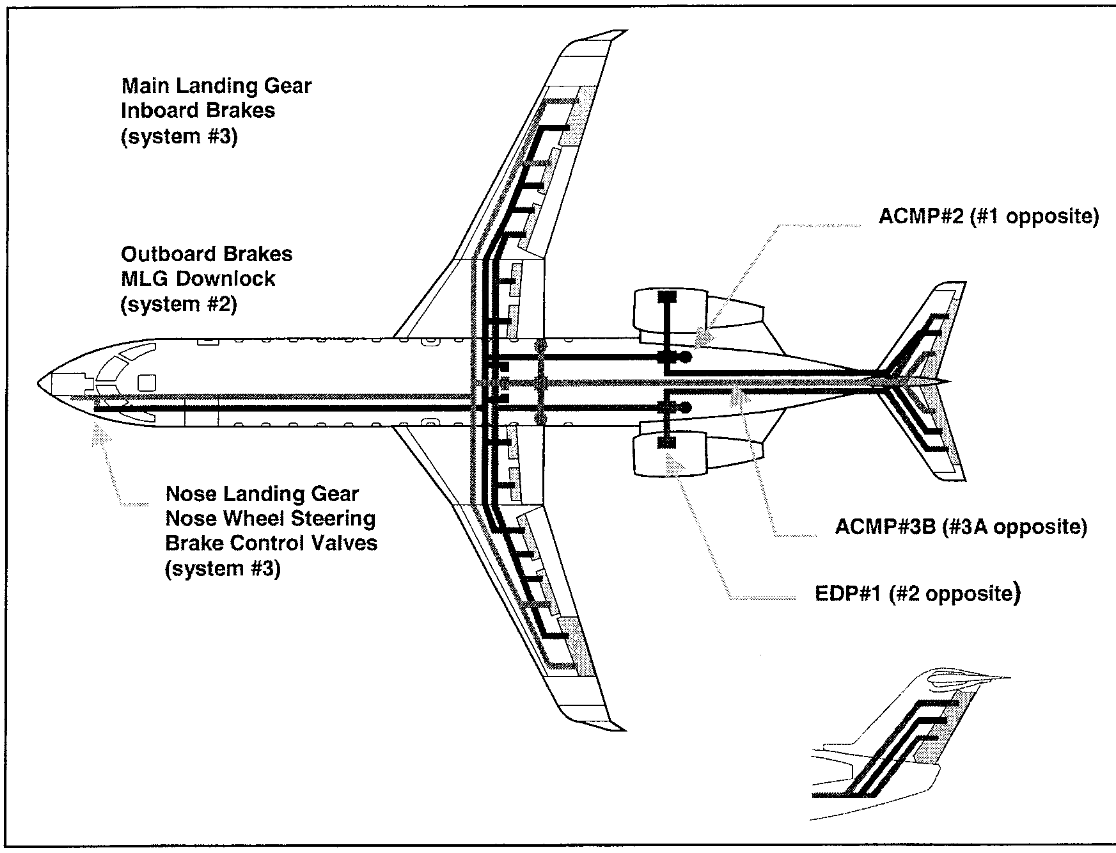

Fig. 5.4: Hydraulic systems location on the *XYZ* aircraft

The three hydraulic systems installed on the aircraft are completely separated units. They are located such that they ensure the *survivability* of the hydraulic circuits in case of foreseeable failures: engine rotor burst, tire burst, or wheel rim release.

The hydraulic systems #1 and #2 have the same architecture. This architecture is presented in Fig. 5.5 below.

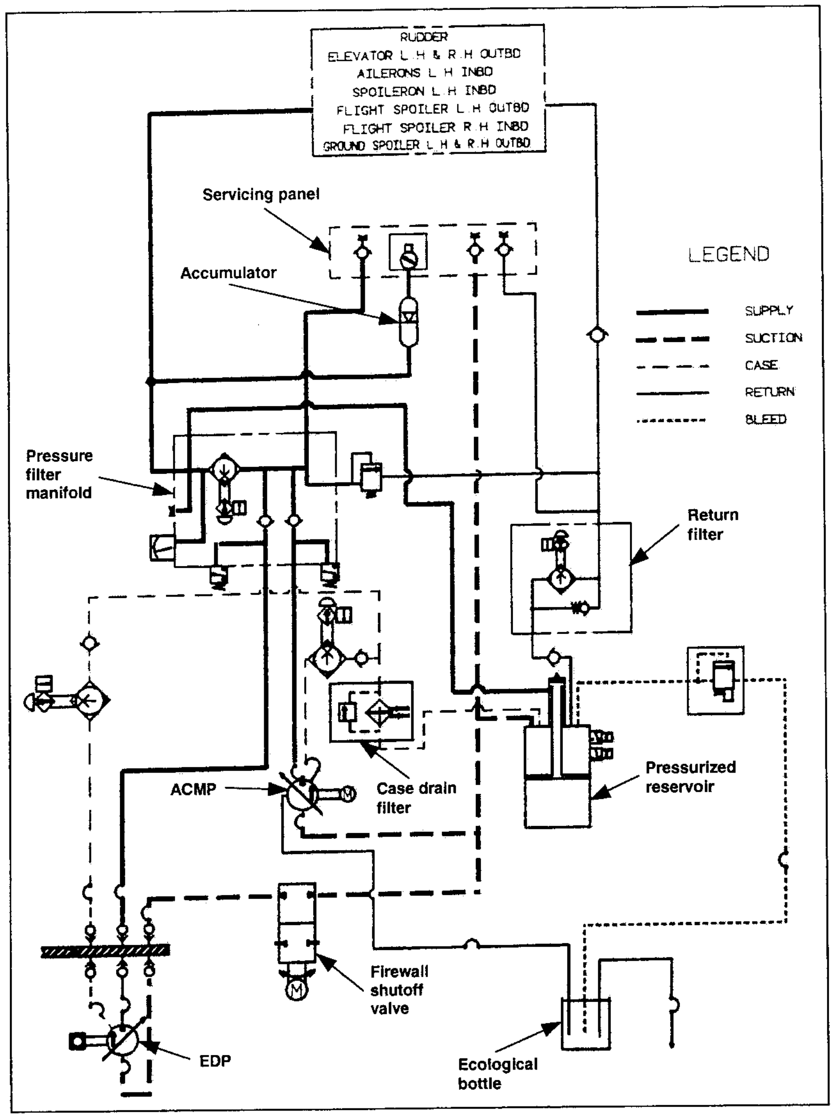

Fig. 5.5: Hydraulic Systems #1 and #2 – Architecture

Systems #1 and #2 are also identified as *Main systems*, while system #3 is referred to as the *Auxiliary system* since it is only used in the event of dual engine failure. For this reason, the distribution of users between the three systems is different: at systems #1 and #2 are connected all users that ensure the aircraft operation in normal conditions, while at system #3 are connected only the users that ensure the aircraft operation in emergency conditions. Therefore, the flow capacity of systems #1 and #2 is higher then the flow capacity of system #3.

Systems #1 and #2 are each powered by one Engine Driven Pump (EDP), which is backed up during flight phases with high flow demand by a single AC Motor Pump (ACMP). The ACMP is also used for ground maintenance of the hydraulic system.

For redundancy reasons, each hydraulic system ACMP is powered by the electrical AC bus supplied by the generator installed on the opposite engine (Fig. 5.6). Thus, the functioning of both hydraulic systems #1 and #2 is ensured in case of one engine failure.

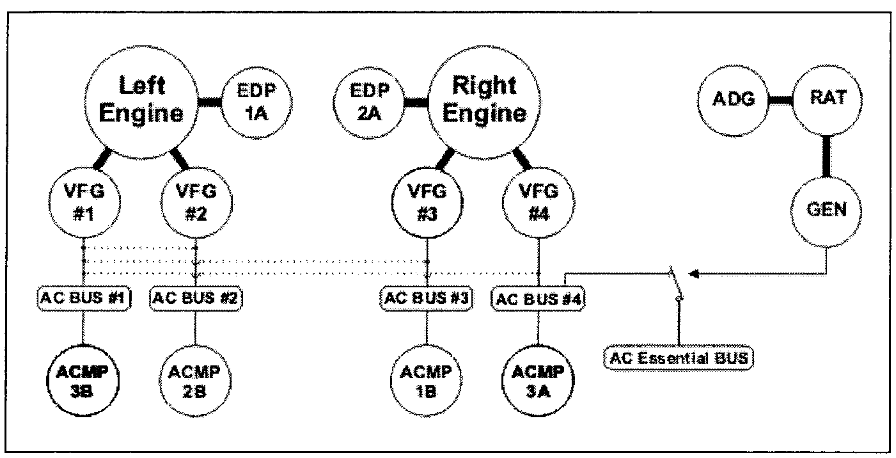

Fig. 5.6: Electrical and hydraulic power distribution on the *XYZ* aircraft

The suction line of each EDP is provided with a Firewall Shut-Off Valve (FWSOV) installed close to the engine nacelle firewall. The FWSOV cuts the flow of hydraulic fluid to the engine areas in case of an engine fire or an EDP compensator failure.

An air-to-hydraulic fluid heat exchanger is installed in the case drain lines of the pumps to control the hydraulic fluid temperature.

The hydraulic reservoirs are pressurized type (bootstrap) and incorporate the necessary sensors and switches for pressure and temperature control and monitoring. The pressurized hydraulic reservoirs are intended to reduce the occurrence of cavitation phenomenon that may be induced by rapid variation of the flow demand.

The pressure manifold of each hydraulic system incorporates the pressure line filter, the check valves protecting each pump against back-flow, and the system pressure transducer and pump pressure switches used for system control and monitoring.

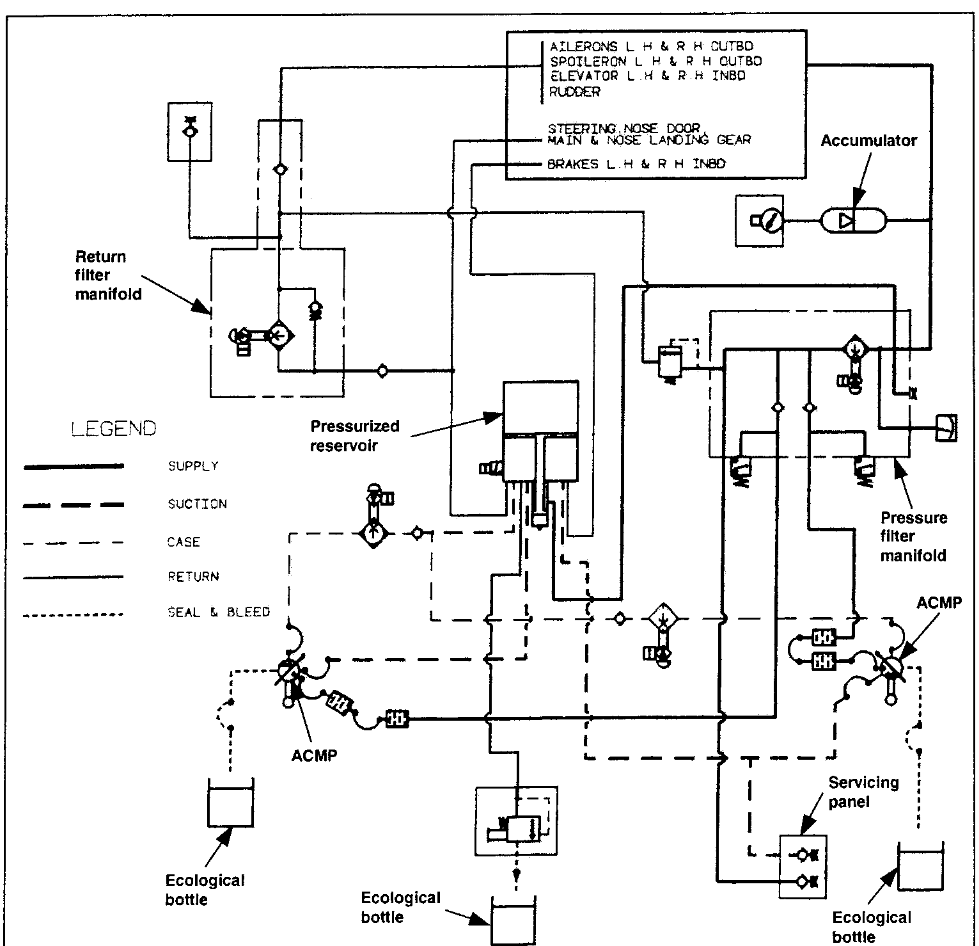

Fig. 5.7: Hydraulic System #3 – Architecture

The hydraulic system #3 is powered by one AC Motor Pump (ACMP), which it is backed up by another ACMP. One Ram Air Turbine (RAT) is driving an Air Driven Generator (ADG) in case a failure on both engines or on the electrical system occurs.

This arrangement of hydraulic pumps provides flexibility and redundancy of the hydraulic power sources by allowing continuous operation of all three systems with only one engine running, or in event of a single pump failure in any system.

In each hydraulic system, an accumulator nitrogen-charged at 1500 psi is installed on the pressure line, downstream of the pressure manifold.

The fluid employed by all three hydraulic systems is generally a low-density hydraulic fluid, Type IV/Type V phosphate ester based. This type of fluid preserves the viscosity inside a restricted range of temperature variation.

5.3 AC MOTOR PUMP

As it was previously mentioned, the necessity for a study of pump cavitation is determined by the frequent occurrence of this phenomenon within the hydraulic power system of the aircraft. There are two potential causes responsible of cavitation occurrence at the pump level: *pump design* and *pump installation*.

The goal of this study is to evaluate what design characteristics of the pump are involved in cavitation development in order to provide a simple method to evaluate the pump susceptibility to cavitation before it is installed on the hydraulic system.

This study was conducted using as reference the ACMP 3A from system #3 of the *XYZ* aircraft, for which has been recorded an abnormal number of failures in service attributed to cavitation effects. The pump ACMP 3B is used as backup for 3A pump and it is in stand-by mode. Both pumps are identical as design and performances and they are identically installed on the aircraft. Damages caused by cavitation were only recorded on the ACMP 3A.

There are two reasons that make this ACMP 3A more susceptible to cavitation:

- The pump is the main pump of system #3 and it is continuously operated during the entire flight mission in order to ensure the redundancy of the actuation systems connected to hydraulic system #3;
- Under flow demand of system #3 users, the pump ACMP 3A develops high accelerations that cannot be followed by the inertial mass of the fluid. This inertia represents the installation premises for pump cavitation. Due to the inertial mass of the fluid, the pressure from the ACMP suction line may drop instantaneously under a critical value that corresponds to cavity inception stage, in spite of the fact that the bootstrap reservoir pressurizes the suction line of the pump. This brings forward a *sensitivity* of the pump to variations of the input pressure, which may be a consequence of detail design of its *geometrical characteristics*.

5.3.1 Pump Description

The construction of the variable displacement axial piston AC Motor Pump is presented below in relation with Fig. 5.8, Fig. 5.9, Fig. 5.10, and Fig. 5.10.

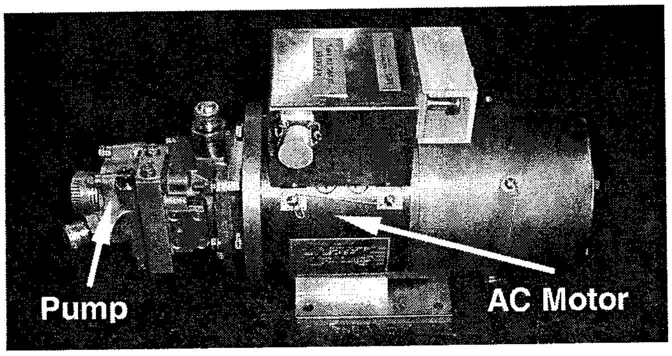

Fig. 5.8: ACMP package – Variable displacement axial piston pump

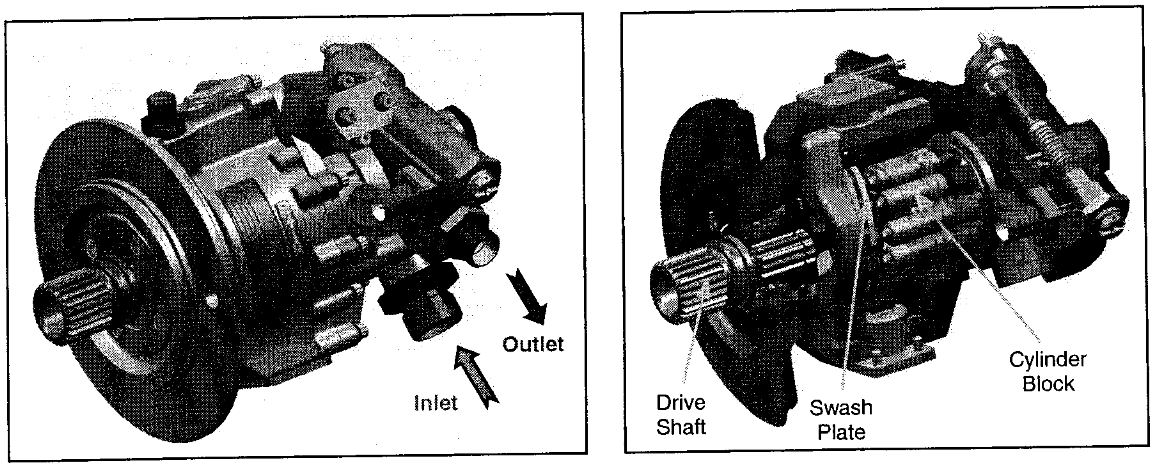

Fig. 5.9: Construction details of the variable displacement axial piston pump

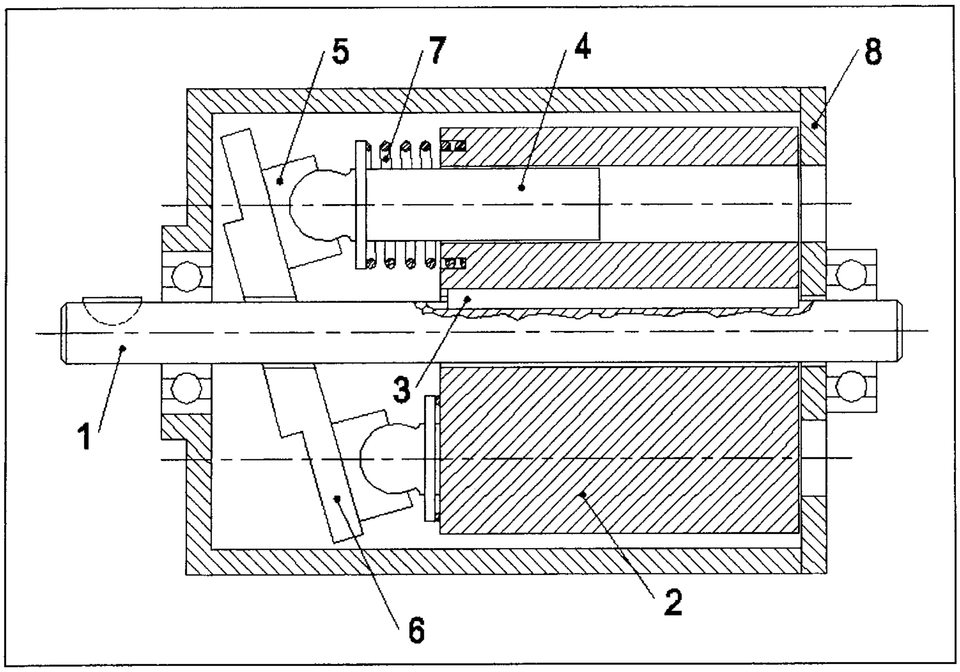

Fig. 5.10: Variable displacement axial piston pump – Schematic

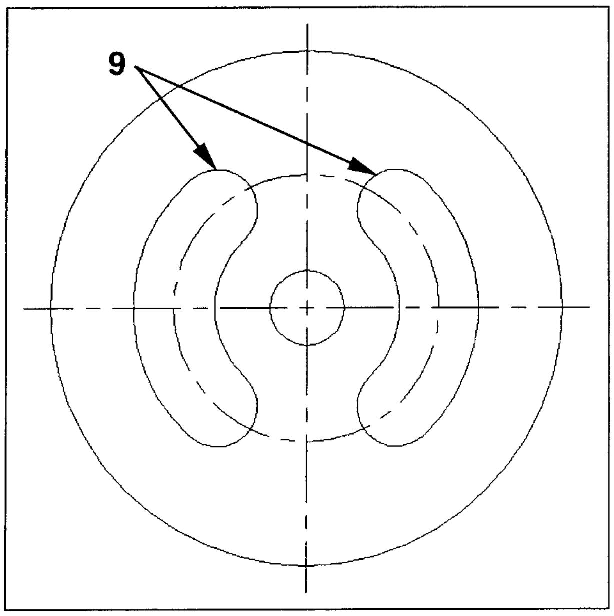

Fig. 5.11: Valve plate – Schematic

The considered Variable Displacement Axial Piston AC Motor Pump meets the following rated performance:

Table 5.1: Variable displacement axial piston AC motor pump rated performance

Input power	115/200 VAC, 400 Hz
Ambient temperature	-65° F to +225° F continuous
Inlet fluid temperature	+20° F to +200° F continuous
Rated discharge pressure for zero flow	3100 ± 50 psig
Rated inlet pressure	min. 55 psia at rated delivery
Case drain port proof pressure	500 psig
Case drain flow	max. 0.5 US gpm
Rated full flow pressure	min. 2900 psig
Rated full flow	min. 4.1 US gpm at 2700 psi
Rated current	max.24 amps per phase at rated delivery

The pump is a pressure-compensated variable displacement axial piston pump capable of varying the volume of fluid delivered to maintain the desired hydraulic system pressure (see Figure 5.10 for pump schematic). The AC motor drives the pump via the *drive shaft* (1). The drive shaft is connected to the mobile *cylinder block* (2) by a *key* (3) or any other locking device. The cylinder block has a series of symmetrically distributed bores that accommodate the *pistons* (4) of the pump. Since the pump is axial, the pistons are parallel to each other and to the axis of the drive shaft and cylinder block. The extremity of each piston is connected to a hydrostatically balanced *piston shoe* (5). Each piston shoe presses against the *swash plate* (or cam plate) (6), which may be tilted but does not rotate. The pressing force is created by the pressure in the hydraulic system and by return *springs* (7). As the cylinder block rotates, the pistons revolve against the tilted swash plate and reciprocate within their bores, sucking and discharging fluid through a stationary *valve plate* (8) resting on the port cap. The valve plate allows the alternative connection of the piston chambers to the inlet and outlet ports through its two *"kidney-shaped" orifices* (9).

Since the pump has a variable displacement output, the tilting angle of the swash plate is mechanically adjusted by a *servo control system*. The modification of the tilting angle has a direct incidence on the distance traveled by the pistons, and consequently, on the volume displaced by the pump. The servo control system is directed by the pump discharge pressure through a compensator valve and a stroking piston such that, above a set pressure the swash plate angle decreases, reducing the displaced volume.

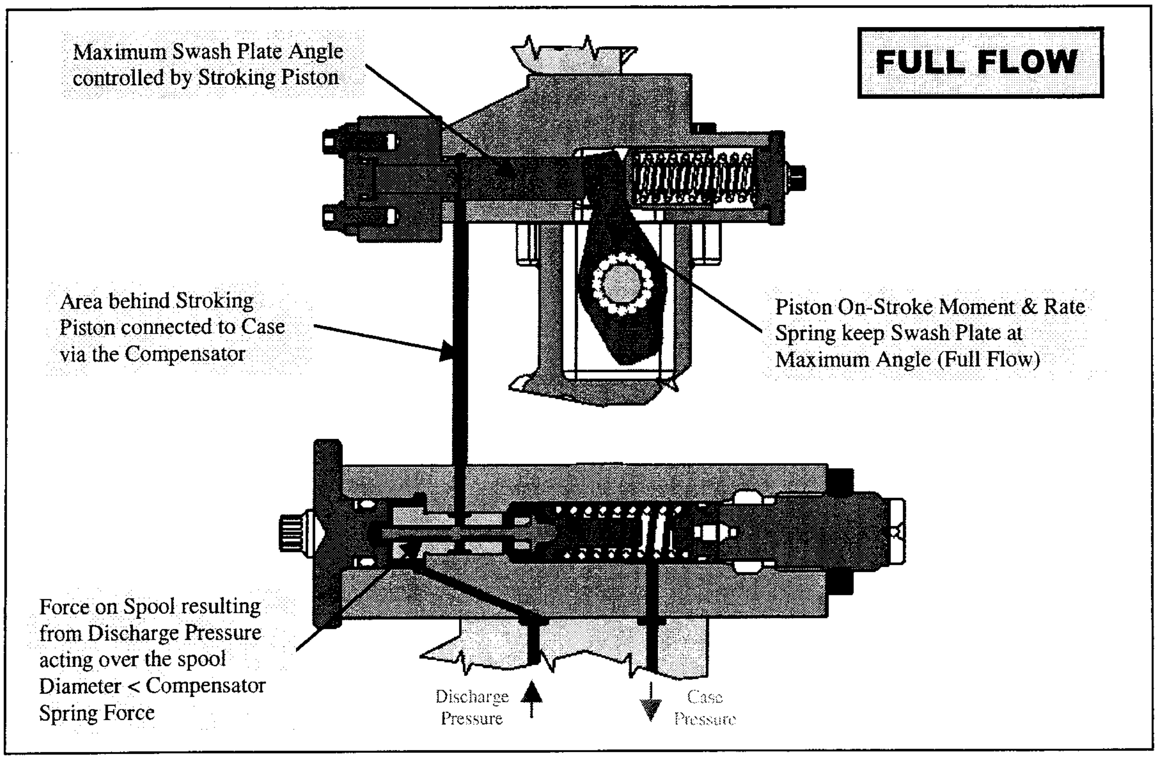

Fig. 5.12: Pump compensator operation

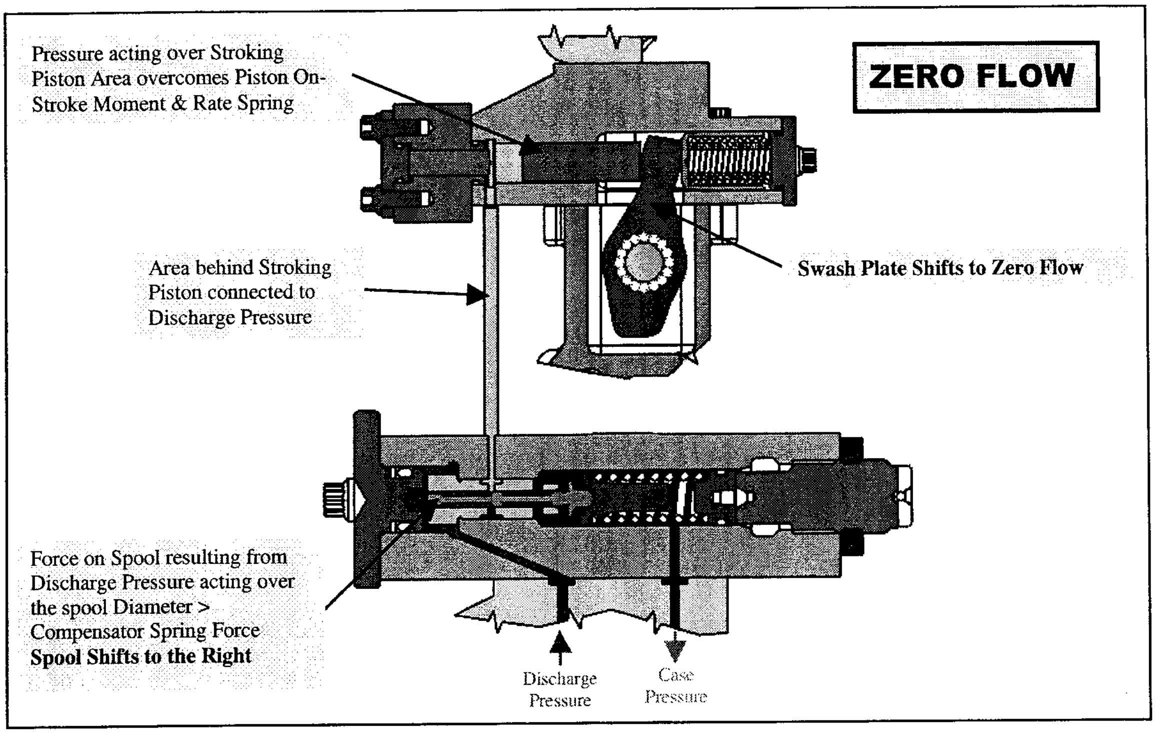

Fig. 5.13: Pump compensator operation (continued)

The compensator controls the pump outlet pressure. The resultant force of the discharge pressure acting across the compensator spool area versus the preset compensator spring force dictates the spool position.

Rated discharge pressure is defined as being the pump maximum pressure that is required to maintain zero flow at rated temperature, rated speed, and rated inlet pressure. The compensator is adjusted such that when discharge pressure reaches 3100 psi, the spool shifts, allowing discharge pressure to be passed to the primary stroking piston (see Fig. 5.12 and Fig. 5.13). Pressure applied across the primary stroking piston area creates sufficient force to decrease the swash plate angle and reduce the pump outlet flow.

The compensator valve performs integration, metering a volume of fluid to the stroking piston proportional to the change in pump output. An increase in system flow demand causes the pump discharge pressure to decrease, reducing the force applied on the compensator spool. When the discharge pressure reaches a value defined by the setting of the spring, the spool shifts, uncovering a port in the sleeve and the valve transfers oil from the stroking piston to the case. The rate piston extends due to the force from its spring, which drives the pump hanger to a larger inclined angle as the stroking piston retracts. The greater cam angle increases the flow output, raising the discharge pressure.

Maximum Full-Flow Pressure is the maximum discharge pressure at which the pump control will not be acting to reduce pump delivery at rated temperature, speed, and inlet pressure. For this pump, maximum full-flow pressure is 2900 psi. At that pressure and any pressure below, the swash plate angle is at its maximum, and the pump is operating at full stroke. Provided that the system flow demand does not exceed the pump capacity, pump discharge pressure will be maintained between 2900 and 3100 psi.

The pump also incorporates a *depressurization circuit* to unload the pump and reduce the input torque required for start-up. The pump utilizes a normally closed 2 position, 3-way solenoid valve. In the de-energized condition, discharge pressure at the valve (P) is blocked, and the control port (C) is connected to the case (R). Application of 28 VDC energizes the solenoid. In the energized position, discharge pressure is routed to the control port, with the return to case port blocked at the valve.

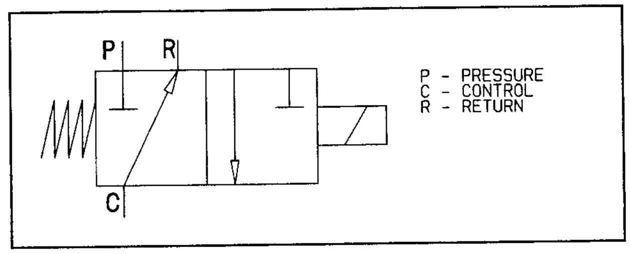

Fig. 5.14: Depressurization solenoid valve positions

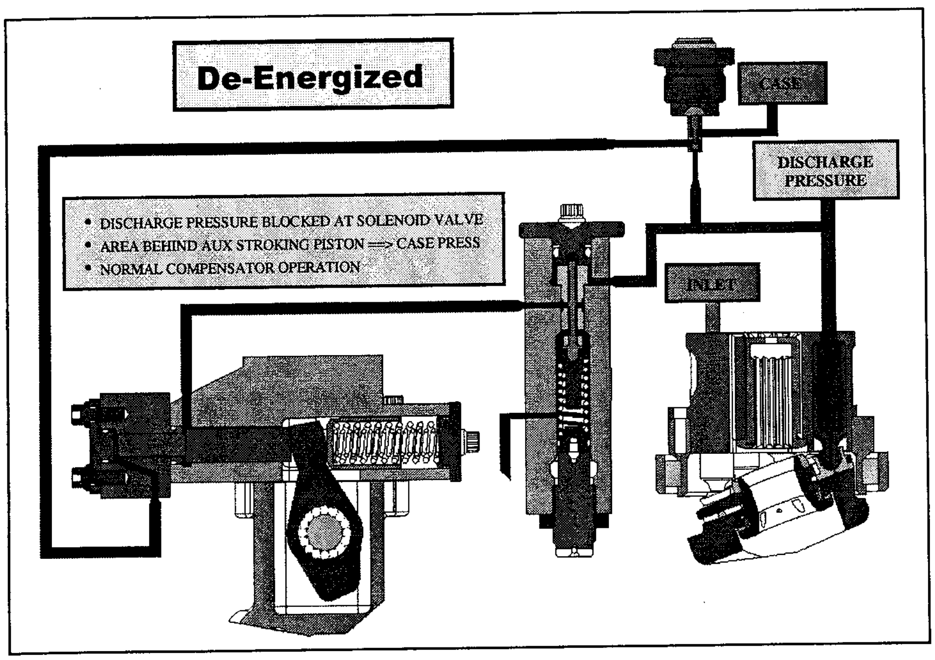

Fig. 5.15: Pump depressurization circuit

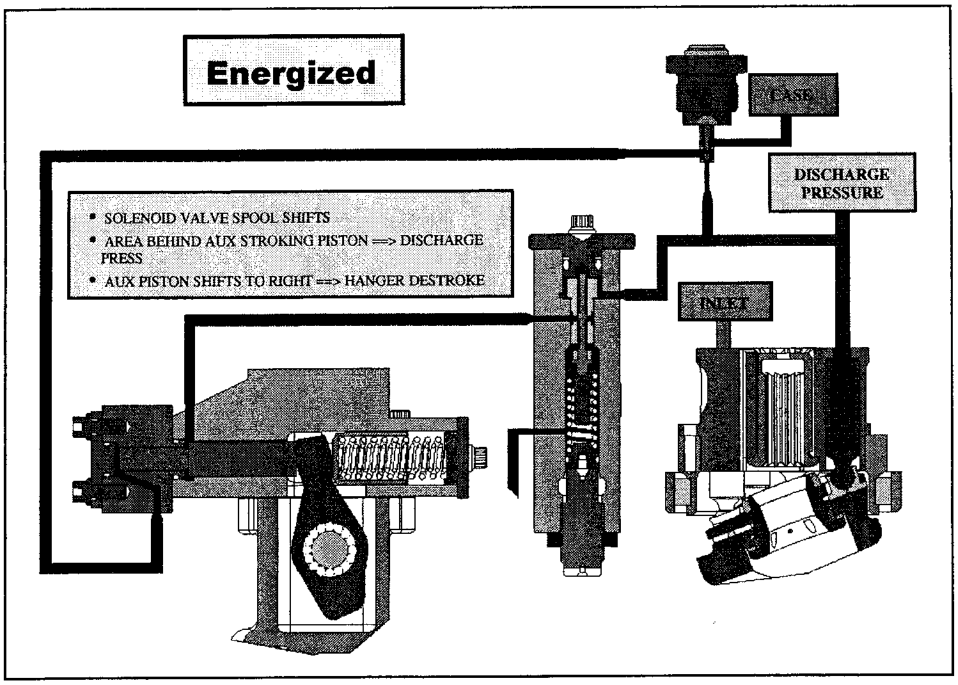

Fig. 5.16: Pump depressurization circuit (continued)

With the depressurization valve de-energized, the pump operates as a pressure compensated variable displacement piston pump. Pump outlet pressure is controlled by the compensator. When the depressurization valve is energized, the solenoid valve position shifts resulting in pump discharge pressure being ported directly behind the stroking piston, bypassing the compensator. With sufficient pressure applied across the stroking piston area, the stroking piston pushes on the swash plate arm, decreasing the swash plate angle and reducing the pump outlet flow (see Fig. 5.15 and 5.16). Because the compensator is bypassed, the pump discharge pressure is reduced to the minimum pressure required to destroke the unit. A shuttle valve is provided to segregate the depressurization circuit and the compensator control. Pressure imbalance dictates the ball position and resulting flow path availability (see Fig. 5.17).

When the applied voltage to the solenoid is removed, the de-energized solenoid valve returns to the normally closed position, venting the pressure applied behind the stroking piston back to the case. Discharge pressure is blocked at the solenoid valve and normal pump operation via the compensator resumes.

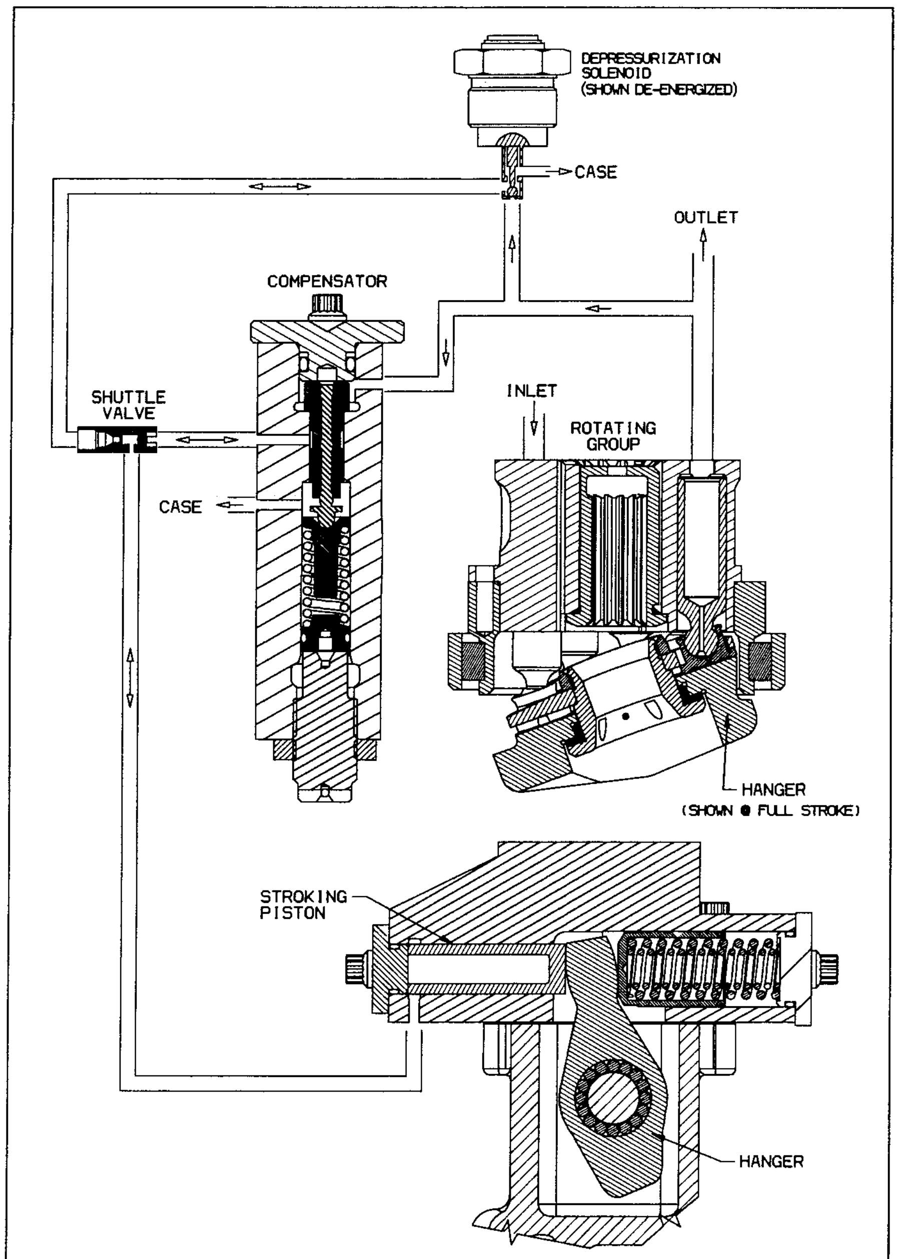

Fig. 5.17: Schematic of servo control system for a variable displacement axial piston pump

CHAPTER 6

MATHEMATICAL MODEL OF VARIABLE DISPLACEMENT AXIAL PISTON PUMP

CHAPTER 6

MATHEMATICAL MODEL OF VARIABLE DISPLACEMENT AXIAL PISTON PUMP

6.1 INTRODUCTION

This chapter presents the mathematical model of the Variable Displacement Axial Piston Pump (VDAPP) installed on *XYZ* aircraft. The mathematical model is validated using related experimental results. Subsequently, the mathematical model is used in Chapter 7 to support the design analysis of this pump with the purpose of reducing the cavitation phenomenon generated by this component.

The mathematical model produced here simulates the dynamic performance of a VDAPP under normal operating conditions using MatLab software.

6.2 MODEL DEFINITION

6.2.1 Modeling Theory

Fluid mechanics theory, mechanics of motion, and geometry rules are used to develop the mathematical model of the pump. Fluid mechanics theory is applied to model the flow conditions of the hydraulic liquid inside the pump. Alternatively, mechanics of motion determine the environment generating the liquid's behaviour (position of piston inside the chamber, position of valve plate etc.). Finally, geometry rules are used to compute the suction and delivery areas of the pistons.

6.2.2 Model Assumptions

The following assumptions were included in the creation of the mathematical model of the VDAPP:

- Steady state flow;
- Compressible liquid medium;
- Thermal effects generated by cavity suppression stage, flow of hydraulic liquid, and movement of pump components are neglected;
- Mass and inertia of pump components are neglected;
- All pump components are rigid and homogeneous bodies.

6.2.3 Model Equations

The mathematical model of the Variable Displacement Axial Piston Pump allows determining the pressure variation, p_k, inside the pump. Using this variation, the pump capability to produce cavitation may be determined. By considering the kinematics of one cylinder of the pump along a complete cycle and the action experienced by the liquid medium contained within this cylinder, the variation of the pressure inside the pump is calculated. The liquid medium contained in the cylinder is represented by a control volume, *c.v.*.

By taking into consideration the compressibility effects for this control volume, the following general equation is written:

$$B = \frac{dp_k}{d(c.v.)/c.v.} \quad [85] \qquad (6.1)$$

where dp_k is the differential change in pressure needed to create a differential change in volume, *d(c.v.)*, of the control volume, *c.v.*.

B represents the *bulk modulus* of the liquid medium.

From Eq. 6.1:

$$dp = \frac{B}{c.v.} d(c.v.) \tag{6.2}$$

By integrating both sides of Eq. 6.2, the pressure, *p*, may be expressed as:

$$\int dp = \int \frac{B}{c.v.} d(c.v.) \quad \Rightarrow \quad p = \frac{B}{c.v.} \int d(c.v.) \tag{6.3}$$

However, the control volume, ∀, may be expressed as: $c.v. = Q * t$ [86] (6.4)

where, Q – Volume flowrate;

t – Time.

Thus, by introducing Eq. 6.4 into Eq. 6.3:

$$p = \frac{B}{c.v.} \int Q \, dt \tag{6.5}$$

However, a series of volume flowrates are considered to enter and exit the given control volume. As a result, the volume flowrate, *Q*, from Eq. 6.5 may be expressed as:

$$Q = \sum Q_{in} - \sum Q_{out} \tag{6.6}$$

By incorporating Eq. 6.6 into Eq. 6.5:

$$p = \frac{B}{c.v.} \int \left(\sum Q_{in} - \sum Q_{out} \right) dt \tag{6.7}$$

For the case considered herein, the volume flowrates associated with each piston chamber are presented in Fig. 6.1:

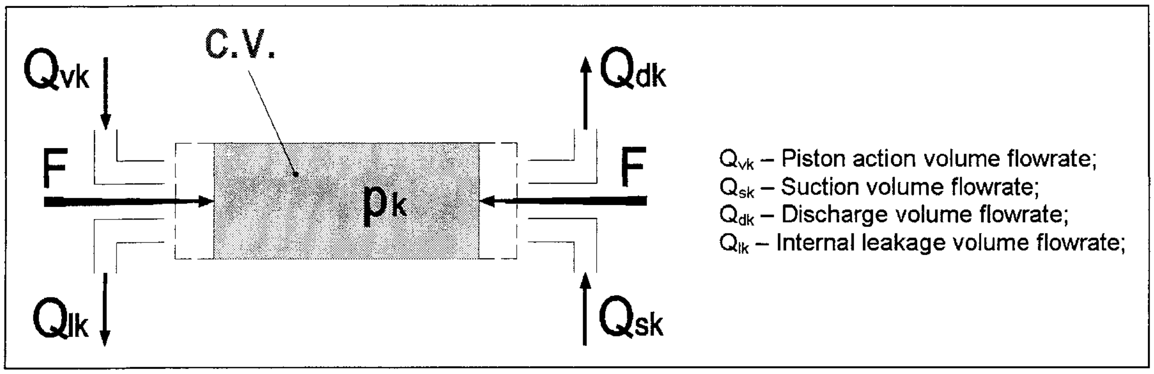

Fig. 6.1: Control volume for one piston chamber

Therefore, Eq. 6.7 may be expressed as:

$$p_k = \frac{B}{c.v.} \int (Q_{vk} + Q_{sk} - Q_{dk} - Q_{lk})\, dt \qquad (6.8)$$

where, Q_{vk} – Volume flowrate due to piston action;

Q_{sk} – Suction volume flowrate;

Q_{dk} – Discharge volume flowrate;

Q_{lk} – Internal leakage volume flowrate.

The volume flowrates Q_{sk} and Q_{dk} are associated with the flow of liquid from one location to another, as seen in Fig. 6.2). They are determined using the following general analysis:

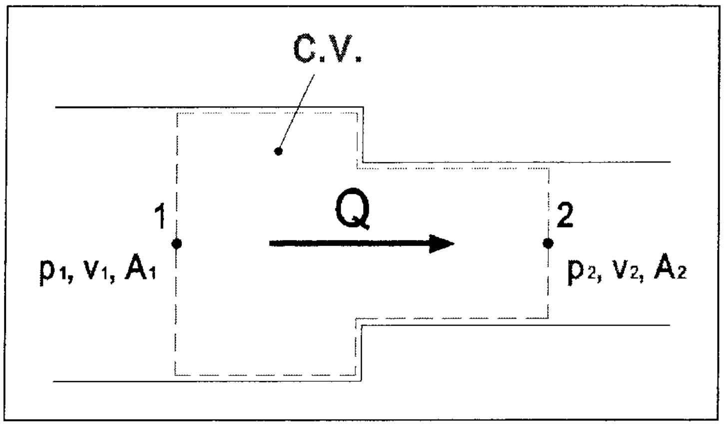

Fig. 6.2: Control volume for volume flowrate analysis

Newton's second law of motion for a system is [87]:

Sum of external forces acting on the system	=	Time rate of change of the linear momentum of the system

Therefore, the application of Newton's second law to the control volume considered in Fig. 6.2 gives:

$$\sum F_{sys} = \left(\frac{dP}{dt}\right)_{sys} \tag{6.9}$$

where, P – Linear momentum of the system.

But, the linear momentum of the system, *P*, may be expressed as:

$$P = \int_{sys} v\, dm \tag{6.10}$$

where, $v = v(x, y, t) = u\,i + v\,j$ – Velocity vector (6.11)

Also, the sum of external forces acting on the system, $\sum F_{sys}$, is represented by:

$$\sum F_{sys} = F_{body} + F_{surface} \tag{6.12}$$

where, F_{body} – Body forces acting on the system;

$F_{surface}$ – Surface forces acting on the system.

Then, from Eqs. 6.9, 6.10, 6.11:

$$dF_{sys} = dm\left(\frac{dv}{dt}\right)_{sys} \tag{6.13}$$

$$dF_{body} + dF_{surface} = dm\left(\frac{\partial v}{\partial t} + u\,\frac{\partial v}{\partial x} + v\,\frac{\partial v}{\partial y}\right) \tag{6.14}$$

The subsequent algebraic manipulation of the differential equation 6.14 exceeds the objective of this study. By assuming a steady ($Q_{in}=Q_{out}$), incompressible (ρ=const.) and inviscid (μ=0) flow, this equation becomes:

$$p+\frac{\rho * v^2}{2}+\gamma * z = const. \quad - \text{ Bernoulli's equation} \tag{6.15}$$

where, p – Pressure along a streamline;

v – Velocity along a streamline;

z – Elevation;

ρ – Liquid density;

γ – Specific weight ($\gamma = \rho$*g);

g – Gravitational acceleration.

The application of Bernoulli's equation to the control volume presented in Fig. 6.2 gives:

$$p_1+\frac{\rho * v_1^2}{2}+\gamma * z_1 = p_2+\frac{\rho * v_2^2}{2}+\gamma * z_2 \tag{6.16}$$

where, p_1, p_2 – Pressures at locations (1) and (2);

v_1, v_2 – Velocities at locations (1) and (2);

z_1, z_2 – Elevations of locations (1) and (2);

ρ – Liquid density;

γ – Specific weight ($\gamma = \rho$*g);

g – Gravitational acceleration.

But $z_1 = z_2$. Thus, Eq. 6.16 becomes:

$$p_1+\frac{\rho * v_1^2}{2} = p_2+\frac{\rho * v_2^2}{2} \tag{6.17}$$

Also, $Q = v_1 * A_1 = v_2 * A_2$ [88] (6.18)

where, A_1, A_2 – Cross-sectional areas at locations (1) and (2)

Thus, by incorporating Eq. 6.18 into 6.17:

$$p_1 + \frac{1}{2} * \rho * \frac{Q^2}{A_1^2} = p_2 + \frac{1}{2} * \rho * \frac{Q^2}{A_2^2} \quad (6.19)$$

$$\frac{\rho}{2} * \left(\frac{Q^2}{A_2^2} - \frac{Q^2}{A_1^2} \right) = p_1 - p_2 \quad (6.20)$$

$$\frac{Q^2 * A_1^2 - Q^2 * A_2^2}{A_1^2 * A_2^2} = \frac{2*(p_1 - p_2)}{\rho} \quad (6.21)$$

$$Q^2 = \frac{2*(p_1 - p_2)}{\rho} * \frac{A_1^2 * A_2^2}{A_1^2 - A_2^2} \quad (6.22)$$

Therefore, $Q = \frac{A_1 * A_2}{\sqrt{A_1^2 - A_2^2}} * \sqrt{\frac{2*(p_1 - p_2)}{\rho}}$ (6.23)

Let $C_0 = \frac{A_1 * A_2}{\sqrt{A_1^2 - A_2^2}}$ – *Ideal flow coefficient* (6.24)

Hence, Eq. 6.23 becomes:

$$Q = C_0 * \sqrt{\frac{2*(p_1 - p_2)}{\rho}} = Q_{ideal} \quad (6.25)$$

Eq. 6.25 allows the calculation of the *Ideal volume flowrate* since *no losses are associated with the flow of liquid between locations (1) and (2).*

However, in any application, losses are present and they are grouped in two categories: *major losses* (represented by the friction taking place between the liquid and solid boundaries) and *minor losses* (represented by the reduction of area created by the *vena contracta* phenomenon) [89].

The addition of major and minor losses forms the *head loss* (h_L).

Thus, the unfolded Bernoulli's equation (Eq. 6.16) as applied to the control volume presented in Fig. 6.2 for a real liquid flow becomes:

$$p_1 + \frac{\rho * v_1^2}{2} + \gamma * z_1 = p_2 + \frac{\rho * v_2^2}{2} + \gamma * z_2 + h_L \quad \text{– Energy equation} \tag{6.26}$$

Although a formula is available to compute the head loss, its use is limited. Often, for more elaborate applications, an empirical coefficient is determined and used in the volume flowrate equation to account for the head loss effect. This constant and dimensionless coefficient, named *Actual flow coefficient, C_A*, is a function of v_1, A_1, and A_2 and it may be found in specialized charts [90].

Therefore, $Q_{actual} = C_A * Q_{ideal} \quad \Leftrightarrow$ (6.27)

$$\Leftrightarrow \quad Q_{actual} = C_A * C_0 * \sqrt{\frac{2*(p_1 - p_2)}{\rho}} \tag{6.28}$$

Going back to the volume flow rates associated with the flow of liquid from one location to another (see Eq. 6.8), Eq. 6.28 allows expressing Q_{sk} and Q_{dk} as:

$$Q_{sk} = C_{As} * C_{0s} * \sqrt{\frac{2*(p_s - p_k)}{\rho}} \qquad \text{– Suction volume flowrate} \qquad (6.29)$$

where, $$C_{0s} = \frac{A_{sk} * A_p}{\sqrt{A_{sk}^2 - A_p^2}} \qquad (6.30)$$

C_{As} – Actual flow coefficient of suction

C_{0s} – Ideal flow coefficient of suction

p_k – Pressure inside piston chamber;

p_s – Suction pressure;

A_p – Piston cross-sectional area;

A_{sk} – Suction area.

$$Q_{dk} = C_{Ad} * C_{0d} * \sqrt{\frac{2*(p_k - p_d)}{\rho}} \qquad \text{– Discharge volume flowrate} \qquad (6.31)$$

where, $$C_{0d} = \frac{A_p * A_{dk}}{\sqrt{A_p^2 - A_{dk}^2}} \qquad (6.32)$$

C_{Ad} – Actual flow coefficient of discharge

C_{0d} – Ideal flow coefficient of discharge

p_k – Pressure inside piston chamber;

p_d – Discharge pressure;

A_p – Piston cross-sectional area;

A_{dk} – Discharge area.

Although Eq. 6.28 may be used to theoretically calculate the internal leakage volume flowrate, an equivalent formula is empirically determined. The deviation from the theoretical procedure is caused by the complexity of the internal leakage process that occurs between the piston and the cylinder and between the valve plate and the cylinder block. The empirical formula, which is used within the definite operating limits of the pump, allows a more exact computation of the internal leakage volume flowrate.

Thus,

$Q_{lk} = K_L * (p_k - p_c)$ – Internal leakage volume flowrate (6.33)

where, K_L – Leakage empirical factor;

p_k – Pressure inside piston chamber;

p_c – Pump casing pressure.

The volume flowrate, Q_{vk}, associated with the piston action is determined from the expression (see Fig. 6.3):

$Q_{vk} = v_{pk} * A_p$ [88] (6.34)

where, v_{pk} – Piston velocity;

A_p – Piston cross-sectional area.

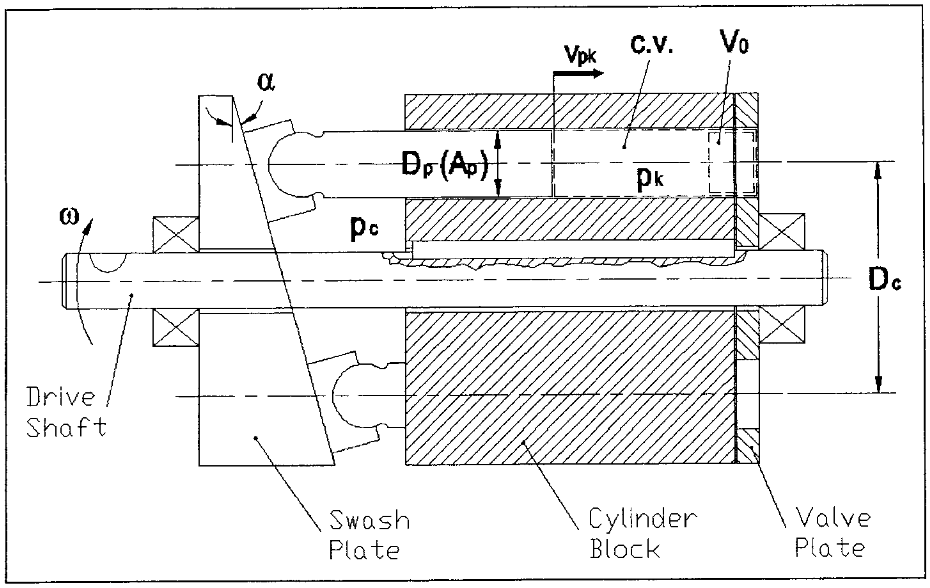

Fig. 6.3: Kinematic scheme of variable displacement axial piston pump

In order to establish the expression of the piston velocity, v_{pk}, and determine the variation of the volume flowrate associated with the piston action, Q_{vk}, a detailed kinematic scheme of the variable displacement axial piston pump is used (see Fig. 6.4 below):

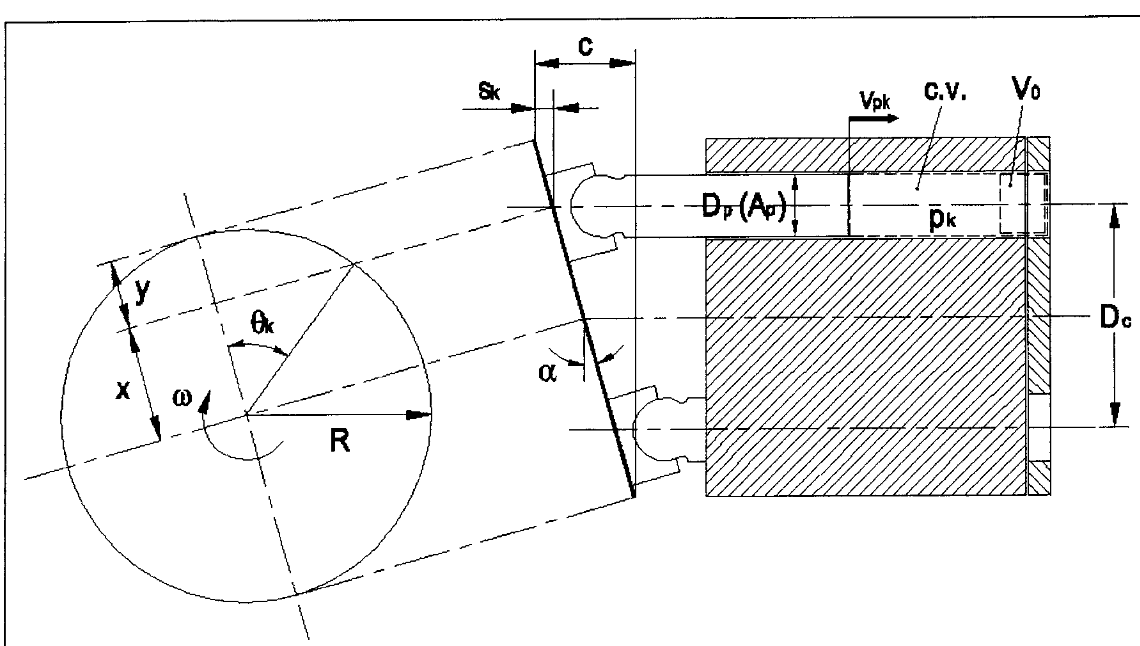

Fig. 6.4: Detailed kinematic scheme of variable displacement axial piston pump

The piston velocity, v_{pk}, may be expressed as:

$$v_{pk} = \frac{ds_k}{dt} \tag{6.35}$$

where, s_k – Linear displacement of piston.

However, Eq. 6.35 may also be written as:

$$v_{pk} = \frac{ds_k}{d\theta_k} \cdot \frac{d\theta_k}{dt} \tag{6.36}$$

where, θ_k – Angular displacement of piston.

The angular displacement (or position) of the piston, θ_k, is represented by:

$$\theta_k = \theta_{av} + \theta_{pn} \tag{6.37}$$

where, θ_{av} – Angular position of piston produced by drive shaft rotation;

θ_{pn} – Angular position of piston related to the total number of pistons.

Therefore, the angular displacement of the piston, θ_k, may also be written as:

$$\theta_k = \omega * t + \frac{2 * \pi * (k-1)}{q} \tag{6.38}$$

where, ω – Angular velocity of drive shaft;

t – Time;

k – Piston number;

q – Total number of pistons.

But the angular velocity of the drive shaft, ω, is:

$$\omega = 2 * \pi * f = 2 * \pi * \frac{n}{60} \tag{6.39}$$

where, f – Frequency;

n – Drive shaft speed of rotation.

Thus, from Eqs. 6.38 and 6.39, the angular displacement of the piston, θ_k, becomes:

$$\theta_k = \left(2 * \pi * \frac{n}{60}\right) * t + \frac{2 * \pi * (k-1)}{q} \tag{6.40}$$

In order determine the expression of the linear displacement of piston, s_k, additional analysis is required.

Thus, with reference to Fig. 6.4:

$$x = R * \cos \theta_k \tag{6.41}$$

where, R – Radius of circle on which the pump pistons revolve.

But, $y = R - x = R - R * \cos \theta_k = R * (1 - \cos \theta_k)$ (6.42)

Now, $s_k = y * \sin \alpha$ (6.43)

where, α – Angle of swash plate.

Hence, from Eqs. 6.42 and 6.43:

$$s_k = y * \sin \alpha = R * \sin \alpha * (1 - \cos \theta_k) \tag{6.44}$$

But,

$$R = \frac{\frac{D_C}{2}}{\cos\alpha} = \frac{D_C}{2} * \frac{1}{\cos\alpha} \tag{6.45}$$

where, D_C – Diameter of cylinders positioning (or Distance between centers of pistons).

Thus, by incorporating Eq. 6.45 into Eq. 6.44:

$$s_k = \frac{D_C}{2} * \tan\alpha * (1 - \cos\theta_k) \tag{6.46}$$

Now, going back to Eq. 6.36 and using Eqs. 6.46 and 6.40:

$$\frac{ds_k}{d\theta_k} = \frac{d}{d\theta_k}\left[\frac{D_C}{2} * \tan\alpha * (1 - \cos\theta_k)\right] = \frac{D_C}{2} * \tan\alpha * \sin\theta_k \tag{6.47}$$

and,

$$\frac{d\theta_k}{dt} = \frac{d}{dt}\left[\left(2 * \pi * \frac{n}{60}\right) * t + \frac{2 * \pi * (k-1)}{z}\right] = 2 * \pi * \frac{n}{60} \tag{6.48}$$

The expression in Eq. 6.48 is obtained by assuming that the drive shaft speed of rotation, *n*, is constant (not varying with time).

Therefore, by incorporating Eqs. 6.47 and 6.48 into Eq. 6.36:

$$v_k = \left(2 * \pi * \frac{n}{60}\right) * \left(\frac{D_C}{2}\right) * \tan\alpha * \sin\theta_k \tag{6.49}$$

Consequently, from Eqs. 6.34 and 6.49, the volume flowrate associated with the piston action, Q_{vk}, becomes:

$$Q_{vk} = \left(2*\pi*\frac{n}{60}\right)*\left(\frac{D_C}{2}\right)*\tan\alpha*\sin\theta_k*A_p \tag{6.50}$$

From Fig. 6.4, the formula allowing the calculation of the control volume, *c.v.*, at any time is:

$$c.v. = \forall_0 + A_p * c - A_p * s_k \tag{6.51}$$

where, $\forall_0$ – “Dead” volume of cylinder;

c – Maximum travel of piston.

Again, from Fig. 6.4, the maximum travel of the piston, *c*, is determined as:

$$c = 2*R*\sin\alpha = \frac{D_C}{\cos\alpha}*\sin\alpha = D_C*\tan\alpha \tag{6.52}$$

Thus, by incorporating Eqs. 6.46 and 6.52 into Eq. 6.51:

$$c.v. = \forall_0 + A_p*(D_C*\tan\alpha) - A_p*\left[\frac{D_C}{2}*\tan\alpha*(1-\cos\theta_k)\right] \Rightarrow$$

$$\Rightarrow \quad c.v. = \forall_0 + A_p*\frac{D_C}{2}*\tan\alpha*(1+\cos\theta_k) \tag{6.53}$$

Finally, the pressure inside the cylinder of the pump, p_k, is obtained by replacing the expressions of Q_{vk} (Eq. 6.50), Q_{sk} (Eq. 6.29), Q_{dk} (Eq. 6.31), Q_{lk} (Eq. 6.33), and c.v. (Eq. 6.53) in Eq. 6.8:

$$p_k = \frac{B}{\forall_0 + A_p \frac{D_C}{2} \tan\alpha (1+\cos\theta_k)} \int \begin{bmatrix} \left(2\pi \frac{n}{60}\right)\left(\frac{D_C}{2}\right) \tan\alpha \sin\theta_k A_p + \\ + C_{As} \frac{A_{sk} A_p}{\sqrt{A_{sk}^2 - A_p^2}} \sqrt{\frac{2(p_s - p_k)}{\rho}} - \\ - C_{Ad} \frac{A_p A_{dk}}{\sqrt{A_p^2 - A_{dk}^2}} \sqrt{\frac{2(p_k - p_d)}{\rho}} - \\ - K_L (p_k - p_c) \end{bmatrix} dt \qquad (6.54)$$

This analysis is subsequently used to create the mathematical model of the Variable Displacement Axial Piston Pump.

6.3 MATLAB MATHEMATICAL MODEL

From the formulas presented above, the mathematical model of the Variable Displacement Axial Piston Pump is generated using the *MatLab* software and *Simulink* modeling package. This section presents the MatLab mathematical model of the Variable Displacement Axial Piston Pump, as well as a brief description of the block-diagrams that compose it.

Subsequently, the data and pseudo-code used by the mathematical model are presented.

Finally, the model input data, along with the method of computing the suction and discharge areas and the pseudo-code used to introduce these values into the mathematical model are also presented in this section.

6.3.1 Block Diagrams

6.3.1.1 Pump Model

Fig. 6.5 illustrates the top level block-diagram of the VDAPP model. The model is composed of four main superblocks: (theta)k, Kinematics, Control Volume, and Flowrates.

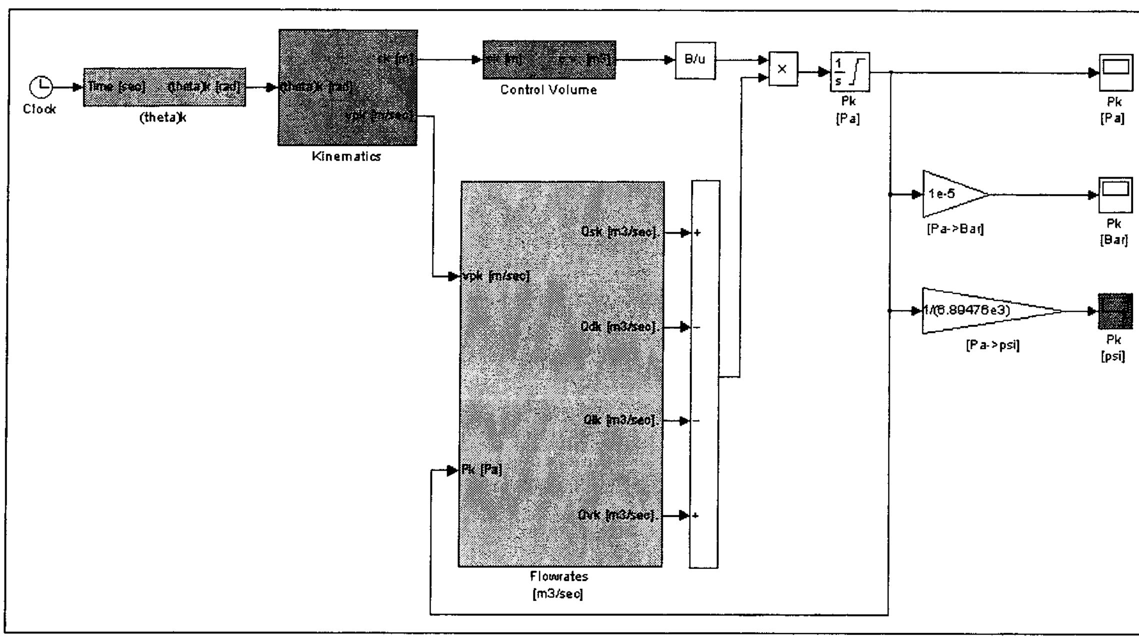

Fig. 6.5: Pump model

6.3.1.2 (theta)k

Fig. 6.6 illustrates the superblock containing the theory used for determining the angular displacement of the piston, θ_k. The input to this superblock is the time used for the piston to complete one cycle.

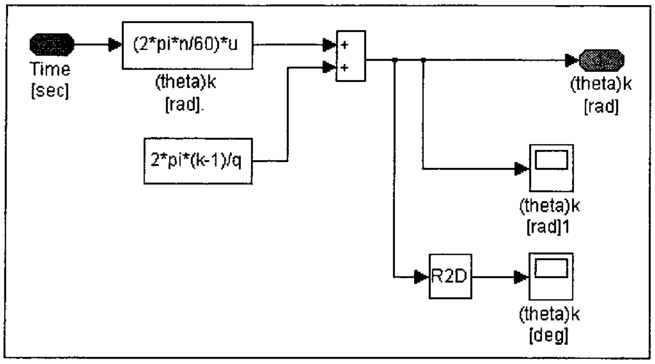

Fig. 6.6: Angular displacement of piston, θ_k

6.3.1.3 Kinematics

Fig. 6.7 illustrates the superblock that determines the kinematics of the pump by calculating the linear displacement of the piston, s_k, and the piston velocity, v_{pk}, during one cycle. The input to this superblock is the angular displacement of the piston, θ_k.

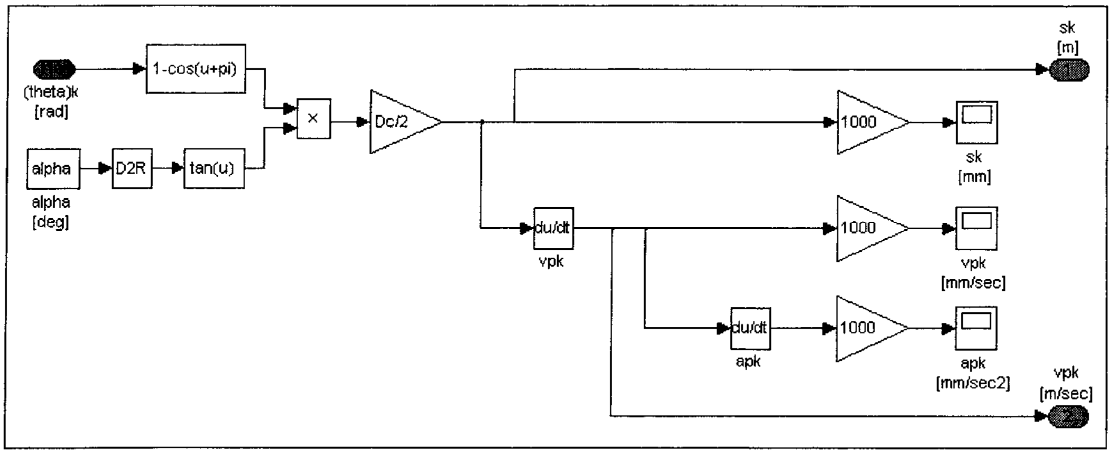

Fig. 6.7: Kinematics

6.3.1.4 Control Volume

Fig. 6.8 illustrates the superblock that determines the control volume of the cylinder chamber, *c.v.*. The input to this superblock is the linear displacement of the piston, s_k.

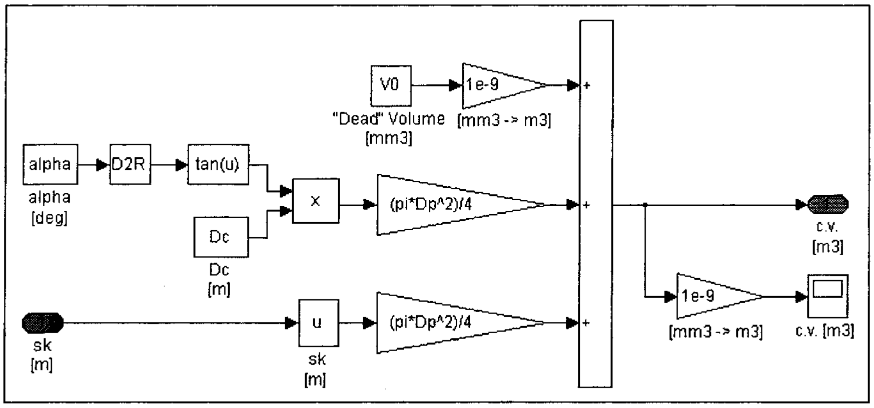

Fig. 6.8: Control Volume, *c.v.*

6.3.1.5 Flowrates

Fig. 6.9 illustrates the superblock that determines the flowrates involved into the control volume, Q_{sk}, Q_{dk}, Q_{lk}, and Q_{vk}. The inputs to this superblock are the pressure inside the cylinder, p_k, and piston velocity, v_{pk}.

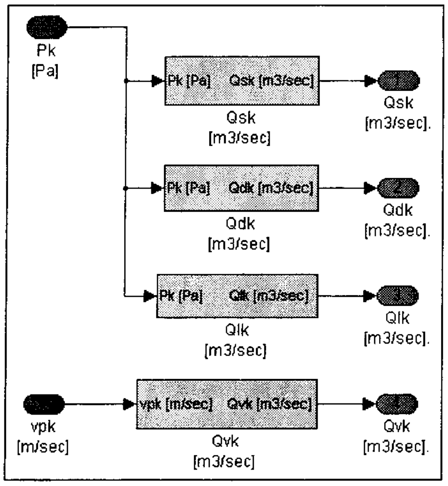

Fig. 6.9: Flowrates

6.3.1.6 Suction Flowrate

Fig. 6.10 illustrates the superblock that determines the suction flowrate, Q_{sk}. The input to this superblock is the pressure inside the cylinder, p_k.

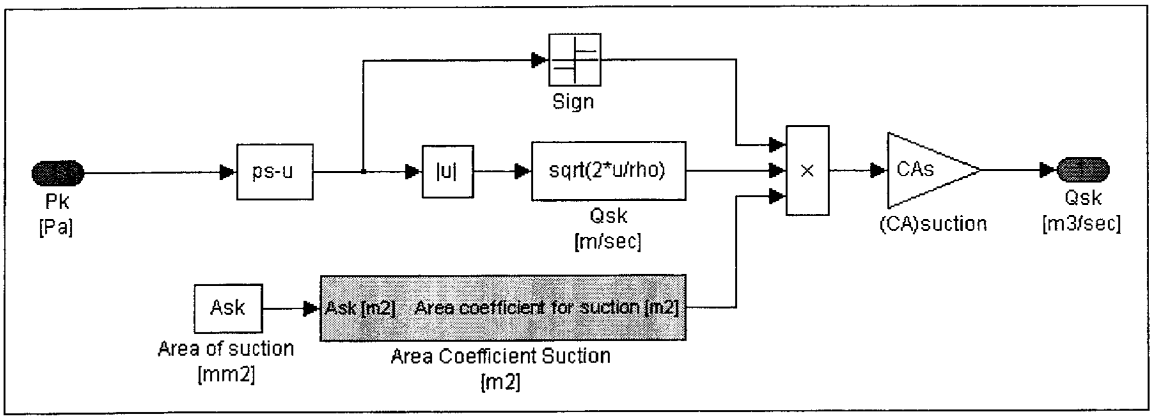

Fig. 6.10: Suction Flowrate, Q_{sk}

6.3.1.7 Area Coefficient for Suction

Fig. 6.11 illustrates the superblock that determines the area coefficient for suction, C_{0s}. The input to this superblock is the area at the suction port, A_{sk}.

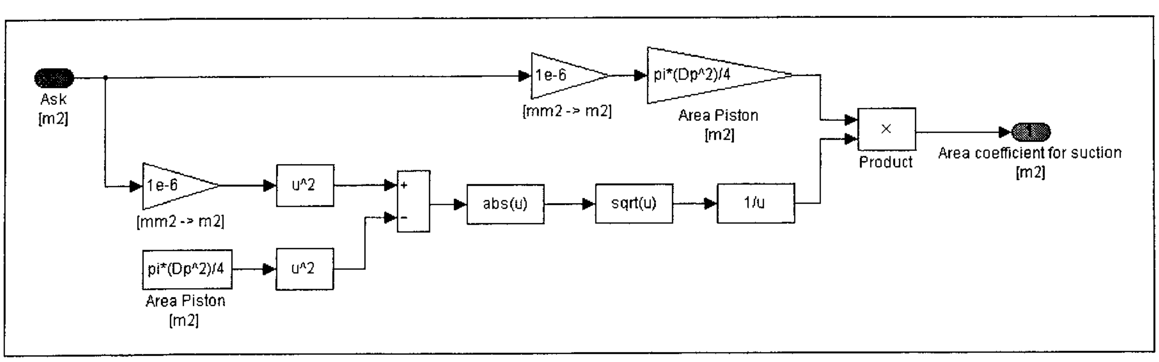

Fig. 6.11: Area coefficient for suction, C_{0s}

6.3.1.8 Discharge Flowrate

Fig. 6.12 illustrates the superblock that determines the discharge flowrate, Q_{dk}. The input to this superblock is the pressure inside the cylinder, p_k.

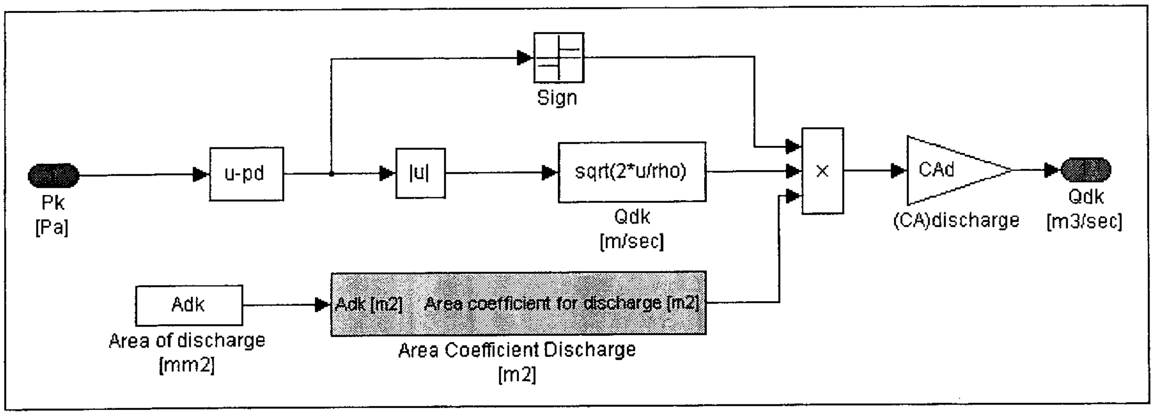

Fig. 6.12: Discharge Flowrate, Q_{dk}

6.3.1.9 Area Coefficient for Discharge

Fig. 6.13 illustrates the superblock that determines the area coefficient for discharge (or delivery), C_{0d}. The input to this superblock is the area at the discharge port, A_{dk}.

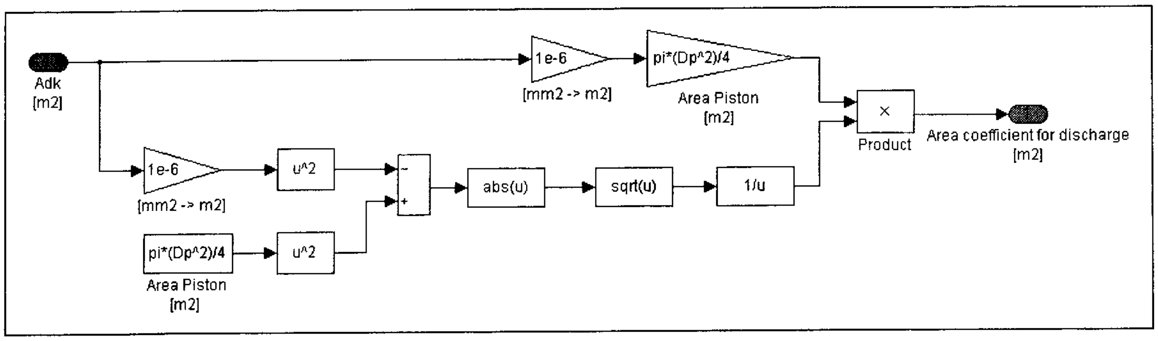

Fig. 6.13: Area coefficient for Discharge, C_{0d}

6.3.1.10 Leak Flowrate

Fig. 6.14 illustrates the superblock that determines the internal leakage flowrate of the pump, Q_{lk}. The input to this superblock is the pressure inside the cylinder, p_k.

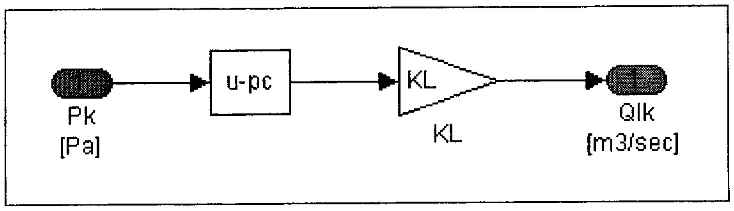

Fig. 6.14: Leak Flowrate, Q_{lk}

6.3.1.11 Volume Flowrate

Fig. 6.15 illustrates the superblock that determines the volume flowrate associated with the piston action, Q_{vk}. The input to this superblock is the piston velocity, v_{pk}.

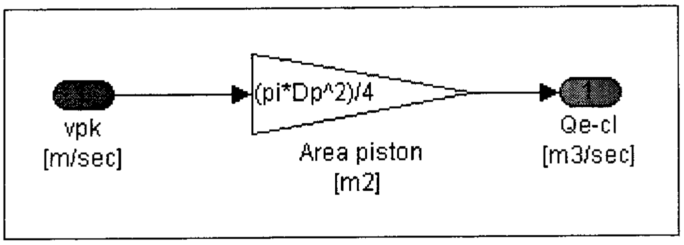

Fig. 6.15: Volume Flowrate, Q_{vk}

6.3.2 Model Input Data

6.3.2.1 Pump Data

The following Table 6.1 documents the data entered into the MatLab mathematical model that corresponds to the pump geometrical characteristics and to the type of hydraulic liquid used by the pump.

Table 6.1: Model input data

Variable	**Description**
n = 1800	Speed of Rotation of Pump Shaft [rpm]
k = 1	Piston Number
z = 9	Total Number of Pistons
alpha = 15	Actual Angle of Swash Plate [deg]
Dc = 0.0228092	Distance between Centers of Pistons [m] - (0.906 in)
Dp=0.0062611	Diameter Piston [m] - (0.2465 in)
V0=50	"Dead" Volume [mm3]
ps=3.79e5	Pressure at Suction [Pa] - (55 psi, 3.79 Bar)
pd=2.07e7	Pressure at Discharge [Pa] - (3000 psi, 2.07e2 Bar)
pc=5.86e5	Pressure in Pump Casing [Pa] - (85 psi, 5.86 Bar)
rho=990	Density of hydraulic liquid [kg/m3]
B=1.30e9	Bulk modulus [Pa]
CAd=0.4	Actual Flow Coefficient of Suction
CAs=0.3	Actual Flow Coefficient of Discharge
KL=1e-13	Leakage Empirical Factor

6.3.2.2 Suction and Discharge Areas

The suction and discharge areas for one cylinder of the pump are geometrically determined by overlapping the cylinder suction / discharge opening located on the rotating Cylinder Block (Fig. 6.16) with the kidney-shaped inlet / outlet ports found on the stationary Valve Plate (Fig. 6.17).

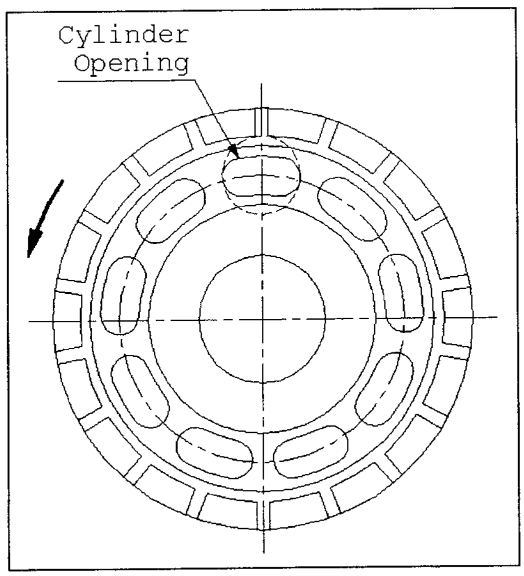

Fig. 6.16: Cylinder Block

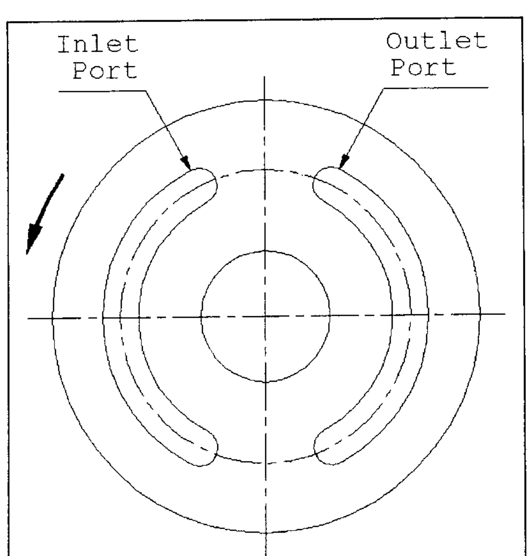

Fig. 6.17: Typical Valve Plate

The overlapping procedure is illustrated in Fig. 6.18 below:

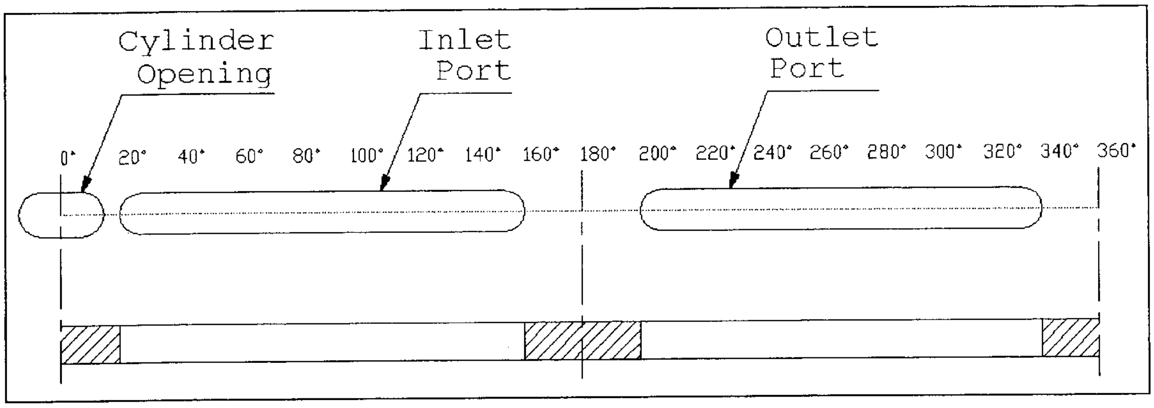

Fig. 6.18: Overlapping of cylinder opening with inlet / outlet ports on valve plate

The following geometry rules and formulas are used to determine the suction and discharge areas as the cylinder opening crosses the valve plate ports:

- Circular sector:

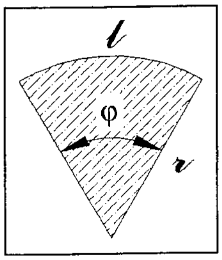

$$l = r * \frac{\varphi * \pi}{180}$$

$$A = \frac{\pi * r^2 * \varphi}{360}$$

- Circular segment:

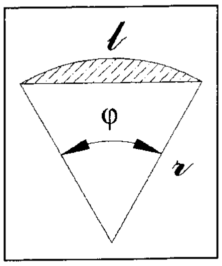

$$A = \frac{r^2}{2} * \left(\frac{\pi * \varphi}{180} - \sin\varphi \right)$$

After the suction and discharge areas for one cylinder of the pump are determined at every degree of rotation of the cylinder block, two individual text files containing this data are created. These files are introduced in the mathematical model using the following pseudo-code:

```
% **** Pseudo-Code Suction and Discharge areas ****
fid1 = fopen('C:\thesis\matlab\model\Ask.dat')
Ask = fscanf(fid1,'%e %e',[2 inf])
Ask = Ask'
fid11 = fopen('G:\thesis\matlab\model\Adk.dat')
Adk = fscanf(fid11,'%e %e',[2 inf])
Adk = Adk'
status = fclose('all')
```

6.4 MATHEMATICAL MODEL VALIDATION

The VDAPP mathematical model is validated by comparing the analytical results obtained from the MatLab model with experimental results obtained from specific tests. These tests were conducted at the supplier facilities using the same procedure employed for the verification of pump performance.

In order to complete the validation stage of the VDAPP mathematical model, one pump was successively fitted with two valve plates having the same geometry and position of their "kidney-shaped" orifices. However, the second valve plate includes a *transition notch* at the beginning of each "kidney-shaped" orifice (see Fig. 6.19 and Fig. 6.20) in order to ensure a progressive connection of the cylinders to the pressure from the suction and discharge lines. Hydraulic pumps fitted with both valve plates were already installed and operated on the aircraft.

The presence of transition notches on each "kidney-shaped" orifice showed a reduction of the cavitation effects.

The geometries of the above mentioned valve plates are initially used for determining the suction and discharge areas supplied to the mathematical model. This allows the *theoretical computation of the pressure inside the cylinder chamber*, as well as other parameters related to the piston performance and control volume evolution. Subsequently, tests conducted on the available pumps allow the measurement of pressure variations at the inlet and outlet ports of the pump.

Due to the impossibility of monitoring the pressure values inside the cylinder chamber along a complete cycle, only the variations of the inlet and outlet pressures were experimentally measured. Because of this condition, the results of the conducted tests may be only used for the *qualitative validation* and not *quantitative*. This means that the measured pressures from the suction and discharge lines are average values obtained by the integration of the pressures variations from all cylinders. Therefore, only the detection of *perturbations* of the input and output pressures corresponding to the duration of one cycle may be used to validate the mathematical model of the pump.

Although alternatives implying major design modifications of the pump could allow the measurement of the pressure inside the cylinder chamber along a complete cycle, the experimental results obtained from these test will greatly diverge from the simulated condition. This is due to the fact that the introduction of any measuring instrument inside the cylinder chamber shall significantly affect the flow field inside the chamber. Consequently, the measuring instrument shall affect the pressure field inside the cylinder chamber, and thus, the occurrence of an already sensitive cavitation phenomenon.

6.4.1 Mathematical Model Results

This section presents the analytical results obtained from the MatLab mathematical model using the valve plate geometries shown in Fig. 6.19 and Fig. 6.20. The presence of two transition notches at the beginning of suction and discharge areas is noted as a significant design difference between the valve plates.

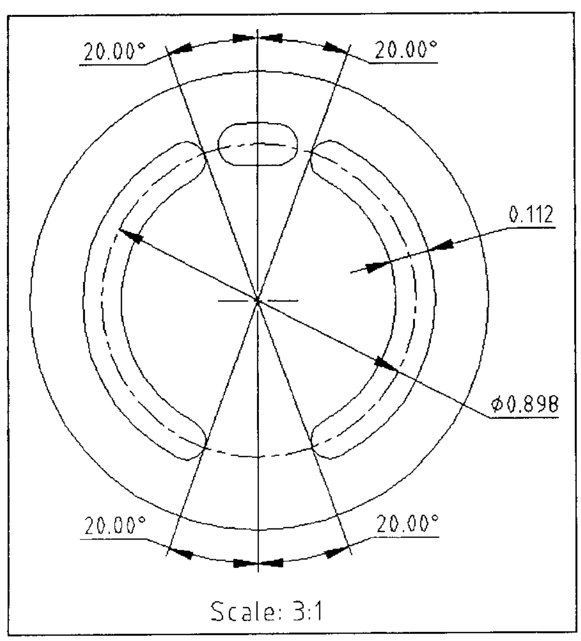

Fig. 6.19: Valve plate # 1

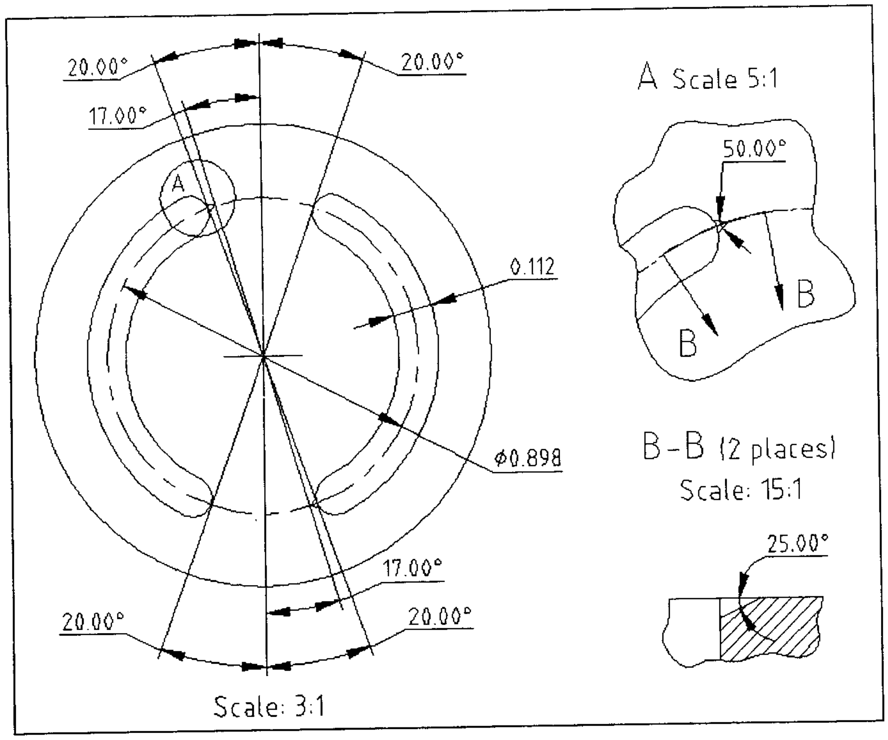

Fig. 6.20: Valve plate # 2

The variations of suction and discharge areas for these two valve plates are shown in Fig. 6.21 and Fig. 6.22. In Fig. 6.21 for the valve plate without transition notches, the opening of suction and discharge areas start at 6 and 186 degrees respectively corresponding to 0.09 mm^2 (Detail A). In Fig. 6.22 for the valve plate with transition notches, the opening of suction and discharge areas start at 3 and 183 degrees respectively corresponding to 0.01 mm^2 (Detail B). This earlier and more progressive opening of the cylinder volume reduces the abrupt increases and decreases of pressure inside the cylinder and consequently it reduces the occurrence of cavitation within the pump.

The variations of pressure inside the cylinder chamber generated by the mathematical model using the selected valve plate geometries are subsequently presented in Fig. 6.23 and Fig. 6.24.

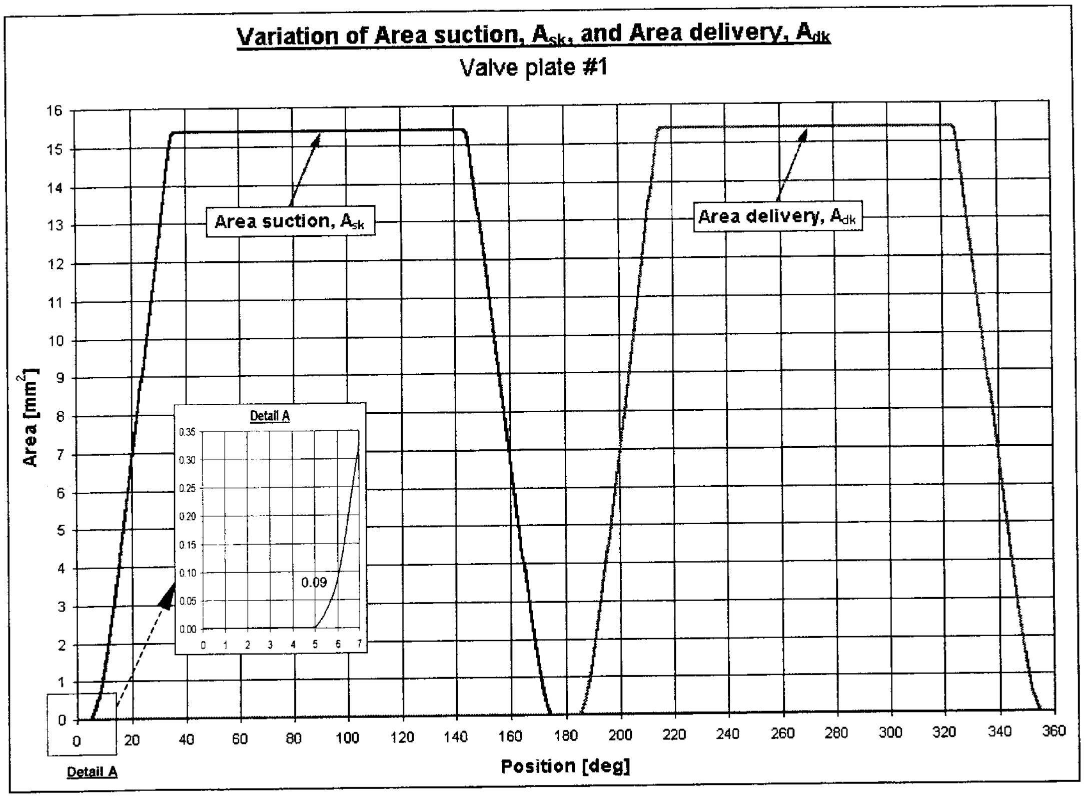

Fig. 6.21: Variation of Area suction, A_{sk}, and Area delivery, A_{dk}, for valve plate # 1

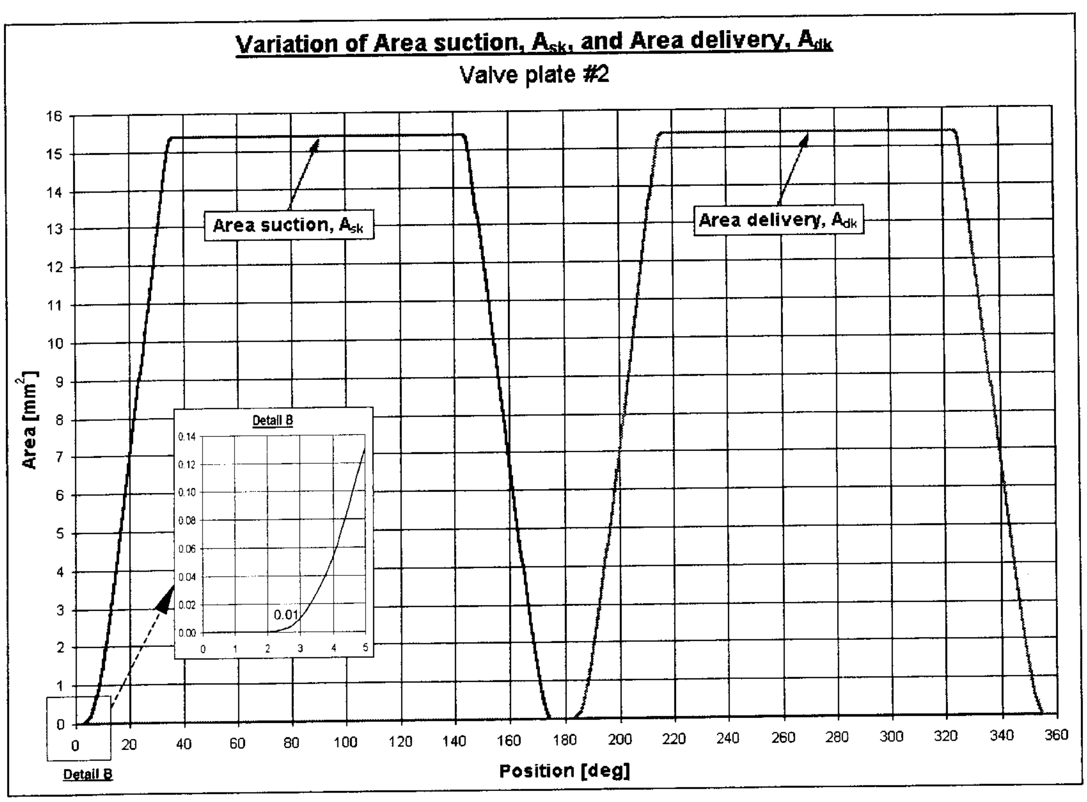

Fig. 6.22: Variation of Area suction, A_{sk}, and Area delivery, A_{dk}, for valve plate # 2

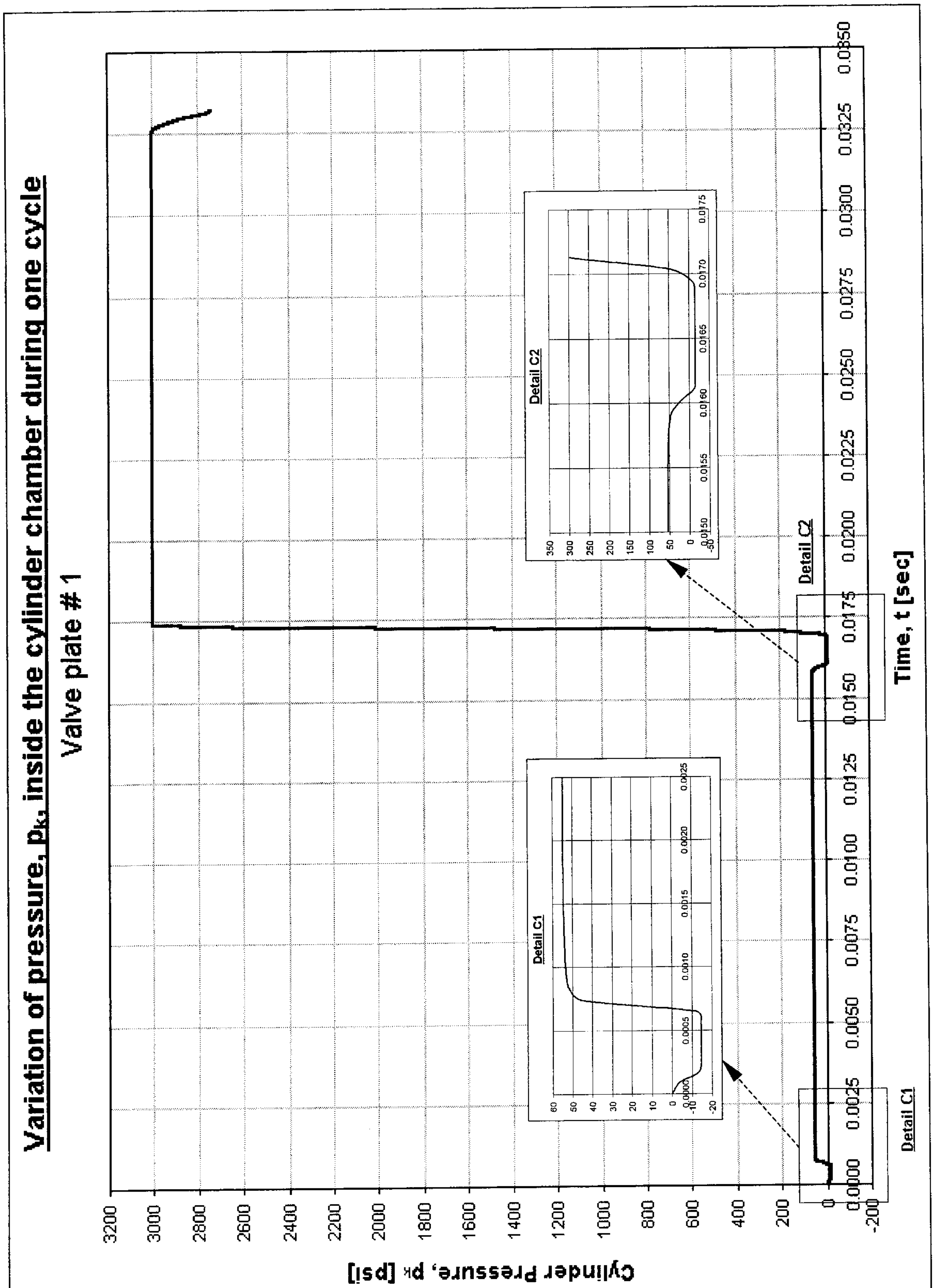

Fig. 6.23: Variation of pressure, p_k, inside the cylinder chamber using valve plate # 1

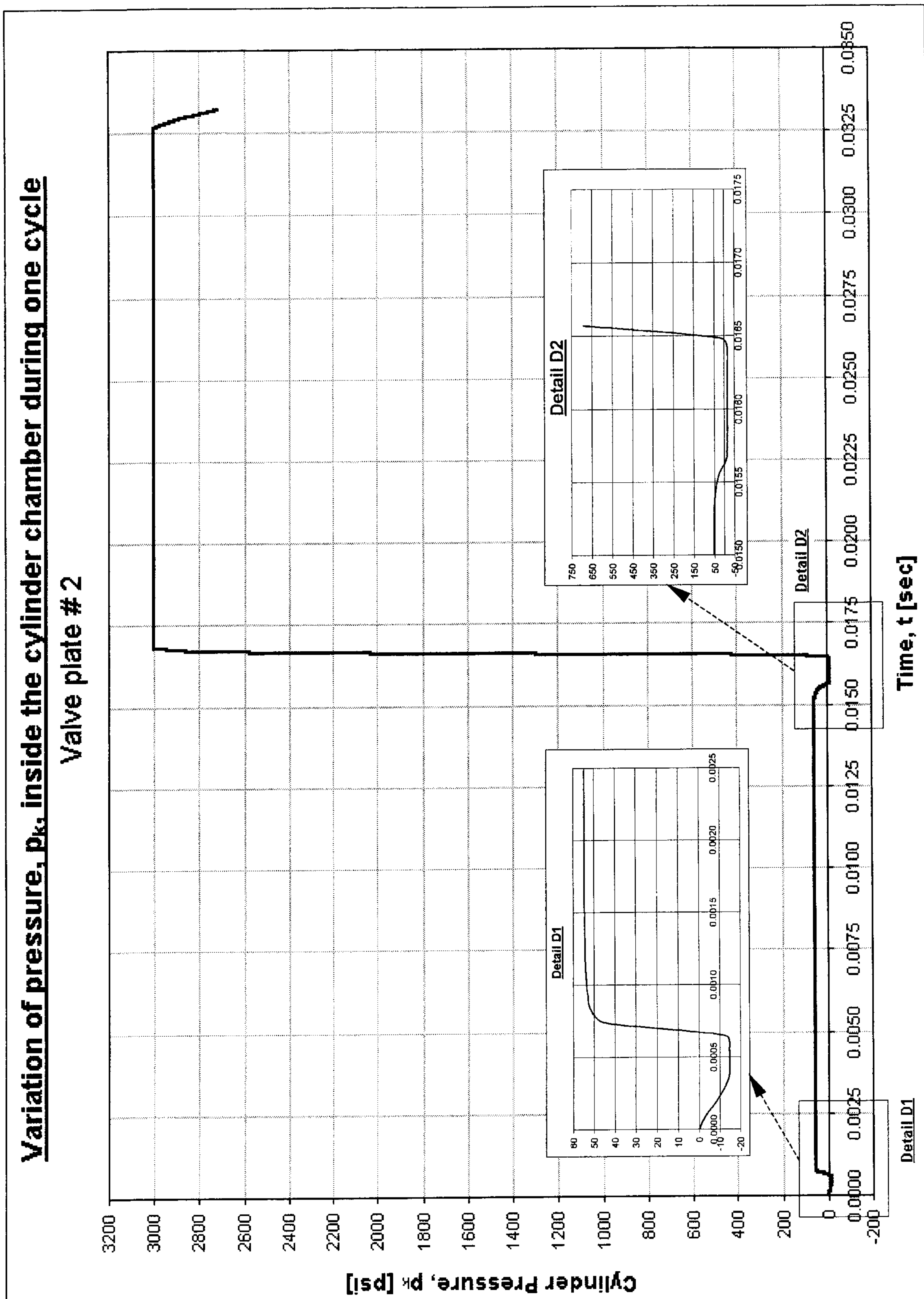

Fig. 6.24: Variation of pressure, p_K, inside the cylinder chamber using valve plate # 2

For the valve plate without transition notches – Fig. 6.23, Details C1 and C2 – the opening of the cylinder to the suction and discharge ports is abrupt and generates sudden variations of the pressure that can produce cavitation. For the valve plate with transition notches – Fig. 6.24, Details D1 and D2 – the opening of the cylinder to the suction and discharge ports is gradual and generates a progressive increase of the pressure that reduces the risk of cavitation occurrence.

In addition, the mathematical model allows determining the evolution of other functional parameters of the pump: variation of piston angular displacement, variation of piston linear displacement, variation of piston velocity, and variation of control volume. These functional parameters are presented in Fig. 6.25 to Fig. 6.28. They are included only to show the capabilities of the mathematical model and they are not employed in the analysis presented in this study, which is dedicated to the cavitation phenomenon.

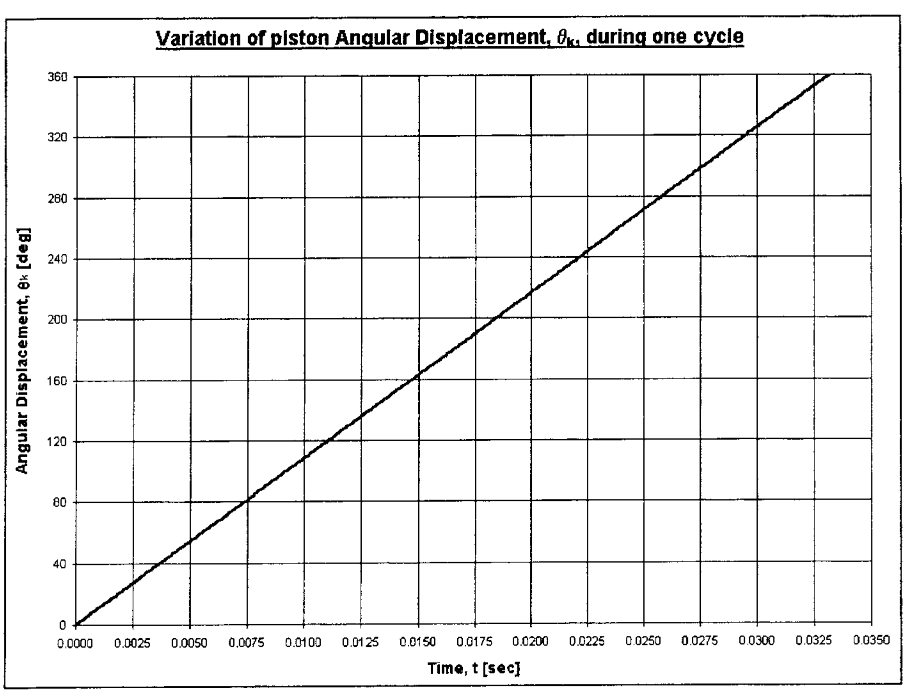

Fig. 6.25: Variation of piston angular displacement, θ_K

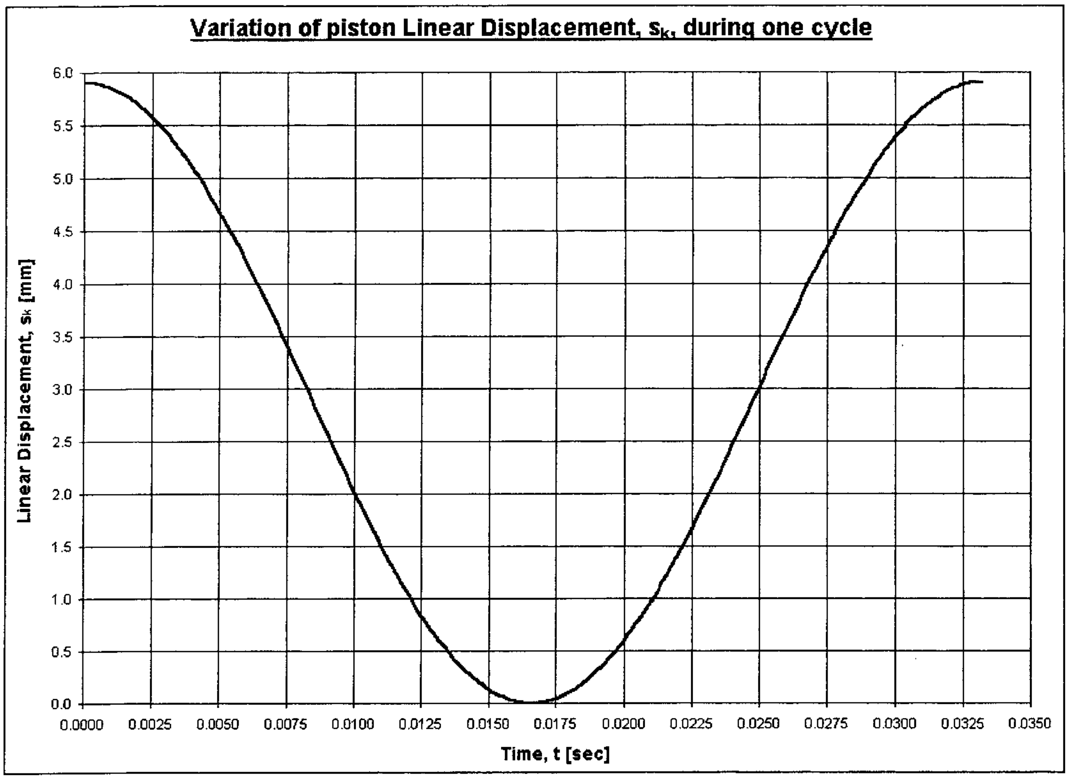

Fig. 6.26: Variation of piston linear displacement, s_k

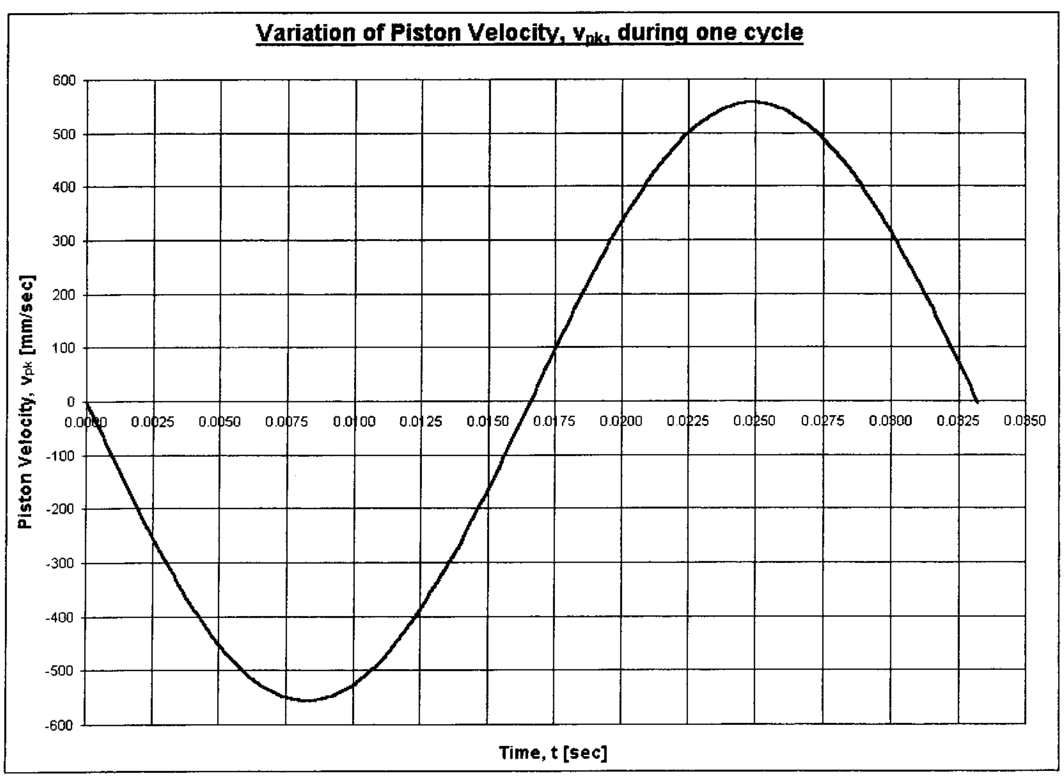

Fig. 6.27: Variation of piston velocity, v_{pk}

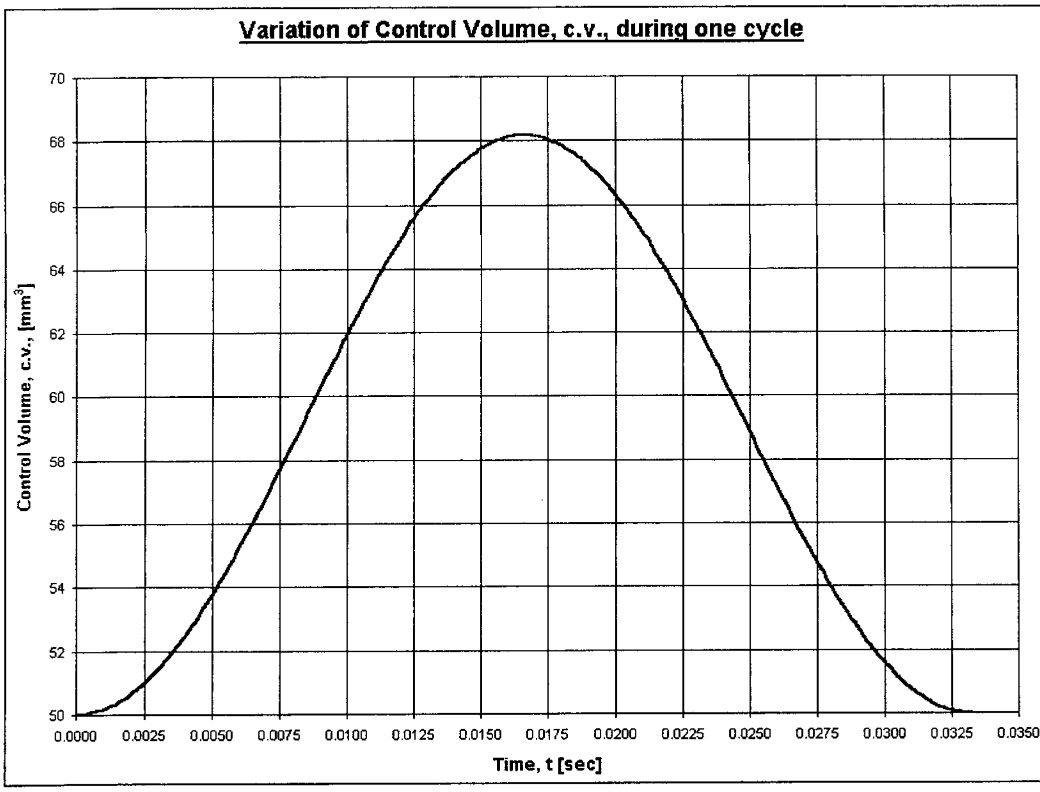

Fig. 6.28: Variation of control volume, c.v.

6.4.2 Experimental Results

6.4.2.1 Experimental Set-up

The tests on the pump fitted with the previously presented valve plates have been conducted at the supplier facilities using a dedicated *test cell*. The test cell, which is specifically conceived for executing performance tests, includes the following elements (see Fig. 6.29 for the experimental set-up diagram):

- *Electrical motor*, equipped with one speed control unit for pump driving at various regimes of functioning;
- *Pressurized reservoir of fluid*, equipped with a pressure control system for conditioning the pump suction line at various pressure values;

- *Heat exchanger* for conditioning the fluid temperature during the tests;
- *Electro-valve* installed on the discharge line to control the hydraulic load of the pump and simulate the flow demand of the hydraulic system users;
- *Filter manifolds* installed on the discharge and case-drain lines to control the fluid cleanliness level;
- *Specific instrumentation* for monitoring the temperature, pressure and flow on the discharge, suction and case drain lines of the pump;
- *Data acquisition system*, represented by one Honeywell computer with 64 acquisition channels and capable of recording at a maximum sampling rate of 10,000 samples per second.

The performance tests of the pump were conducted using the following test conditions:

- Fluid: phosphate ester based base, low density, type IV, Skydrol LD4;
- Cleanliness level: class 7 as per National Aerospace Standards NAS 1638;
- Ambient: temperature 80 ± 5 °F, humidity 10-30%, pressure 15 ± 5 psia;
- Instrumentation: all pressures, temperatures, forces, torques, and flow transducers were calibrated to comply with Military Specifications requirements MIL-C-45662.

The nominal values of the pump operating test parameters are:

- Case-drain pressure: 80 ± 5 psig;
- Inlet pressure: 50 ± 5 psig for zero outlet flow;
- Outlet pressure: 3100 ± 50 psig for zero outlet flow;
- Inlet fluid temperature: 160 ± 10 °F.

In addition, the variation range, accuracy of measurement and sample rate of the pump parameters recorded during the test are presented in Table 6.2 below.

Table 6.2: Specifications of recorded operating test parameters

Parameter	**Range**	**Accuracy**	**Sample Rate**
Temperature	0 – 250 °F	± 5 °F	5 samples / sec
Torque	0 – 2,000 lbf in	± 1% full scale	5 samples / sec
Motor speed	0 – 10,000 rpm	± 25 rpm	5 samples / sec
Outlet flow	1 – 50 gpm	± 1% full scale	5 samples / sec
Outlet pressure	0 – 5,000 psig	± 0.5% full scale	10 samples / sec
Outlet pulsations	0 – 1,500 psig	± 0.5% full scale	10,000 samples / sec
Case-drain flow	0.5 – 5 gpm	± 1% full scale	5 samples / sec
Case-drain pressure	0 – 500 psig	± 1% full scale	5 samples / sec
Inlet pressure	0 – 100 psig	± 1% full scale	10 samples / sec

Fig. 6.30 and Fig. 6.31 provide the exterior of the test cell, while Fig. 6.32 and Fig. 6.33 show the installation of the pump within the test cell.

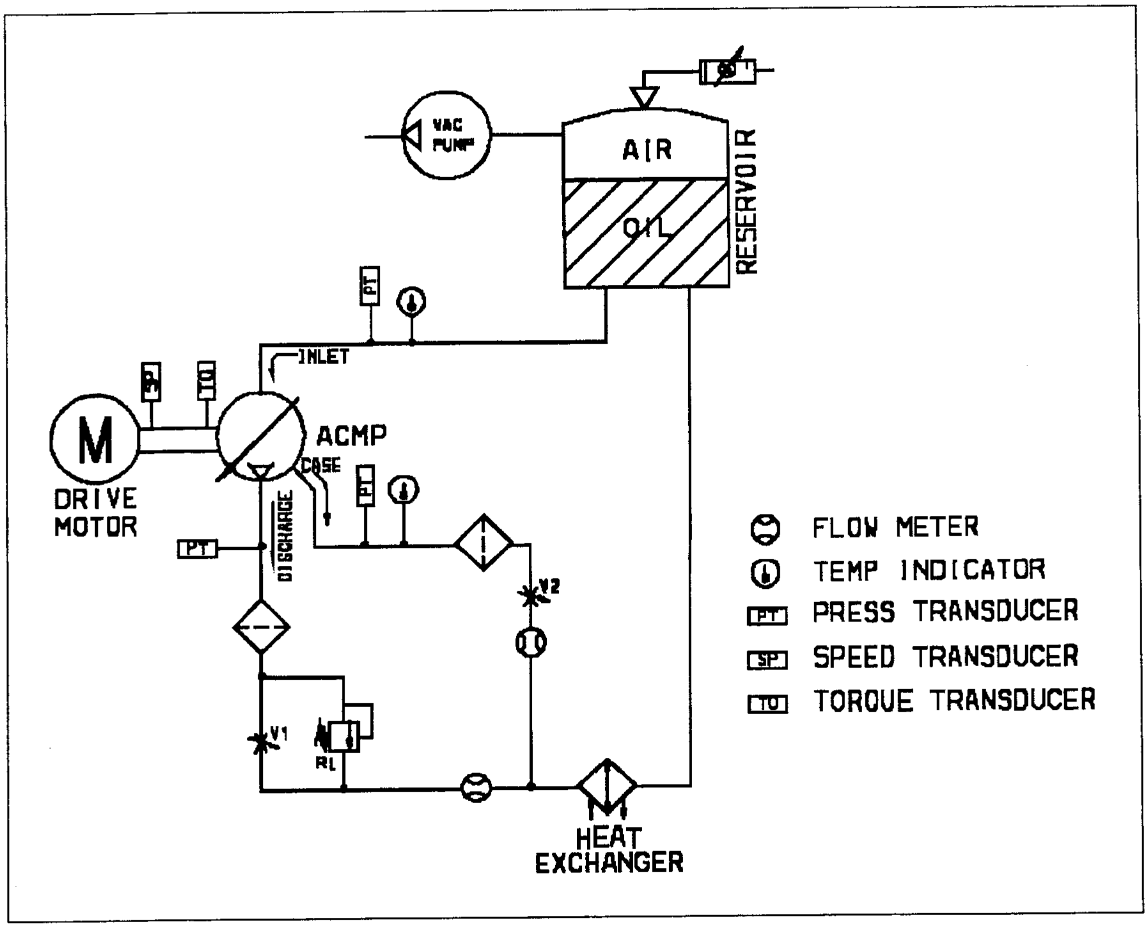

Fig. 6.29: Experimental set-up diagram

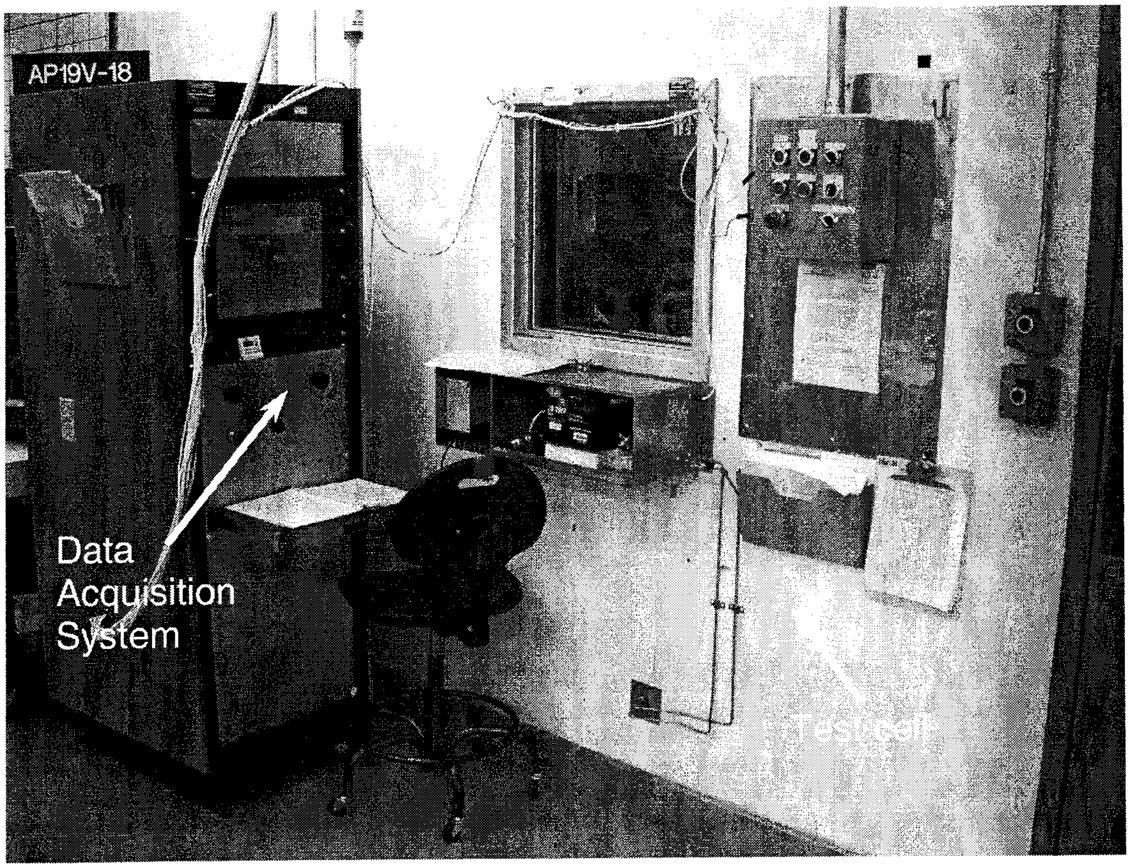

Fig. 6.30: Experimental set-up

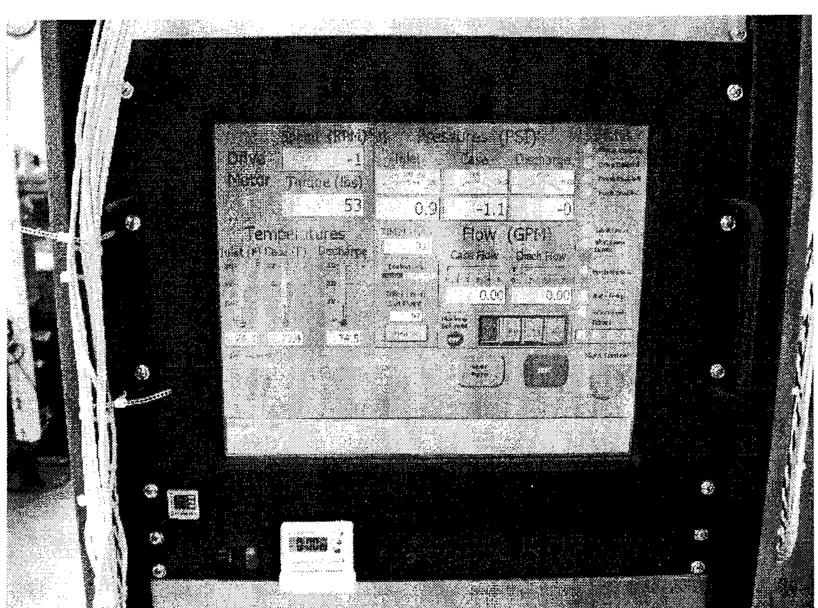

Fig. 6.31: Data acquisition system (detail)

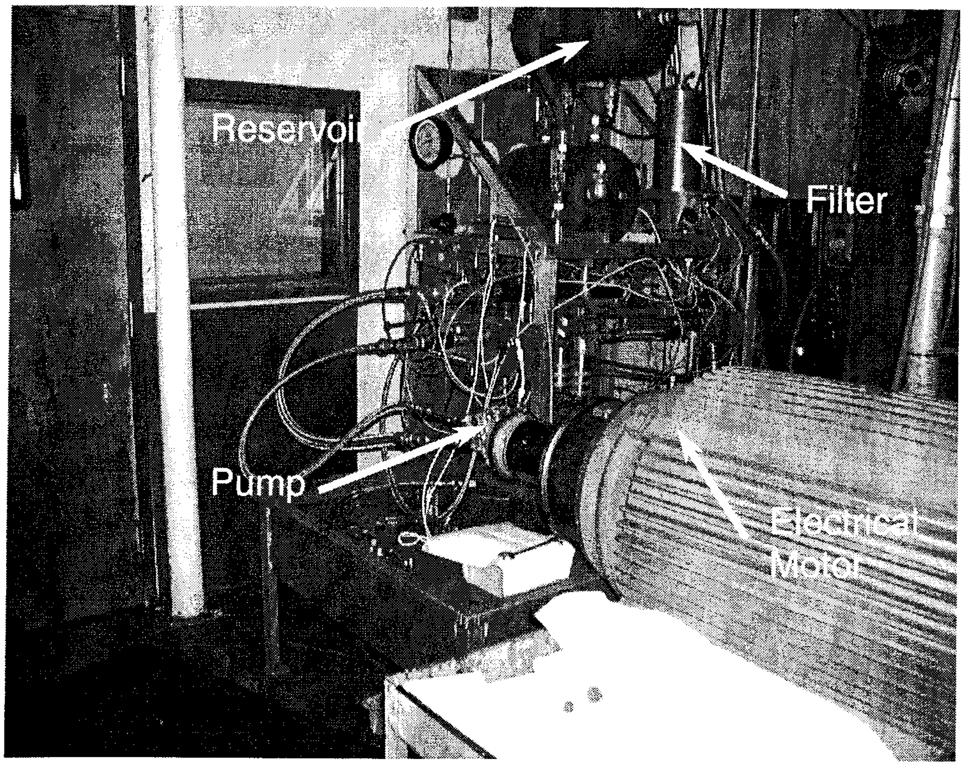

Fig. 6.32: Pump installation within the test cell

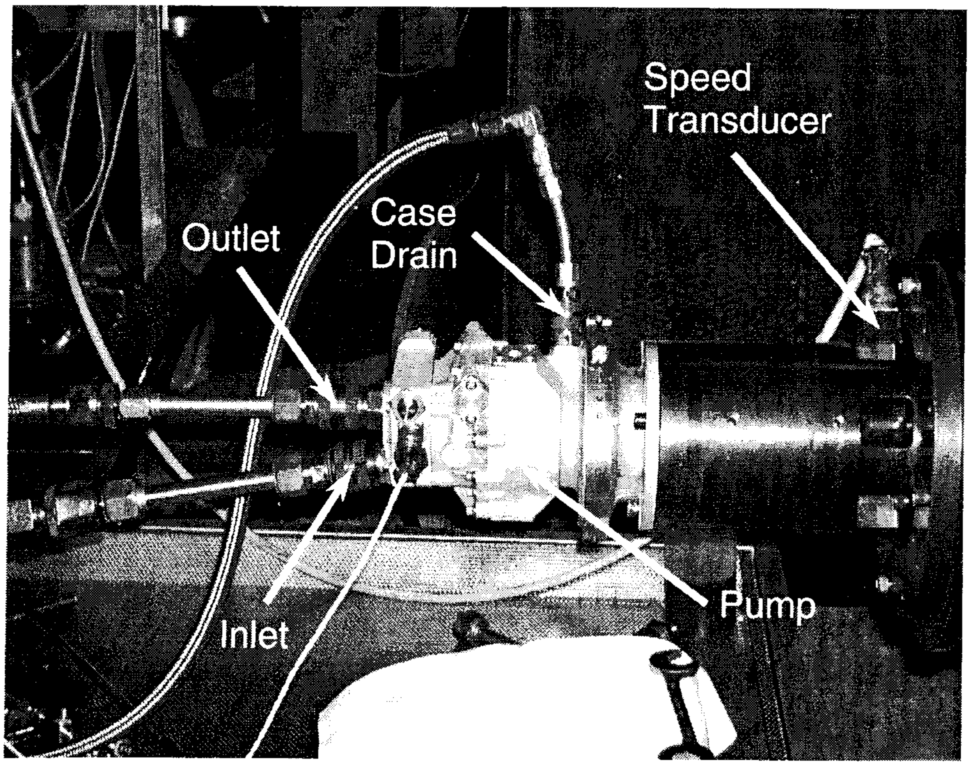

Fig. 6.33: Pump installation within the test cell (detail)

6.4.2.2 Test Procedure

The pump has been submitted to the following tests:

a) *Structural test*

Prior to starting the performance and cavitation tests, the pump is examined for external damage and proper assembly. In order to verify its structural integrity and determine the external leakage value, the pump is submitted to a *proof pressure test* for 2 minutes: 4500 psig for the outlet port, and 900 psig for the inlet and case drain ports.

b) *Discharge pressure set-up*

The pump compensator, which controls the pump outlet pressure in function of the flow demand of the system, is adjusted to deliver 3100 ± 50 psig at zero discharge flow.

c) *Performance tests*

Prior to starting the cavitation tests, the pump is submitted to the following performance tests in order to evaluate the impact of valve plate configuration (geometrical characteristics) on the pump performance:

– *Maximum flow, torque and discharge pressure*: with the pump set-up as shown in Fig. 6.14, the discharge flow, running torque and discharge pressure are measured at various pump speeds;

– *Pressure stability:* for various operating speeds, the response of the pump compensator to flow demands is verified if its functioning is free of persistent oscillations from the flow control;

– *Discharge pressure pulsations*: for various operating speeds and discharge flow values, peak-to-peak discharge pressure pulsations during nominally steady operating conditions are recorded;

- *Case-drain flow*: the case-drain flow is recorded at various speeds, case-drain pressures, and discharge flow values;
- *Response time*: the time interval between the instant when an increase/decrease of discharge pressure is initiated and the subsequent instant when discharge pressure reaches its first value is recorded.

During these performance tests, no unusual low noise, chatter or vibrations, low frequency pulsations or compensator cycling have been recorded. Thus, it was concluded that the *geometrical characteristics of the valve plates do not degrade the designed performance of the pump.*

d) *Cavitation test*

The results of this test are used to validate the pump mathematical model. The cavitation test is conducted in conformity with the Aerospace Standards AS595 requirements using the following procedure:

- By gradually opening the valve on the discharge line, the pump is brought at 3000 psi discharge pressure, value which corresponds to maximum discharge flow of the pump;
- The suction pressure is adjusted to 65 psi (120% of the rated suction pressure) by gradual opening the valve on the suction line;
- After stabilisation of this operating regime, the suction line valve is gradually closed in steps small enough to clearly bring on the on-set of cavitation and its effects at the output.

In conformity with this AS595 procedure, the first degradation of the discharge flow and pressure shown in Fig. 6.34 is recorded at 55 psi suction pressure, and it is indicating the initiation of cavitation. *These operating conditions of the pump and the cavitation occurrence duplicate the behaviour of the pump on the aircraft.*

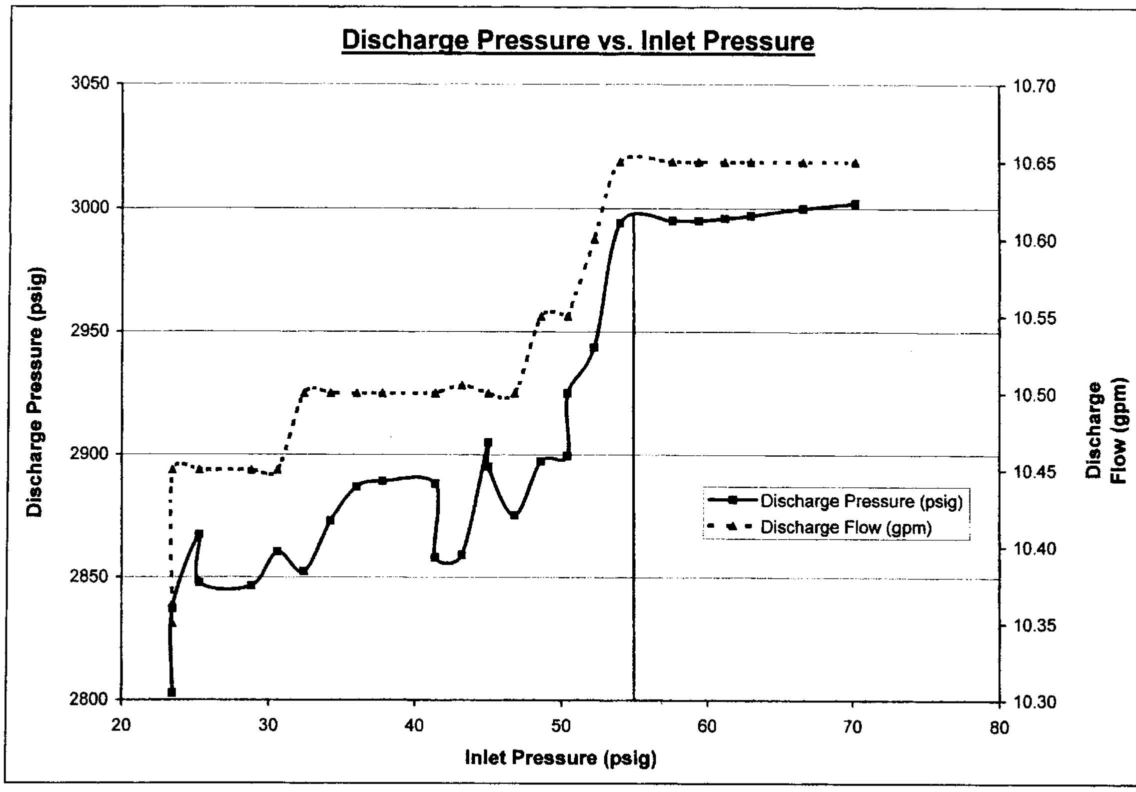

Fig. 6.34: Cavitation test results

The results from this operating point of the pump were extracted and plotted on an expanded time scale in Fig. 6.35 to Fig. 6.38 in order to make them compatible with the time scale used in the mathematical model.

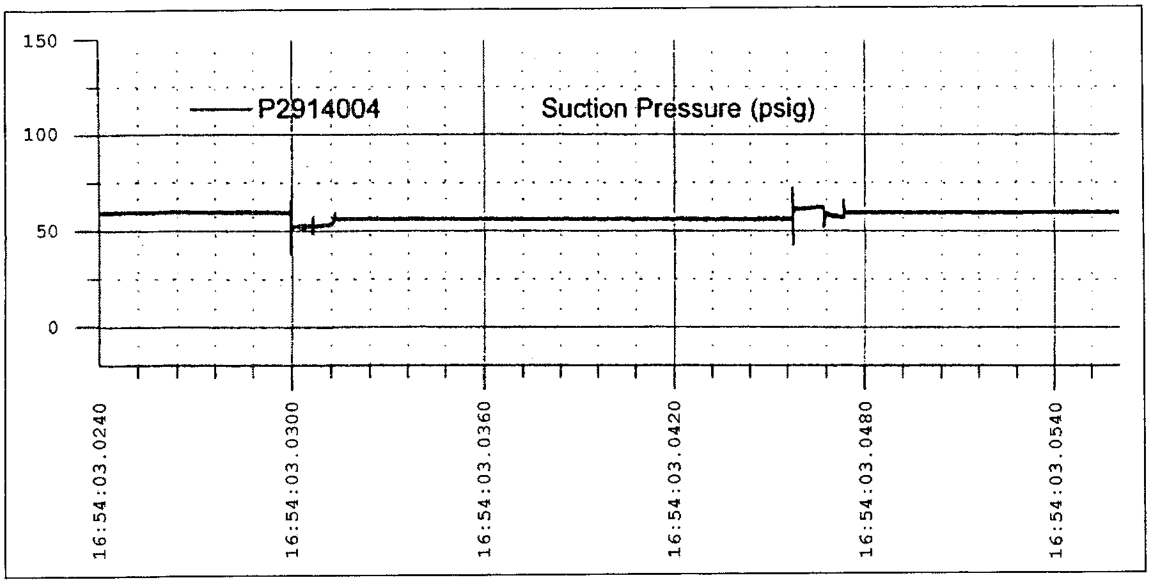

Fig. 6.35: Valve plate # 1 – Variation of Suction pressure for one cylinder during one cycle

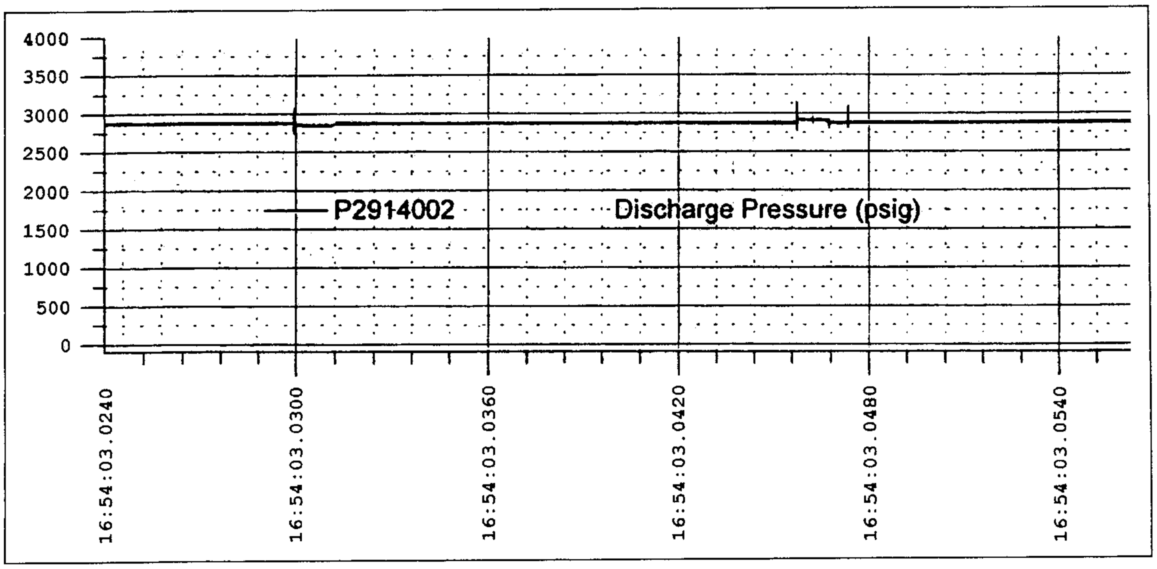

Fig. 6.36: Valve plate # 1 – Variation of Discharge pressure for one cylinder during one cycle

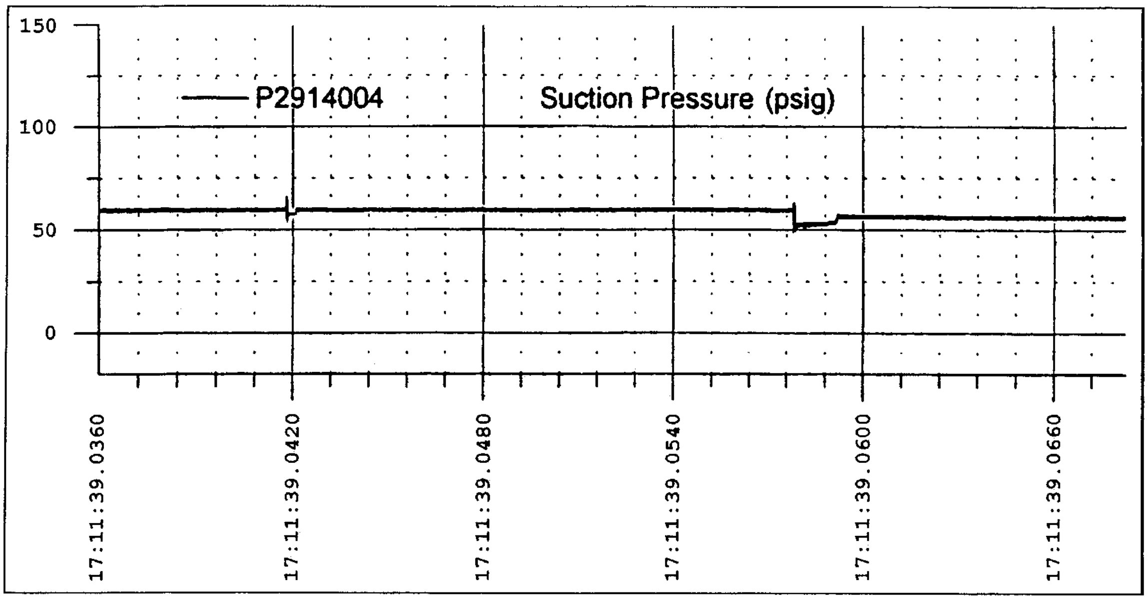

Fig. 6.37: Valve plate # 2 – Variation of Suction pressure for one cylinder during one cycle

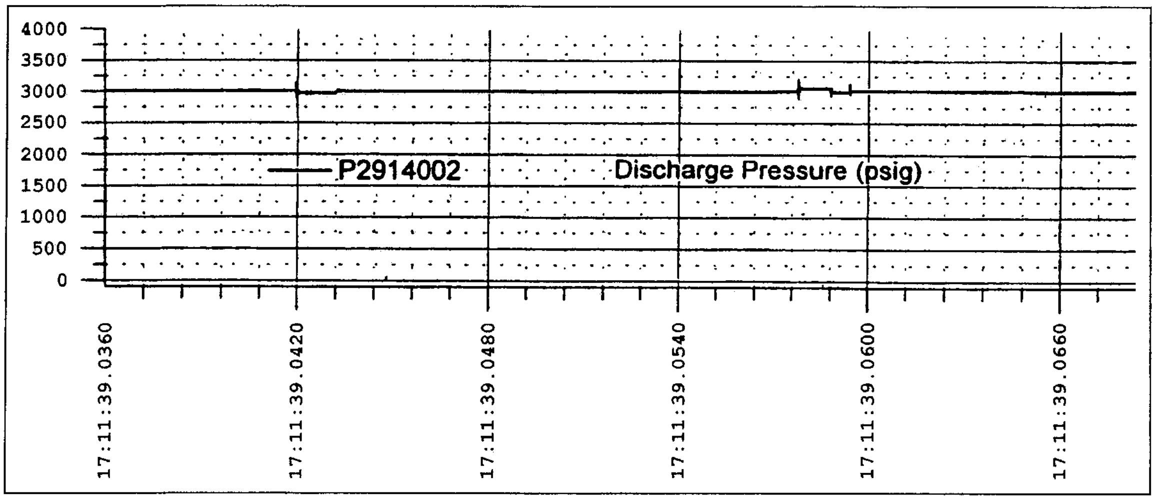

Fig. 6.38: Valve plate # 2 – Variation of Discharge pressure for one cylinder during one cycle

The evolution of suction and discharge pressures for one cycle of the pump obtained from tests is compared, on the same graph, with the pressure evolution inside one cylinder calculated by the model.

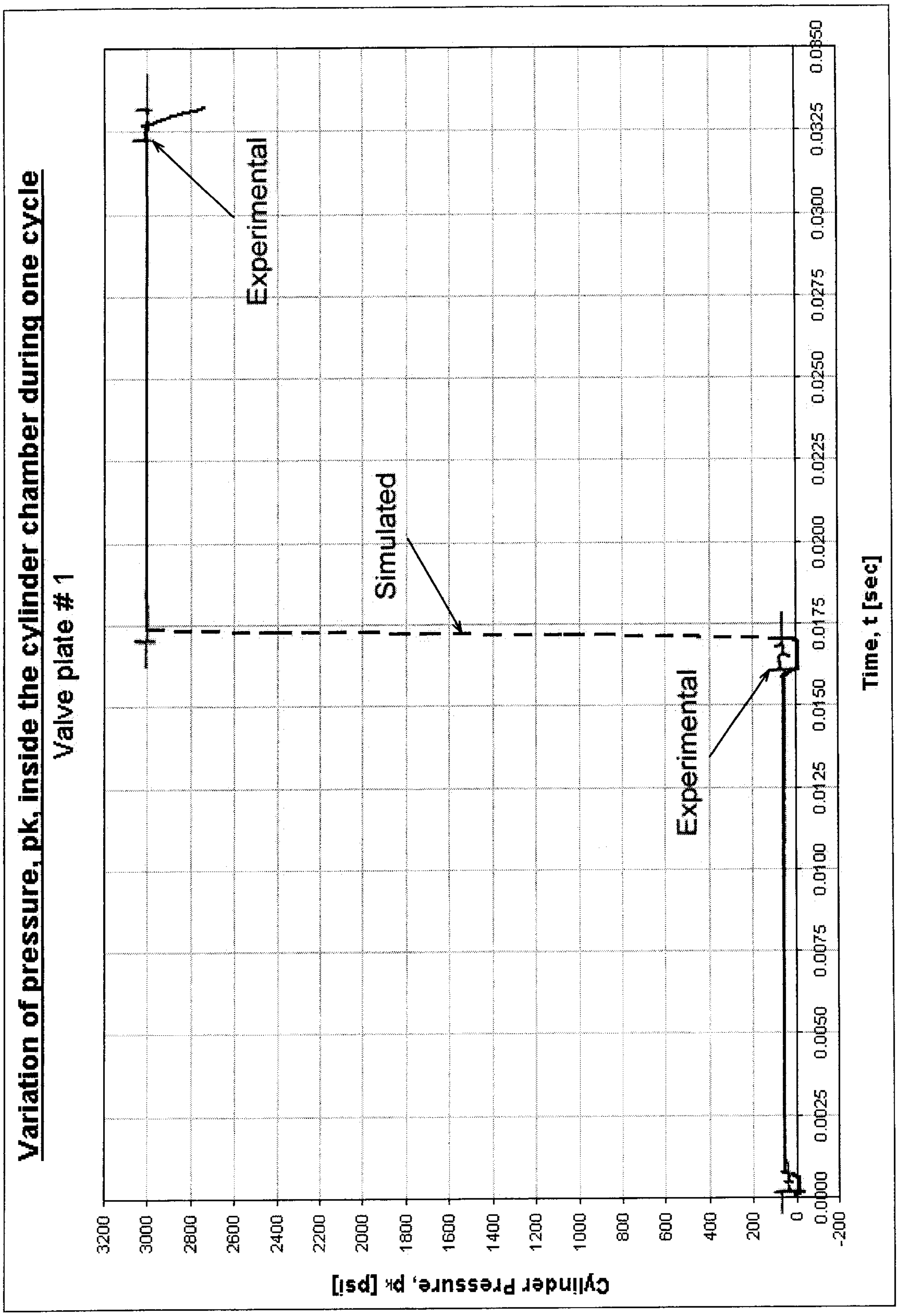

Fig. 6.39: Valve plate # 1 – Validation of variable displacement axial piston pump mathematical model

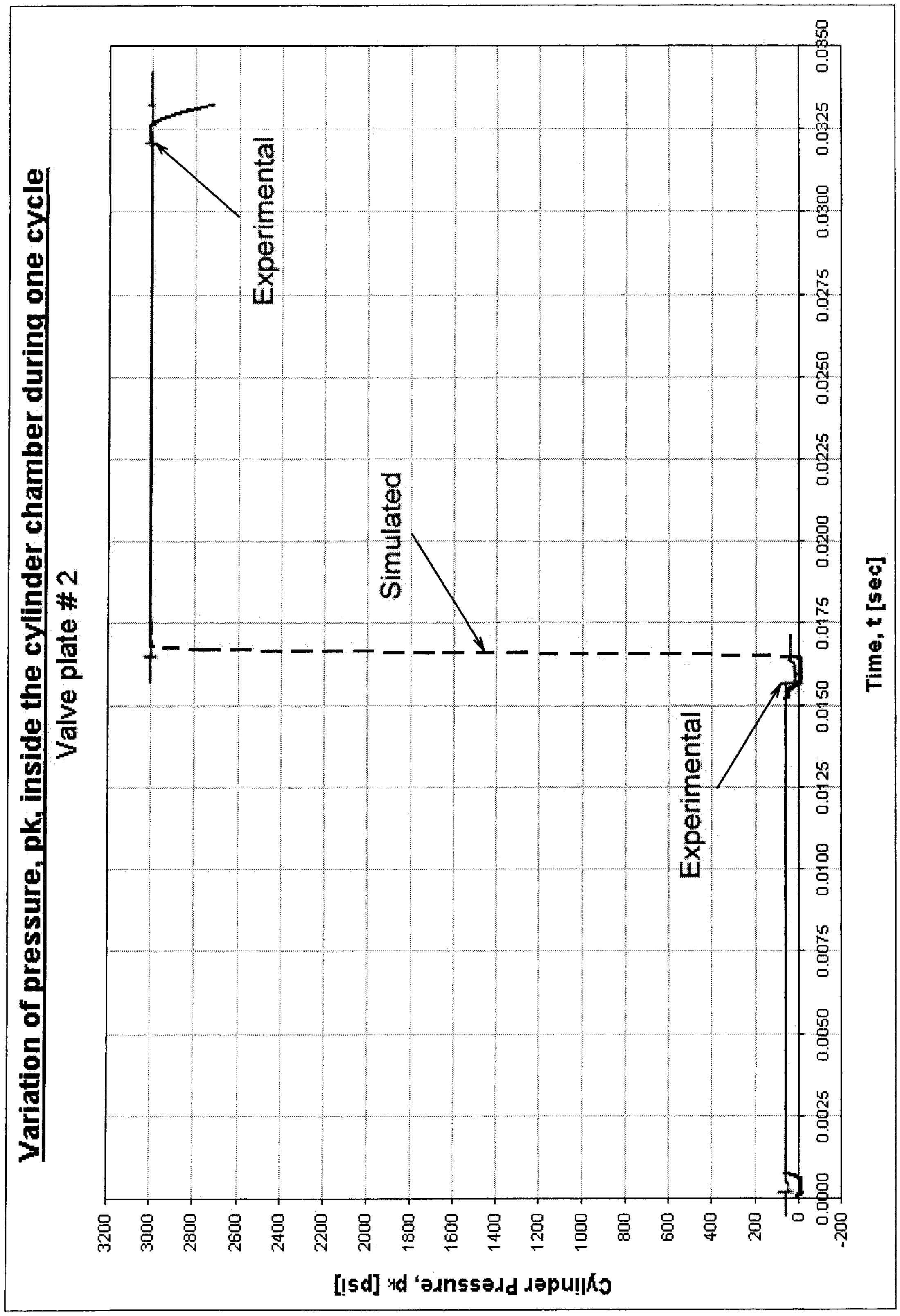

Fig. 6.40: Valve plate # 2 – Validation of variable displacement axial piston pump mathematical model

Fig. 6.39 presents the comparison between the experimental data and the numerical simulated values for the valve plate without the transition notches.

Fig. 6.40 presents the comparison between the experimental data and the numerical simulated values for the valve plate with the transition notches.

For both experimental and simulated results, the perturbations of the pressure inside the cylinder occur at the same moment of the cycle. The same locations of the pressure perturbations for the suction and discharge ports corresponding to one cycle validate the mathematical model of the pump.

The impact on the pressure variation at suction and discharge ports of the transition notches is the change in amplitude of pressure variation:

- For the valve plate without the transition notches, the amplitude is higher and it is accompanied by signal noise. This indicates a momentary flow instability that may be associated with the occurrence of cavitation.
- For the valve plate with the transition notches, the amplitude is lower and the signal noise is reduced. This indicates a reduced momentary flow instability that may make it less sensitive to cavitation occurrence.

CHAPTER 7

VARIABLE DISPLACEMENT AXIAL PISTON PUMP REDESIGN SOLUTIONS

CHAPTER 7

VARIABLE DISPLACEMENT AXIAL PISTON PUMP REDESIGN SOLUTIONS

Multiple factors influence the occurrence of cavitation process in variable displacement axial piston pumps. These factors may be organized in the following categories:

- *Factors associated with the pump's geometrical characteristics*;
- *Factors associated with the pump's inlet port conditions*; and
- *Factors associated with the pump's working regime.*

The factors associated with the pump's geometrical characteristics include the *geometry of suction and discharge ports* located on the valve plate (see Fig. 5.11), as well as the *swash plate angle* (see Fig. 6.3). The geometry of suction and discharge ports deals with the presence of transition notches at the beginning of the "kidney-shaped" orifices, as well as with the length of the transition period between the suction and discharge areas.

The swash plate angle also influences the occurrence of cavitation in the pump as a variation of this angle generates a variation of the cylinder volume. Subsequently, the occurrence of cavitation process is affected since the available cylinder volume influences the degree of stretching/compressing to which the liquid medium inside is subjected.

The factors associated with the pump's inlet port conditions are the *pressure* and *flowrate characteristics* of the hydraulic system where the pump is installed. The inlet pressure affects the inception and development stages of the cavitation process: as the suction pressure increases, the occurrence of the cavitation process in the pump is reduced. Alternatively, the inlet flowrate influences the pressure inside the pump's cylinders during the suction period: as the flowrate increases, the occurrence of the cavitation process in the pump is reduced.

The factors associated with the pump's working regime involve the *angular velocity* (rotation speed) *of the pump shaft*. This element affects the linear velocity of the pistons inside the cylinder block. A series of studies, independent of the analysis of cavitation occurrence in axial piston pumps, investigated the possibility of cavitation occurrence behind a moving disc [91]. As observed in these studies, gas-filled cavities may occur and develop as a result of the linear motion of a disc within a liquid medium. Fig. 7.1 below depicts this phenomenon.

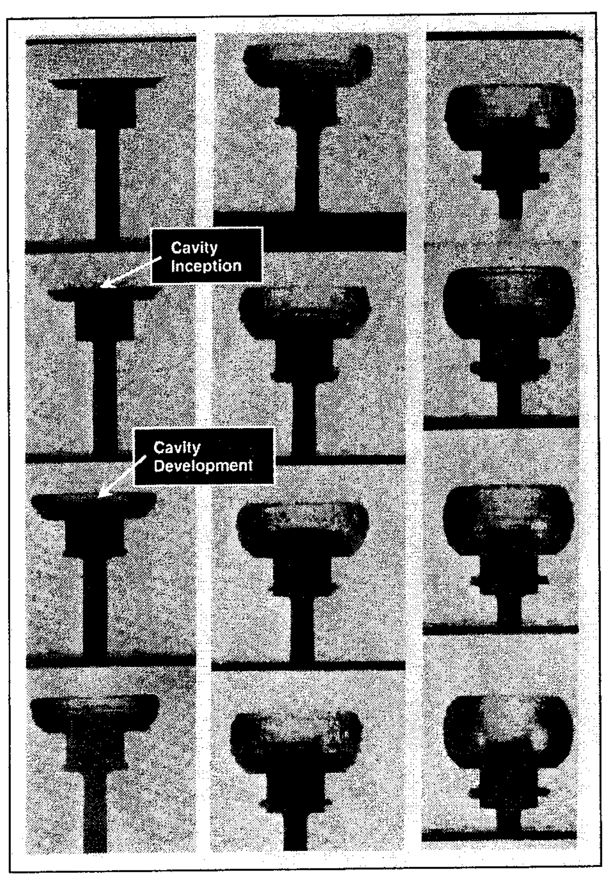

Fig. 7.1: Occurrence of cavitation behind a moving disc [92]

Although all factors presented above may be used to reduce or eliminate the cavitation process generated by the pump, most of them cannot be considered by this study due to the operating conditions of the hydraulic system and the pump's working regime.

The pump considered in this study operates within a hydraulic system that limits its inlet conditions (pressure and flowrate). As a result, the factors associated with the pump's inlet port conditions shall not be considered by the redesign process presented herein.

In this study, the swash plate angle was selected constant and it corresponds to the maximum flowrate operating condition. Under this circumstance the pump is must susceptible to cavitate. Therefore, the swash plate angle, as part of the factors associated with the pump's geometrical characteristics, it is not a variable of the mathematical model. Hence, the variation of the swash plate angle may safely be excluded from the analysis.

Finally, the factors associated with the pump's working regime (rotation speed) may also be excluded from the analysis performed for the redesign process. The independent studies previously mentioned allow concluding that more significant velocity and acceleration values are required to stretch and crack the liquid medium contained by the pump's cylinders. This condition is confirmed by the lack of physical evidence (damage) on the inner circular surface of the pump pistons exposed to the hydraulic fluid.

Therefore, the only element that shall be considered by the redesign solutions presented in this study is the *geometry of suction and discharge ports*. A comprehensive theoretical study that evaluates the design solutions associated with this element with the purpose of controlling the occurrence of cavitation in the pump is presented below.

7.1 DESIGN SOLUTIONS CORRESPONDING TO THE GEOMETRY OF SUCTION AND DISCHARGE PORTS – VALVE PLATE REDESIGN

As presented before, the geometry of suction and discharge ports located on the valve plate involves two design solutions that affect the occurrence of cavitation phenomenon in the pump. These solutions are:

- The introduction of *transition notches* at the beginning of the "kidney-shaped" orifices; and
- The *length of the transition period* between the suction and discharge areas.

The results obtained during the creation of the pump mathematical model allow stating that the presence of *transition notches* at the beginning of the "kidney-shaped" orifices reduces the level of cavitation produced by the pump. This effect results from the additional port area available, which reduces the degree of stretching/compressing of the liquid medium inside the cylinders. From this condition it may be assumed that, as the area of the notch increases, the cavitation process is reduced. In this study, triangular section notches are selected as this geometry can be easily implemented using the current fabrication technology. The area of a triangular section notch may be increased through the augmentation of its opening angle, φ, and depth angle, δ, (Fig. 7.2).

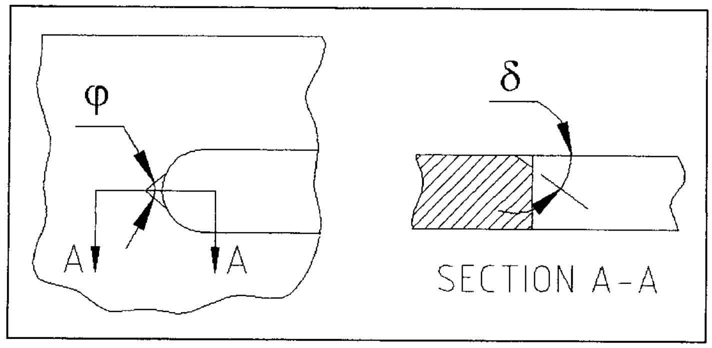

Fig. 7.2: Geometry of the notch

Alternatively, the *transition period* included in the valve plate design (see Fig. 7.3) is the second element that may affect the occurrence of cavitation in the pump. The transition period, which produces the individual closing all pump cylinders as they traverse the suction and discharge areas, ensures that hydraulic fluid from the outlet port does not pass into the inlet port. However, during this period, the pump pistons continue to travel, subjecting the liquid medium inside the cylinders to relatively high levels of stretching/compressing. A brief analysis of the transition period and its effect allows stating that, when its length is reduced until it equals the cylinder opening length, the cavitation phenomenon produced by the stretching/compressing of liquid through piston movement is eliminated. Under these circumstances, only the flow in and out of the cylinders shall be accounted for generating cavitation in the pump.

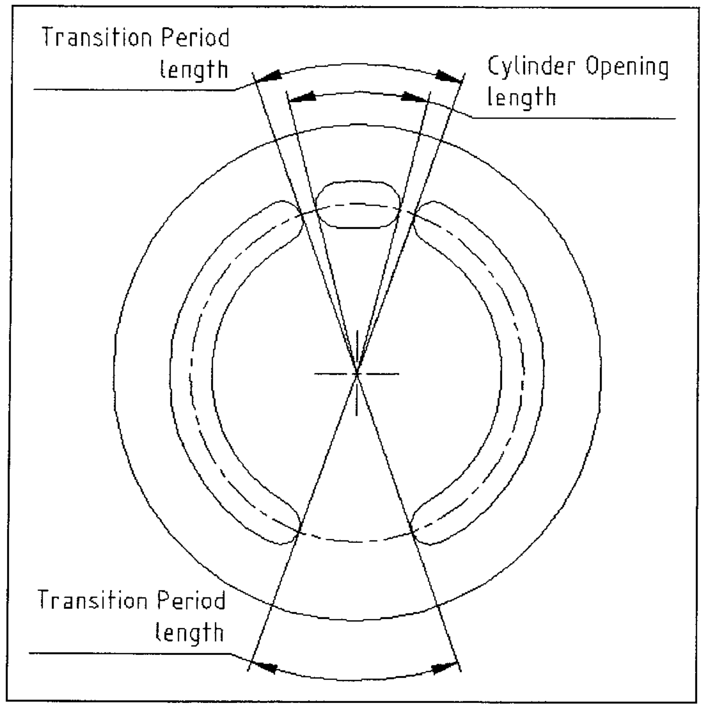

Fig. 7.3: Transition period

Based on these assumptions, the valve plate may be redesigned with the purpose of reducing/eliminating the cavitation process produced by the pump. The mathematical model created in Chapter 6 is used to investigate these designs.

For the first redesigned configuration, the transition notch area is increased by modifying the opening and depth angles ($\varphi = 55°$ and $\delta = 30°$). In addition, the transition period is made equal to the cylinder opening length. The valve plate incorporating these changes is shown in Fig. 7.4. The pressure variation inside the cylinder chamber using this initial redesign is presented in Fig. 7.5. From the results obtained it is observed that, as the notch area increases and the transition period is reduced to a minimum, the cavitation process generated by the pump is decreased.

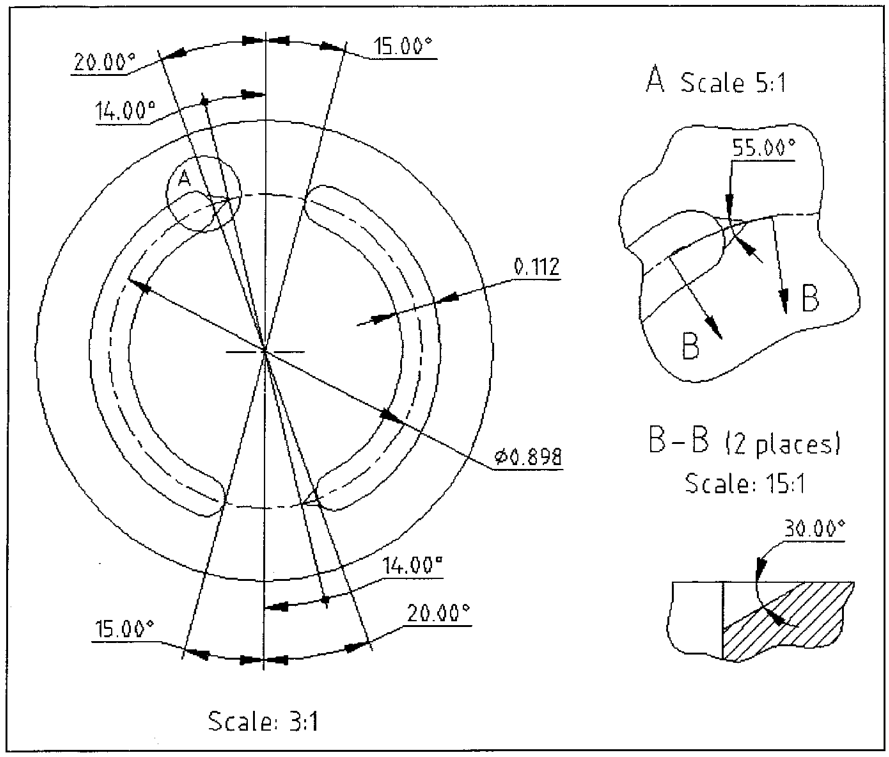

Fig. 7.4: Valve plate redesign # 1

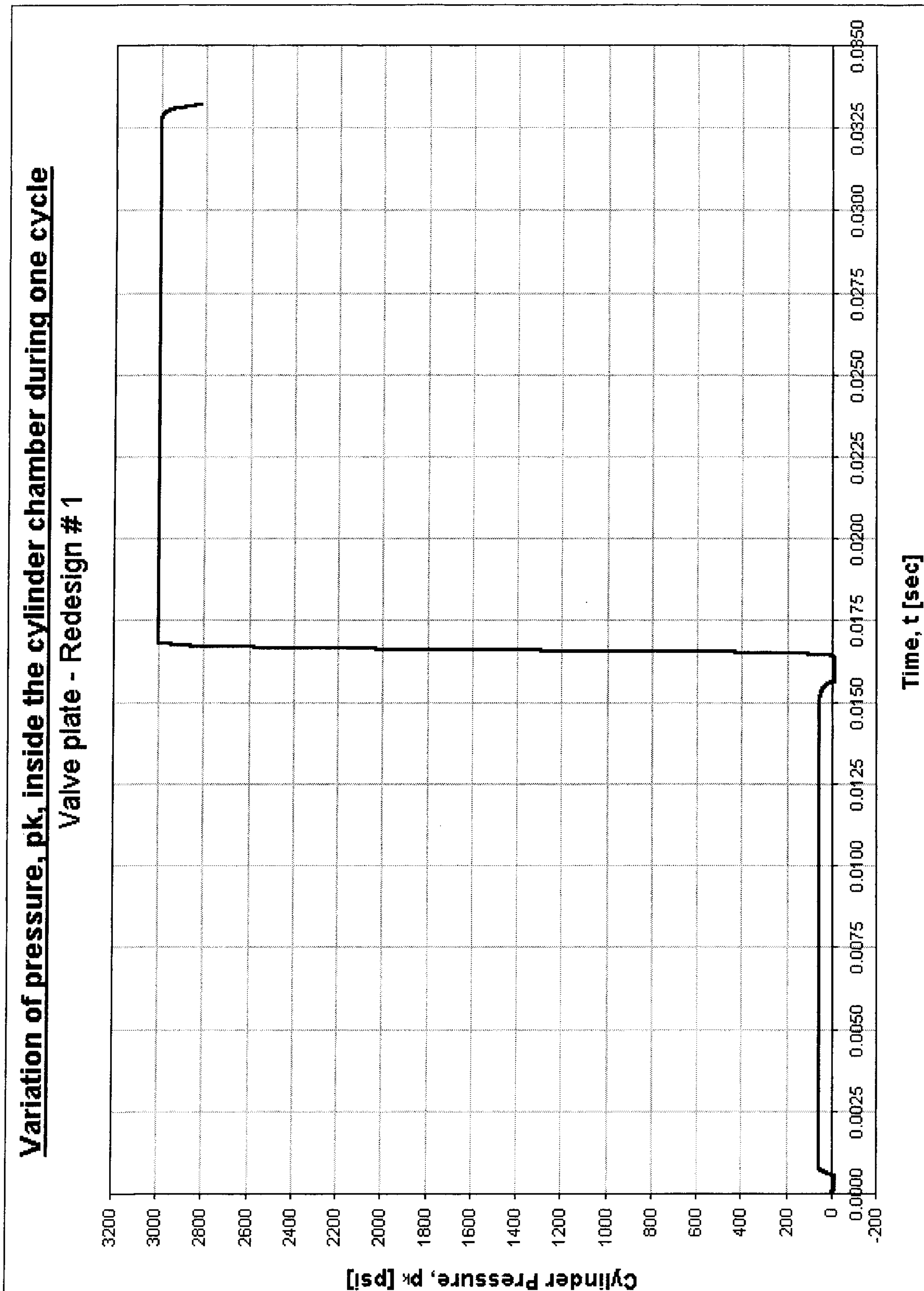

Fig. 7.5: Variation of pressure, p_k, inside the cylinder chamber using valve plate redesign # 1

For the second redesign, the notch area is further increased (φ = 60° and δ = 35°), while the transition period is maintained equal to the cylinder opening length. This new valve plate configuration is shown in Fig. 7.6. The pressure variation inside the cylinder chamber using this second redesign is presented in Fig. 7.7. Once again, from the results obtained it is observed that, as the notch area is further increased and the transition period is maintained equal to the cylinder opening length, the cavitation process generated by the pump is further decreased.

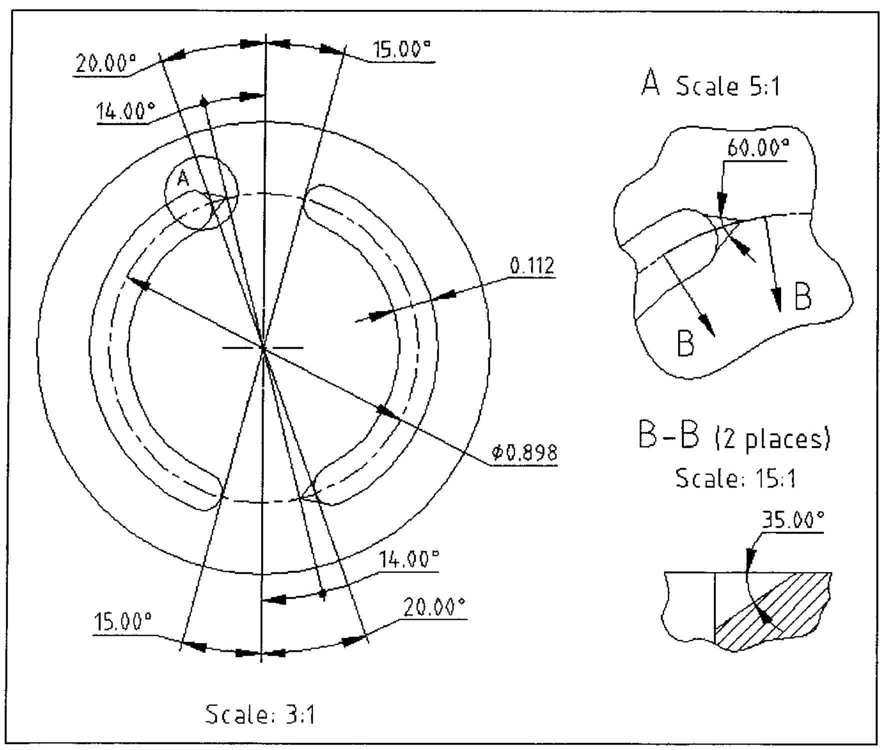

Fig. 7.6: Valve plate redesign # 2

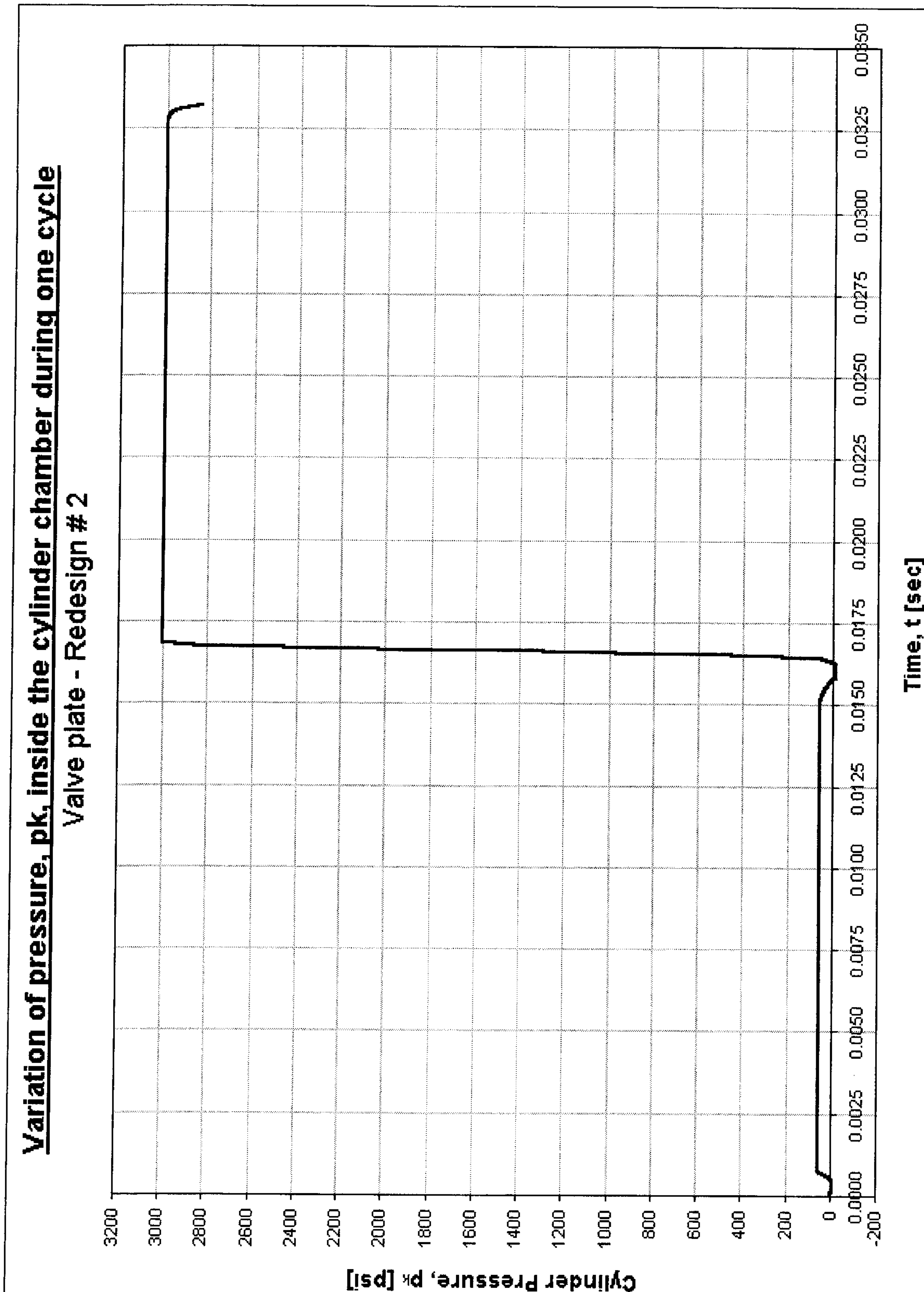

Fig. 7.7: Variation of pressure, p_k, inside the cylinder chamber using valve plate redesign # 2

Therefore, from the results obtained using the presented valve plate redesigns it may first be concluded that, as the notch area is increased, the sensitivity of the pump to cavitation is reduced. Consequently, it may be stated that the notch effect on cavitation occurrence is maximized when the notch area is maximum. The maximum notch area is obtained when its opening angle reaches 180° and the depth angle is 90°. Furthermore, *the geometry of the cylinder opening shall match the geometry of the valve plate* as the suction/discharge areas obtained from overlapping of the inlet/outlet ports with the cylinder opening must also be maximized.

In addition, from the transition period analysis it is observed that its effect on pump cavitation is minimized when the transition period length equals the cylinder opening length.

The configuration of the valve plate incorporating these design elements is shown in Fig. 7.8.

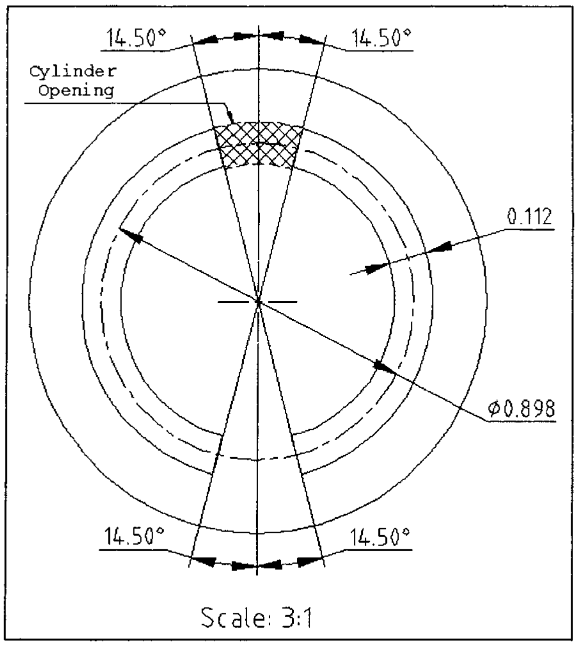

Fig. 7.8: Ideal valve plate configuration

While the proposed depth angle and transition period length can be obtained with relative ease, the current technological capabilities lead to a *conversion of the ideal "square" transition notch configuration into a "circular" transition notch configuration*.

Thus, *the final configuration of the valve plate that satisfies all cavitation reduction, and manufacturing requirements is characterized by circular openings of the "kidney-shaped" orifices and by an instantaneous connection of the pump cylinders to the inlet and outlet ports*. The configuration of the valve plate is shown in Fig. 7.9. The pressure variation inside the cylinder chamber using this optimized design is presented in Fig. 7.10.

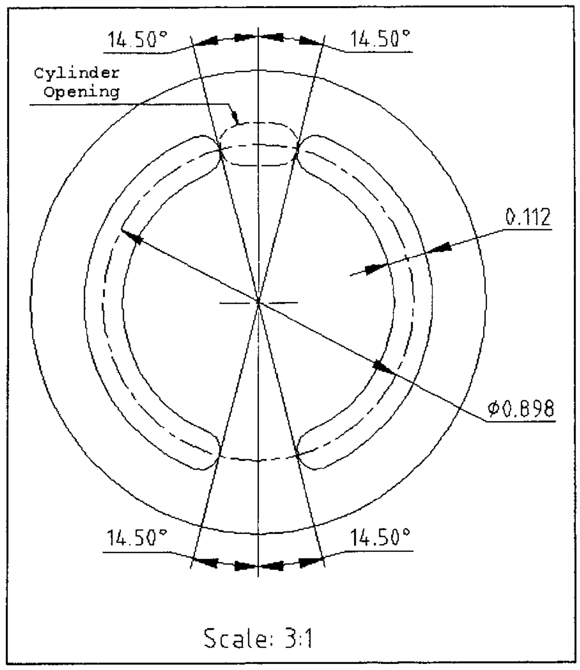

Fig. 7.9: Valve plate redesign # 3 – Final

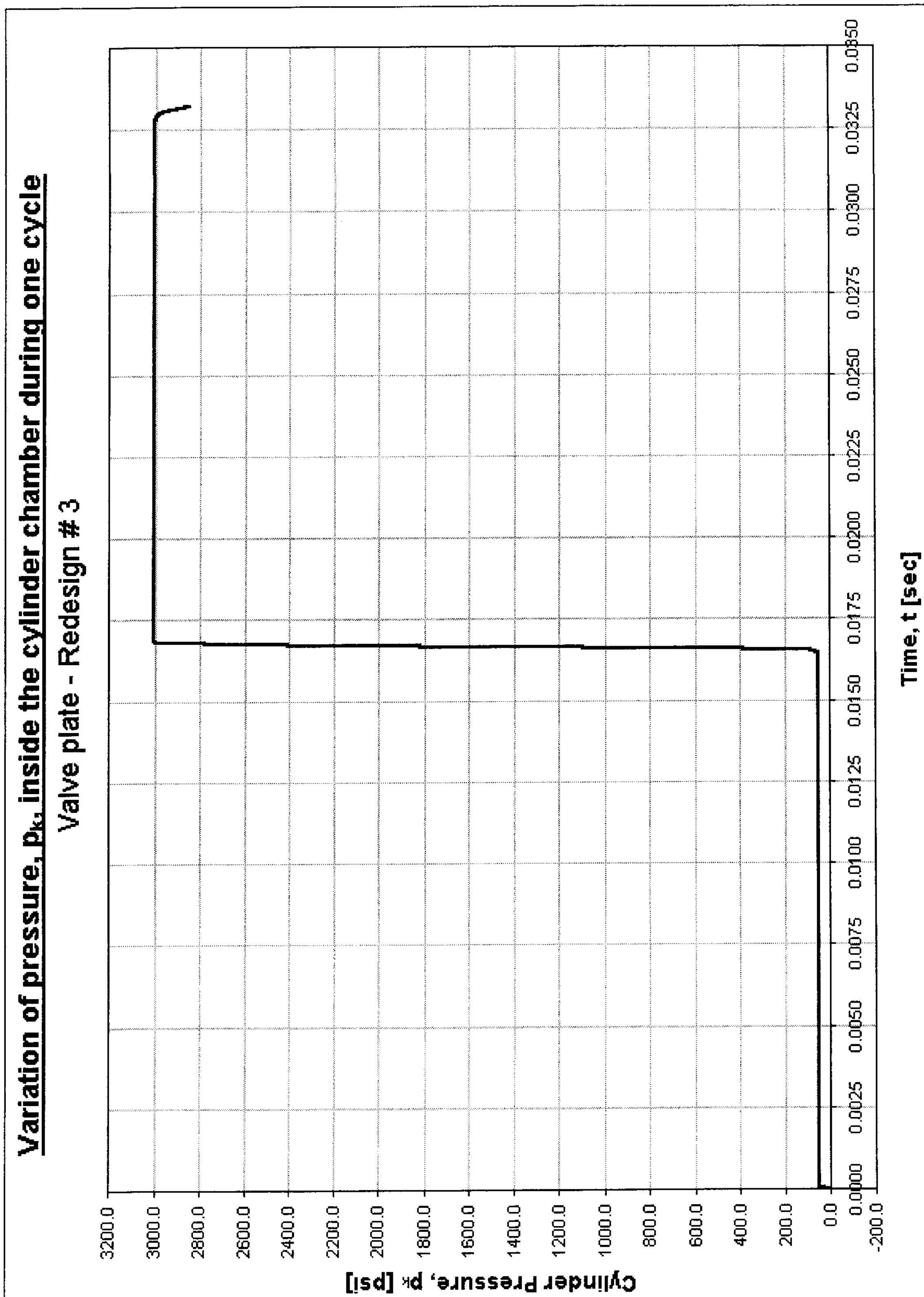

Fig. 7.10: Variation of pressure, p_k, inside the cylinder chamber using valve plate redesign # 3

From Fig. 7.10 it is observed that the pump considered in this study shall not produce cavitation when equipped with the determined valve plate design. However, it is important to recall that this condition is supported by the other geometrical characteristics of the pump, the selected operating conditions (inlet port conditions and working regime), and the physical characteristics of the liquid medium (viscosity). As it was previously stated, these elements were not altered given the operating context of the pump and thus, only the valve plate redesign was considered by this study.

CHAPTER 8

CONCLUSION

CHAPTER 8

CONCLUSION

1. Presently, the pump design is driven by only functional parameters and does not include cavitation pressure criterion. The pump is designed for full flow and pressure, as well as for maximum efficiency and minimum rejected heat. The inlet pressure value corresponding to the cavitation occurrence is determined only by tests, when the pump is ready for undergoing qualification analysis and no other modifications are envisaged. For this reason, the cavitation pressure resulting from the functional design criteria is imposed as a limitation condition for the operation of hydraulic system where the pump is installed.
2. At the aircraft level, mitigation of this restrictive condition requires specific solutions for the hydraulic system architecture, which has to guarantee that the inlet pressure will never drop below the value corresponding to cavitation occurrence. In spite of an appropriate design of the hydraulic system architecture and sizing, the interface complexity between various users may cause unforeseeable pressure drops below cavitation value. For this reason, a lower value of cavitation pressure of the pump is more desirable.
3. The effects of random occurrence of cavitation are cumulative and they will degrade the performance of actuation systems of the aircraft. The performance degradation of actuation systems may ultimately impact the aircraft safety.
4. Therefore, the pump sensitivity to cavitation occurrence shall be considered as a design criterion for the pump itself and not to be transferred as an operating limitation to the hydraulic system design for mitigation.

Means to reduce cavitation occurrence in the pump

As mentioned in the previous chapters of this study, the following means shall be used to reduce the occurrence of cavitation phenomenon.

a) At pump level:

- Modify the geometrical characteristics of the pump (geometry of suction and discharge ports located on the valve plate and angle of swash plate);
- Determine the working regime interval (angular velocity) at which the pump shall operate.

b) At system level:

- Adjust the pump's inlet port conditions (pressure and flowrate values of the hydraulic system where the pump is installed).

Contributions to cavitation understanding

The present study includes the following personal contributions to the understanding of the cavitation phenomenon:

- Improved description of all cavitation stages based on an exhaustive analysis of fundamental theories and principles of physics;
- Introduced the interpretation of cavitation occurrence conditions based on matter – energy relationship;
- Definition of the mathematical model of the variable displacement axial piston pump;
- Validation of the mathematical model using results from tests performed with two valve plate configurations;
- Identification of factors involved in the occurrence of cavitation phenomenon in the pump;
- Establishment of design solutions for the valve plate to reduce the pump sensitivity to cavitation conditions.

CHAPTER 9

SUGGESTIONS FOR FUTURE WORK

CHAPTER 9

SUGGESTIONS FOR FUTURE WORK

This study may be continued with the following activities:

- Definition of the mathematical model for the entire hydraulic system where the pump is installed in order to establish the interface between the operating conditions of the pump and the operating conditions of the hydraulic system users;
- Validation of this mathematical model using results of tests performed on the aircraft.

Although these activities may require more significant computational capabilities, the analysis involved in deriving and validating the mathematical model of the entire hydraulic system shall remain similar to the process presented in this study.

REFERENCES

1. Reynolds, O., "The causes of the racing of the engines of screw steamers investigated theoretically and by experiment", Institute of Naval Architecture, London, 1963, pp. 14, 56-57.
2. Pearsall, I. S., "Cavitation", Mills & Boon Limited, London, 1977, pp. 13.
3. Robertson, J. M., and Wislicenus, G. F., "Cavitation state of knowledge", The American Society of Mechanical Engineers, New York, 1969, pp. 5.
4. "Webster's new collegiate dictionary", G. & C. Merriam Company, Massachsetts, 1974, pp. 178.
5. Serway, R. A., "Physics for scientists and engineers", Saunders College Publishing, Montreal, 1990, pp. 393-394, 560-581.
6. Kurtus, R., "Theories of matter", http://www.school-for-champions.com/science/matter.htm, 2004.
7. Harrison, D., "Forces between molecules", http://www.newi.ac.uk/beckleyc/fbmolecules.htm, 2004.
8. Serway, R. A., "Physics for scientists and engineers", Saunders College Publishing, Montreal, 1990, pp. 161-164, 183-184.
9. Anton, I., "Cavitation", Romanian Academy Publishing House, Bucharest, 1984, pp. 7.
10. Robertson, J. M., and Wislicenus, G. F., "Cavitation state of knowledge", The American Society of Mechanical Engineers, New York, pp. 15-16.
11. Anton, I., "Cavitation", Romanian Academy Publishing House, Bucharest, 1984, pp. 13.
12. Munson, B. R., Young, D. F., and Okiishi, T. H., "Fundamentals of fluid mechanics", John Wiley & Sons, New York, 1990, pp. 17.

13. Serway, R. A., "Physics for scientists and engineers", Saunders College Publishing, Montreal, 1990, pp. 183-184.

14. Serway, R. A., "Physics for scientists and engineers", Saunders College Publishing, Montreal, 1990, pp. 161-164.

15. Lamb, W. S., "Cavitation and aeration in hydraulic systems", The Fluid Engineering Centre, Bedford, 1987, pp. 4.

16. Plesset, M. S., "The tensile strength of liquids", University of Illinois, Urbana, 1969, pp. 15-25.

17. Knapp, R. T., Daily, J. W., and Hammitt, F. G., "Cavitation", McGraw-Hill Book Company, New York, 1970, pp. 59-60.

18. Lamb, W. S., "Cavitation and aeration in hydraulic systems", The Fluid Engineering Centre, Bedford, 1987, pp. 4.

19. Robertson, J. M., and Wislicenus, G. F., "Cavitation state of knowledge", The American Society of Mechanical Engineers, New York, 1969, pp. 15-25.

20. Anton, I., "Cavitation", Romanian Academy Publishing House, Bucharest, 1984, pp. 13-19.

21. Lamb, W. S., "Cavitation and aeration in hydraulic systems", The Fluid Engineering Centre, Bedford, 1987, pp. 4.

22. Van Wylen, G. J., Sonntag, R. E., and Borgnakke, C., "Fundamentals of classical thermodynamics", ", John Wiley & Sons, New York, 1994, pp. 755-756.

23. Lamb, W. S., "Cavitation and aeration in hydraulic systems", The Fluid Engineering Centre, Bedford, 1987, pp. 54-93.

24. Harvey, E. N., McElroy, W. D., and Whiteley, A. H., "On cavity formation in water", Journal of Applied Physics, New York, 1947, pp. 162-172.

25. Munson, B. R., Young, D. F., and Okiishi, T. H., "Fundamentals of fluid mechanics", John Wiley & Sons, New York, 1990, pp. 502.

26. Miller, G., "The inception of cavitation from a solid surface", University Microfilms Limited, Michigan, 1973, pp. 7.

27. Munson, B. R., Young, D. F., and Okiishi, T. H., "Fundamentals of fluid mechanics", John Wiley & Sons, New York, 1990, pp. 502.

28. Callister, W. D., "Materials science and engineering", John Wiley & Sons, New York, 1999, pp. 189.

29. Lamb, W. S., "Cavitation and aeration in hydraulic systems", The Fluid Engineering Centre, Bedford, 1987, pp. 3.

30. Morch, K. A., Mortensen, N. A., and Kuhle, A., "Interfacial tension in water at solid surfaces", The American Society of Mechanical Engineers, New York, 1979, pp. 1.

31. Knapp, R. T., Daily, J. W., and Hammitt, F. G., "Cavitation", McGraw-Hill Book Company, New York, 1970, pp. 87-90.

32. Miller, G., "The inception of cavitation from a solid surface", University Microfilms Limited, Michigan, 1973, pp. 13-15.

33. Hammitt, F. G., "Cavitation and Multiphase Flow Phenomena", University of Michigan, Michigan, 1980, pp. 46-47.

34. Brennen, C. E., "Cavitation and bubble dynamics", Oxford University Press, New York, 1995, pp. 9.

35. Brennen, C. E., "Cavitation and bubble dynamics", Oxford University Press, New York, 1995, pp. 65.

36. Pearsall, I. S., "Cavitation", Mills & Boon Limited, London, 1977, pp. 13-14.

37. Miller, G., "The inception of cavitation from a solid surface", University Microfilms Limited, Michigan, 1973, pp. 13-15.

38. Brennen, C. E., "Cavitation and bubble dynamics", Oxford University Press, New York, 1995, pp. 70-71.

39. Brennen, C. E., "Cavitation and bubble dynamics", Oxford University Press, New York, 1995, pp. 70-75.
40. Knapp, R. T., Daily, J. W., and Hammitt, F. G., "Cavitation", McGraw-Hill Book Company, New York, 1970, pp. 345.
41. Anton, I., "Cavitation", Romanian Academy Publishing House, Bucharest, 1984, pp. 31.
42. Brennen, C. E., "Cavitation and bubble dynamics", Oxford University Press, New York, 1995, pp. 65-66.
43. Pearsall, I. S., "Cavitation", Mills & Boon Limited, London, 1977, pp. 16-17.
44. http://focus.aps.org/story/v5/st5
45. Hammitt, F. G., "Cavitation and Multiphase Flow Phenomena", University of Michigan, Michigan, 1980, pp. 171.
46. Knapp, R. T., Daily, J. W., and Hammitt, F. G., "Cavitation", McGraw-Hill Book Company, New York, 1970, pp. 136.
47. Brennen, C. E., "Cavitation and bubble dynamics", Oxford University Press, New York, 1995, pp. 70-75.
48. Anton, I., "Cavitation", Romanian Academy Publishing House, Bucharest, 1984, pp. 36.
49. Brennen, C. E., "Cavitation and bubble dynamics", Oxford University Press, New York, 1995, pp. 65-94.
50. Hammitt, F. G., "Cavitation and Multiphase Flow Phenomena", University of Michigan, Michigan, 1980, pp. 136-214.
51. Pearsall, I. S., "Cavitation", Mills & Boon Limited, London, 1977, pp. 17, 24.
52. Hammitt, F. G., "Cavitation and Multiphase Flow Phenomena", University of Michigan, Michigan, 1980, pp. 181.
53. Pearsall, I. S., "Cavitation", Mills & Boon Limited, London, 1977, pp. 17.

54. Brennen, C. E., "Cavitation and bubble dynamics", Oxford University Press, New York, 1995, pp. 68.
55. Miller, G., "The inception of cavitation from a solid surface", University Microfilms Limited, Michigan, 1973, pp. 13-17.
56. Lamb, W. S., "Cavitation and aeration in hydraulic systems", The Fluid Engineering Centre, Bedford, 1987, pp. 59.
57. Lamb, W. S., "Cavitation and aeration in hydraulic systems", The Fluid Engineering Centre, Bedford, 1987, pp. 66.
58. Pearsall, I. S., "Cavitation", Mills & Boon Limited, London, 1977, pp. 71.
59. Knapp, R. T., Daily, J. W., and Hammitt, F. G., "Cavitation", McGraw-Hill Book Company, New York, 1970, pp. 364-370.
60. Anton, I., "Cavitation", Romanian Academy Publishing House, Bucharest, 1984, pp. 116.
61. Knapp, R. T., Daily, J. W., and Hammitt, F. G., "Cavitation", McGraw-Hill Book Company, New York, 1970, pp. 12-15.
62. Knapp, R. T., Daily, J. W., and Hammitt, F. G., "Cavitation", McGraw-Hill Book Company, New York, 1970, pp. 15-16.
63. Munson, B. R., Young, D. F., and Okiishi, T. H., "Fundamentals of fluid mechanics", John Wiley & Sons, New York, 1990, pp. 504-517.
64. Hammitt, F. G., "Cavitation and Multiphase Flow Phenomena", University of Michigan, Michigan, 1980, pp. 17, 18, 211-213.
65. Lamb, W. S., "Cavitation and aeration in hydraulic systems", The Fluid Engineering Centre, Bedford, 1987, pp. 16-19.
66. Knapp, R. T., Daily, J. W., and Hammitt, F. G., "Cavitation", McGraw-Hill Book Company, New York, 1970, pp. 16.
67. Knapp, R. T., Daily, J. W., and Hammitt, F. G., "Cavitation", McGraw-Hill Book Company, New York, 1970, pp. 364-372.

68. Dawson, D., Godet, M., and Taylor, C. M., "Cavitation and related phenomena in lubrication", The Institution of Mechanical Engineers, London, 1975, pp. 177-184.

69. Brennen, C. E., "Cavitation and bubble dynamics", Oxford University Press, New York, 1995, pp. 65-82.

70. "Cavitation, a Conference arranged by the Fluid Machinery Group of the Institution of Mechanical Engineers", Heriot-Watt University, Edinburgh, 1974, pp. 403.

71. Hammitt, F. G., "Cavitation and Multiphase Flow Phenomena", University of Michigan, Michigan, 1980, pp. 247.

72. Hammitt, F. G., "Cavitation and Multiphase Flow Phenomena", University of Michigan, Michigan, 1980, pp. 223.

73. Lamb, W. S., "Cavitation and aeration in hydraulic systems", The Fluid Engineering Centre, Bedford, 1987, pp. 59.

74. Knapp, R. T., Daily, J. W., and Hammitt, F. G., "Cavitation", McGraw-Hill Book Company, New York, 1970, pp. 17-19.

75. Hammitt, F. G., "Cavitation and Multiphase Flow Phenomena", University of Michigan, Michigan, 1980, pp. 2, 15, 155-157, 185-186.

76. http://www.enstimac. fr/~louisnar/cavitation.html

77. http://wsx.lanl.gov/WebPub/sono.html

78. "Industrial hydraulics manual", Sperry Rand Corporation, Michigan, 1970, pp. 11.1.

79. Pease, D. A., and Pippenger, J. J., "Basic fluid power", Prentice-Hall, 1987, pp. 90

80. "Industrial hydraulics manual", Sperry Rand Corporation, Michigan, 1970, pp. 11.1-11.2.

81. Pease, D. A., and Pippenger, J. J., "Basic fluid power", Prentice-Hall, 1987, pp. 93-95.
82. Pease, D. A., and Pippenger, J. J., "Basic fluid power", Prentice-Hall, 1987, pp. 90-94, 109.
83. "Industrial hydraulics manual", Sperry Rand Corporation, Michigan, 1970, pp. 11.1-11.2, 11-23.
84. http://www.globalspec.com.
85. Munson, B. R., Young, D. F., and Okiishi, T. H., "Fundamentals of fluid mechanics", John Wiley & Sons, New York, 1990, pp. 25.
86. Fox, R. W., and McDonald A. T., "Introduction to fluid mechanics", John Wiley & Sons, New York, 1992, pp. 106.
87. Fox, R. W., and McDonald A. T., "Introduction to fluid mechanics", John Wiley & Sons, New York, 1992, pp. 97.
88. Munson, B. R., Young, D. F., and Okiishi, T. H., "Fundamentals of fluid mechanics", John Wiley & Sons, New York, 1990, pp. 127.
89. Munson, B. R., Young, D. F., and Okiishi, T. H., "Fundamentals of fluid mechanics", John Wiley & Sons, New York, 1990, pp. 124-126, 507.
90. Munson, B. R., Young, D. F., and Okiishi, T. H., "Fundamentals of fluid mechanics", John Wiley & Sons, New York, 1990, pp. 509, 510.
91. Numachi, F., "Cavitation and hydraulic machinery", Institute of High Speed Mechanics, Sendai, Japan, 1963, pp. 125-141.
92. Numachi, F., "Cavitation and hydraulic machinery", Institute of High Speed Mechanics, Sendai, Japan, 1963, pp. 133.